National Aeronautics
and
Space Administration

Research Grant NsG-306-63

PULSED ELECTROMAGNETIC GAS ACCELERATION

Ninth Semi-Annual Progress Report
1 July 1966 to 31 December 1966

Report No. 634h

Prepared by: R. G. Jahn
Robert G. Jahn
Associate Professor
and Research Leader

and: Woldemar v. Jaskowsky
Woldemar F. von Jaskowsky
Research Engineer
and Lecturer

January 1, 1967

Guggenheim Laboratories for the Aerospace Propulsion Sciences
Department of Aerospace and Mechanical Sciences
Princeton University
Princeton, New Jersey

Abstract

The distribution of current density throughout the exhaust plume of a pulsed plasma accelerator has been determined by magnetic probing, for discharge currents from 40,000 to 140,000 amperes, and pulse lengths from 20 to 80 microseconds. Back pressures from .05 micron to the ambient discharge chamber level of 100 microns are provided in a large plexiglas vacuum tank, which introduces a minimum of electrical and spatial interference with the plume development. Depending on the particular conditions, some fraction of the discharge current propagates out into the plume and, when pulse length is sufficient, attains a fixed spatial distribution which resembles that of the high current MPD arc. Two new experiments to exploit this similarity, and to study the current stabilization process in more detail have been initiated.

The interior structure of the sharp current sheets found in closed chamber discharges are steadily yielding to coordinated studies with electric, magnetic, and microwave probes, high-speed pressure transducers, and a gas-laser interferometer, each interpreted in the light of particular analytical models which are amenable to the data.

Following a lengthy sequence of design, construction, testing, and revision, a group of "piggy-back" pulse line capacitors is now available, and the long-sought match of driving circuit impedance to discharge dynamics seems nearly in hand.

Table of Contents

List of Illustrations

List of Illustrations-continued

List of Illustrations-continued

Current Student Participation

Student	Period	Degree	Thesis Topic
BAUMGARTH, Siegfried	1966-	Visiting Scholar	Acceleration of Plasma in a Diverging Magnetic Field
BRUCKNER, Adam P.	1966-		Gas Dynamical Models of the Pinch Discharge
BURTON, Rodney L.	1962-1966	Ph.D. August 1966	Structure of the Current Sheet in a Pinch Discharge
COOKE, Kenneth J.	1965-	M.S.E. Cand.	Experimental Studies of Density in Pinch Discharges with Laser Radiation
CLARK, Kenn E.	1965-	Ph.D. Cand.	Quasi-Steady Plasma Acceleration by Long Duration Current Pulses
Di CAPUA Marco S.	1966-		Transient Voltage Measurements in Closed Chamber Pinch Discharges and Plasma Ejectors
ECKBRETH, Alan C.	1964-	Ph.D. Cand.	Ejection of a Plasma from a Discharge Chamber
ELLIS, JR. William R.	1962-	Ph.D. Cand.	Microwave Determinations of Electron Densities in a Pinch Discharge
OBERTH, Ronald C.	1966-		Experimental Study of Current Sheet Bifurcation
TURCHI, Peter J.	1963-	B.S. Cand.	Dynamics of Pinch Discharges
YORK, Thomas M.	1965-	Ph.D. Cand.	Gas Pressure Distributions in Pinch Discharges

I. Introduction

During the present reporting period, the studies of the exhaust of a pulsed plasma discharge, which have developed through several phases over the past two and a half years, were brought to a satisfactory interim conclusion, whereby the questions originally motivating the study could now be answered, and the course of logical future work clearly forseen. Therefore, this semi-annual report will concentrate largely on this topic, providing, as it were, a single repository for the summary data of this series of experiments.

In addition, more concise reviews of four other studies which have provided significant new results, or which are nearing completion are also included, along with a brief summary of the other projects currently in progress. Page vii contains a list of participating students; Appendix A presents the budgetary detail; and the list of references covers all publications issued by this program to date.

II. Exhaust of a Pulsed Plasma (Clark, Eckbreth)

The importance of the ejection phase of a pulsed plasma acceleration cycle to the overall effectiveness of a given device, and a substantial sequence of exploratory experiments dealing with the ejection process have been discussed in several earlier reports [18,19,20,21,29,32,43]. In addition to the phenomenological insight these studies provided, they also emphasized the need for certain sophisticated elements of equipment in order to carry out any systematic and unambiguous study of this complex problem. Most notably among these needs were an ultra-fast gas injection system, provision for simultaneous probing of the exhaust plume at several locations, and a large, dielectric, high vacuum facility. During the present reporting period it was possible for the first time to fulfill all of these requirements in one experimental arrangement incorporating a shock tube gas-injection system, a magnetic probe rake, and a large Plexiglas vacuum tank, each of which has been discussed separately in detail in previous reports [32,43]. Using this arrangement, a detailed sequence of exhaust plume studies were carried out, with the primary purpose of identifying the effect of back pressure, arc current magnitude, and pulse length on the development of the exhaust plume, with particular attention to the process of plume stabilization.

The experimental series described below used as a plasma source a 5" diameter, 2" wide linear pinch discharge in argon. The outer anode surface was 34" in diameter with a 4" diameter exhaust orifice from which the plasma generated in the pinch was ejected (Fig. 1). This orifice opened into the large Plexiglas vacuum tank which is 3' in diameter and approximately 4' long from the face of the anode. In this facility pressures as low as .01 μ have been obtained; however in the present set of experiments the back pressure, when not purposely set to 100 μ, was maintained just below 0.05 μ. Under these circumstances the mean free path of the gas is

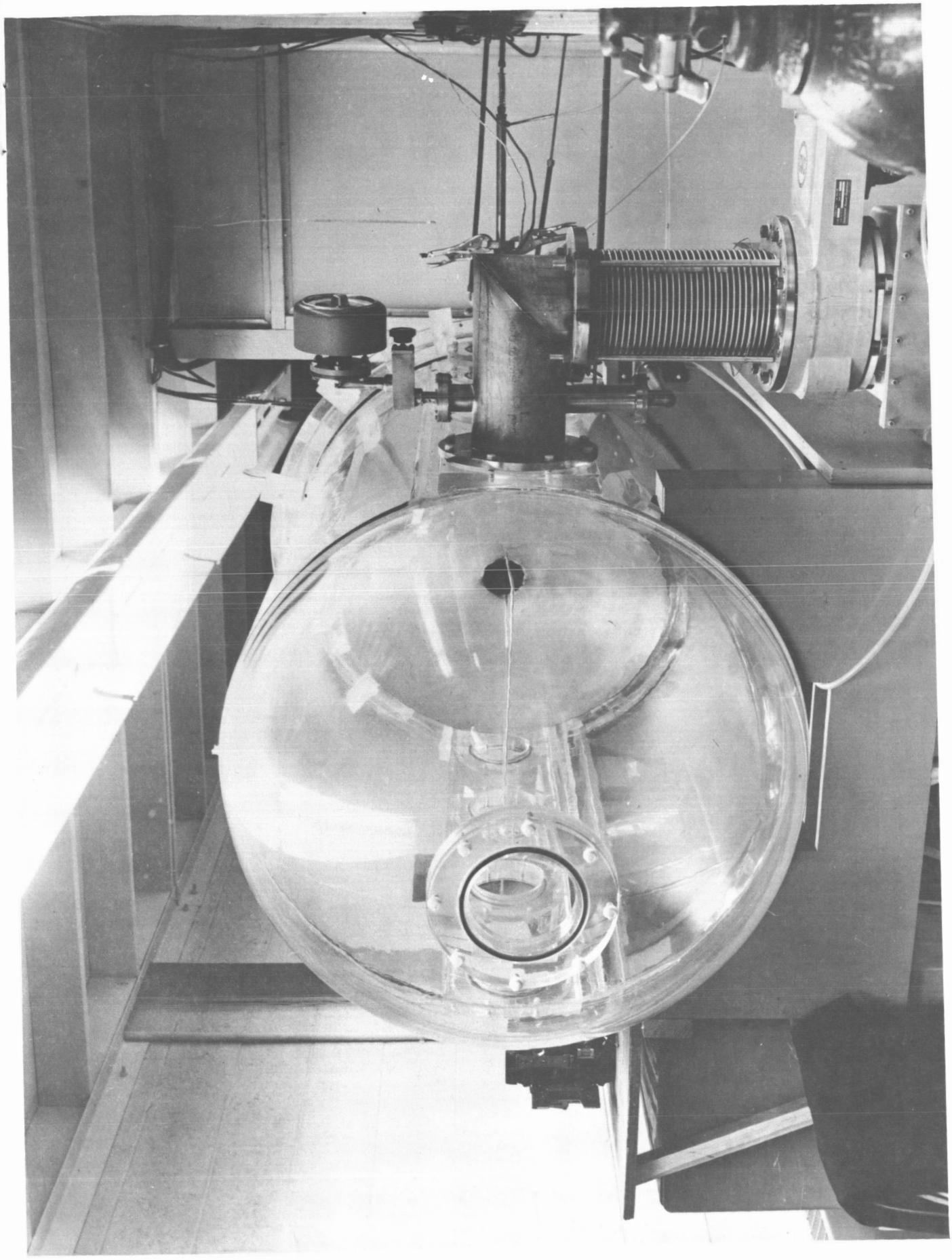

LARGE ANODE WITH EXHAUST ORIFICE INSIDE PLEXIGLAS VACUUM TANK

FIGURE 1

approximately 100 cm, which is comparable to the tank dimensions; thus the situation prior to discharge adequately approximates the space environment.

The pinch discharge was driven by a bank of 40 capacitors divided into 4 individual lines composed of 10 capacitors and 10 inductors in the form of an LC ladder network. Each individual line produced a pulse of roughly 35,000 amps for 20 μsec when charged initially to 10,000 V. When the 4 banks were arranged in parallel, a nearly rectangular pulse of 140,000 amperes for 20 μsec was obtained; series arrangement produced a 70 μsec pulse of 40,000 amperes. Other combinations are possible, but only these two pulse forms were used in the experiments.

The effect of back pressure was explored in two extremes: in one, the "ambient" mode, the exhaust vessel and pinch chamber were both filled to 100 μ; in the other, the pinch chamber and vacuum vessel were both evacuated below .05 μ, and the discharge process was initiated by triggering a shock tube which simultaneously injects argon into the switch and pinch chambers. In the latter mode, no attempt was made to measure the discharge chamber pressure directly, but an average pressure was inferred by matching observed pinch times with those of the ambient mode at the corresponding pressure. For example, in one particular case studied here, it was found that a current pulse of 140,000 amps and 20 μsec duration produced a pinch time of 3.3 μsec in 100 μ ambient argon. Hence, the pinch speed in the shock tube injection case was adjusted by varying the inlet orifices until it also yielded a pinch time of 3.3 μsec.

The principal diagnostic tool employed was a four-element rake of magnetic probes, whose signals were passively integrated on the scope to yield simultaneous records of local magnetic field, B_θ, versus time at the four positions. Direct application of Ampere's law to each probe record yields the total current enclosed in a circular area whose radius is that

of the probe position and whose center is on the axis. The data is thus plotted in the form of contours of enclosed current in the r, z plane at successive times. In addition to the probe-rake used throughout the exhaust plume, straight and bent probes were inserted through the side walls of the pinch chamber to study its interior. All of the probes were calibrated, each with their own integrators, using a shorting post in conjunction with 5 capacitors which produced a damped sinusoidal current pattern. A Rogowski coil, monitoring total discharge current, was calibrated in the same way. Total voltage across the chamber was also measured via a small resistor in series with the ballast resistor.

Of the wide range of possible permutations of discharge current amplitudes, pulse lengths, and tank back pressure available, six were selected for these detailed studies as potentially the most illuminating. They are displayed in the following Table 1:

Current amplitude, I	Pulse length, τ	Back pressure, p_B
140,000 amps	20 μsec	100 μ 0.05 μ
40,000 amps	20 μsec	100 μ 0.05 μ
40,000 amps	70 μsec	100 μ 0.05 μ

It will be noted that this matrix of conditions permits examination of the effect of varying any one parameter with the other two held fixed.

The detailed procedure used in reducing the data was to take a triple overlay at each probe position, a typical trace of which is shown in Fig. 2, and from it to evaluate the three

I414B

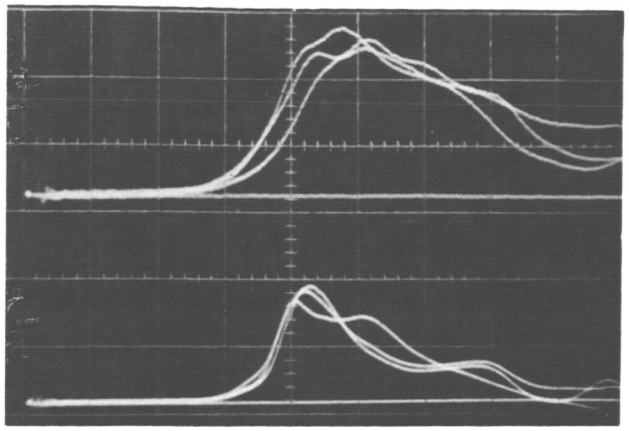

TYPICAL RESPONSE OF MAGNETIC PROBES
a) AT R = $3\frac{1}{8}$ INCHES
b) AT R = $1\frac{1}{8}$ INCHES

FIGURE 2

corresponding magnetic field values at each desired time. From these, an enclosed current was determined by averaging the three readings together at that one time. A typical map of enclosed current profiles obtained in this way is shown in Fig. 3. In Fig. 4 these contours are re-plotted with a few typical error bars representing the uncertainty inherent in the averaging process. With these in mind, the data contours can be smoothed to yield more regular enclosed current contours within the reproducibility of the exhaust patterns. Each contour then represents a mean location of a broad band of enclosed current. All of the results to be presented have been smoothed in this way. In general this leads to an overall uncertainty in the patterns of approximately 10% of the given contour value. One might reasonably dispute whether the irregularities in the original enclosed current pattern results from a slight shot-to-shot irreproducibility in the development of basically smooth plume patterns, or whether the actual

JPR 4241-67

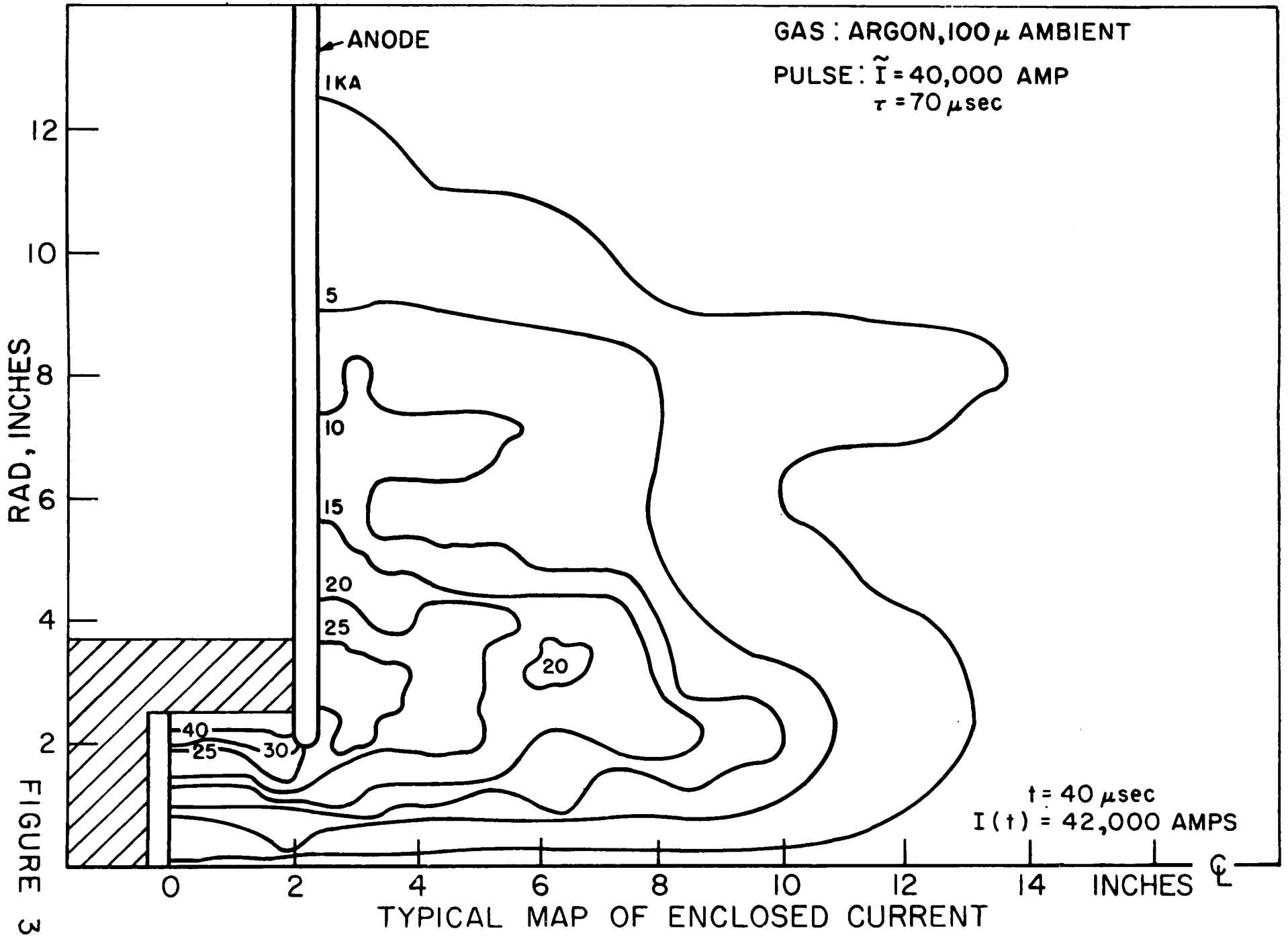

FIGURE 3 TYPICAL MAP OF ENCLOSED CURRENT

JPR 4242-67

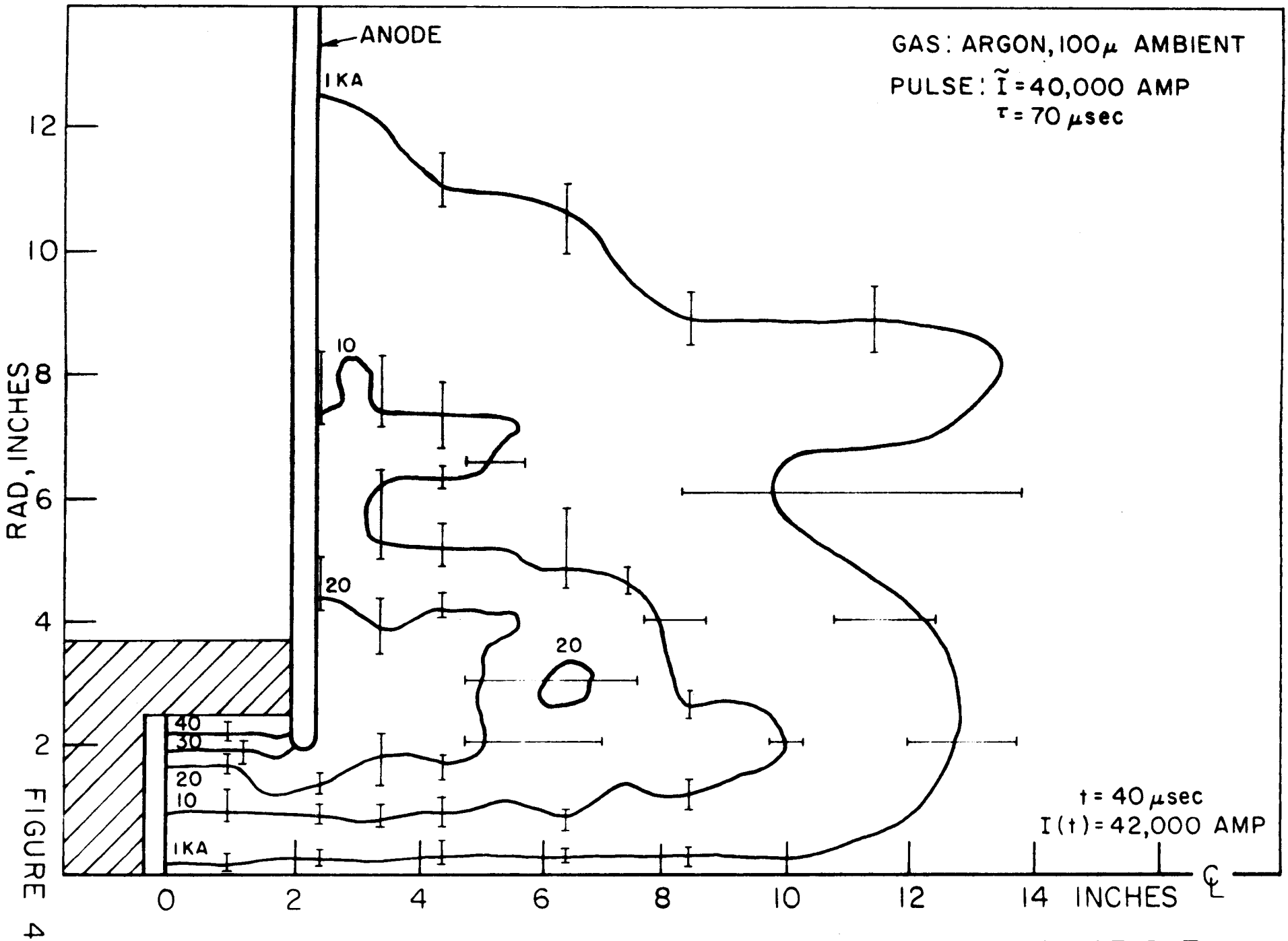

FIGURE 4

TYPICAL MAP OF ENCLOSED CURRENT INDICATING ACCURACY OF DATA

patterns are more closely represented by the original wiggly lines. The data does not permit unambiguous resolution of this question, but as long as the variations are small, it is probably an academic point.

Considering the 100 μ back pressure results first, the plume profiles produced by the 140,000 ampere, 20 μ sec pulse are shown in Figs. 5a through 5i. It is apparent that only approximately 30% of the total current participates in the actually pinching process (the rest remain back near the outer wall of the pinch chamber) and it is this portion that is found in the exhaust plume. No enclosed current contour of significantly greater than 40,000 amps is found in the exhaust. Radial progression of the contours ceases after about 8 μsec, after which their attachment location on the anode remains constant until the end of the pulse. The axial behavior is not as clear. On the one hand, the exterior edge of the pattern appears to progress slowly outward throughout the pulse, but some of the higher value interior contours regress backward toward the orifice.

Maintaining the same pulse duration of 20 μsec but decreasing the current amplitude from 140,000 amps to 40,000 amps yields the current contours shown in Figs. 6a through 6i. Here again, not of all the current takes part in the pinch, but now the fraction is 60%, which is roughly twice the result found in the previous higher current case. As before only that portion of the total current which pinches participates in the exhaust plume. In this case both radial and axial progression continue throughout the duration of the pulse. This may be related to the fact that the driving current is down by a factor 3.5 and hence the driving force of the current sheet is down by an order of magnitude. Hence, the pinch time becomes comparable to the pulse time and one would naively expect an unsteady process throughout the duration of the pulse.

When the pulse time is increased to 70 μsec at the same current level, the plume behavior shown in Figs. 7a

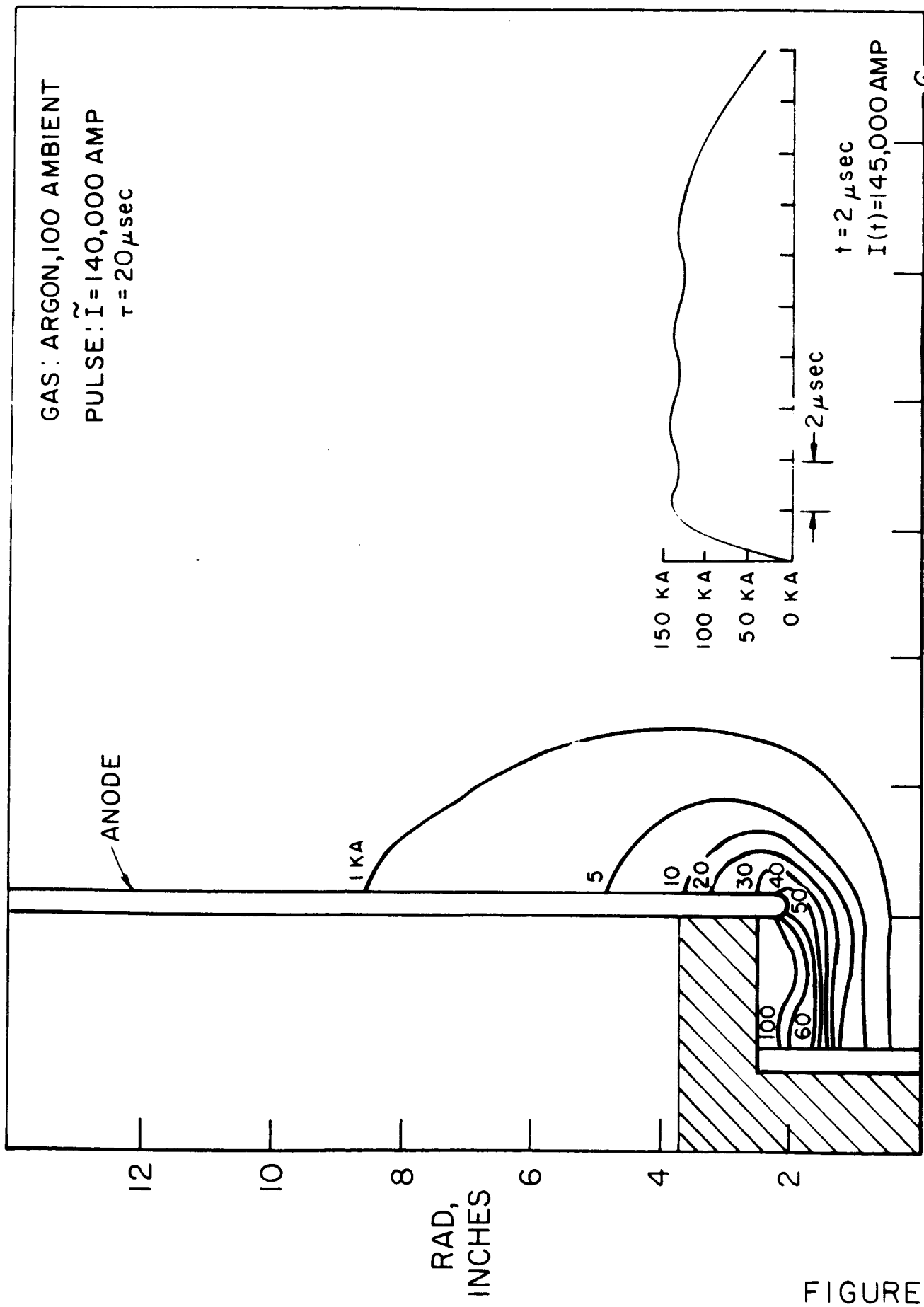

MAP OF ENCLOSED CURRENT

FIGURE 5a

AP 25-4205-67

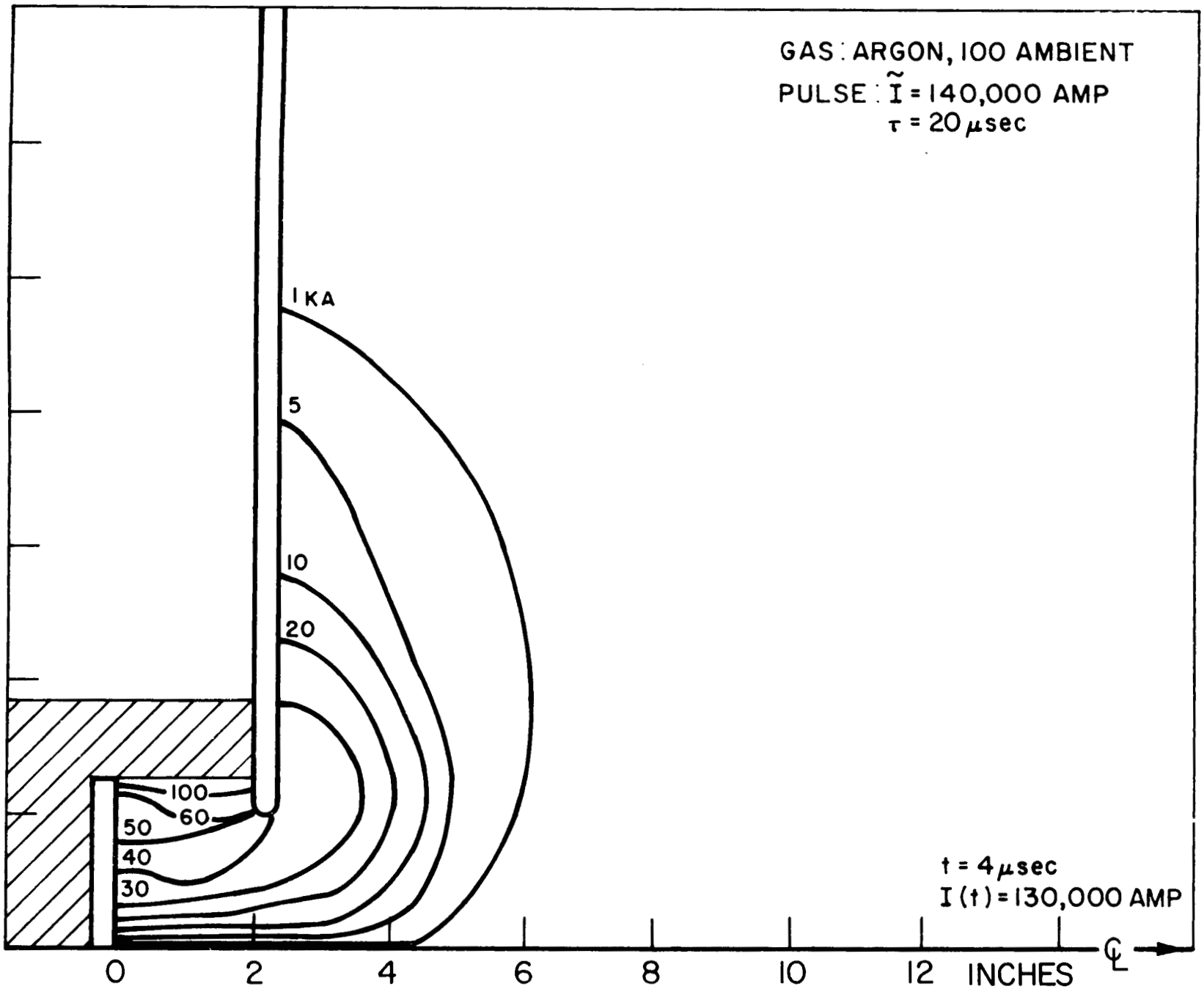

MAP OF ENCLOSED CURRENT

FIGURE 5b

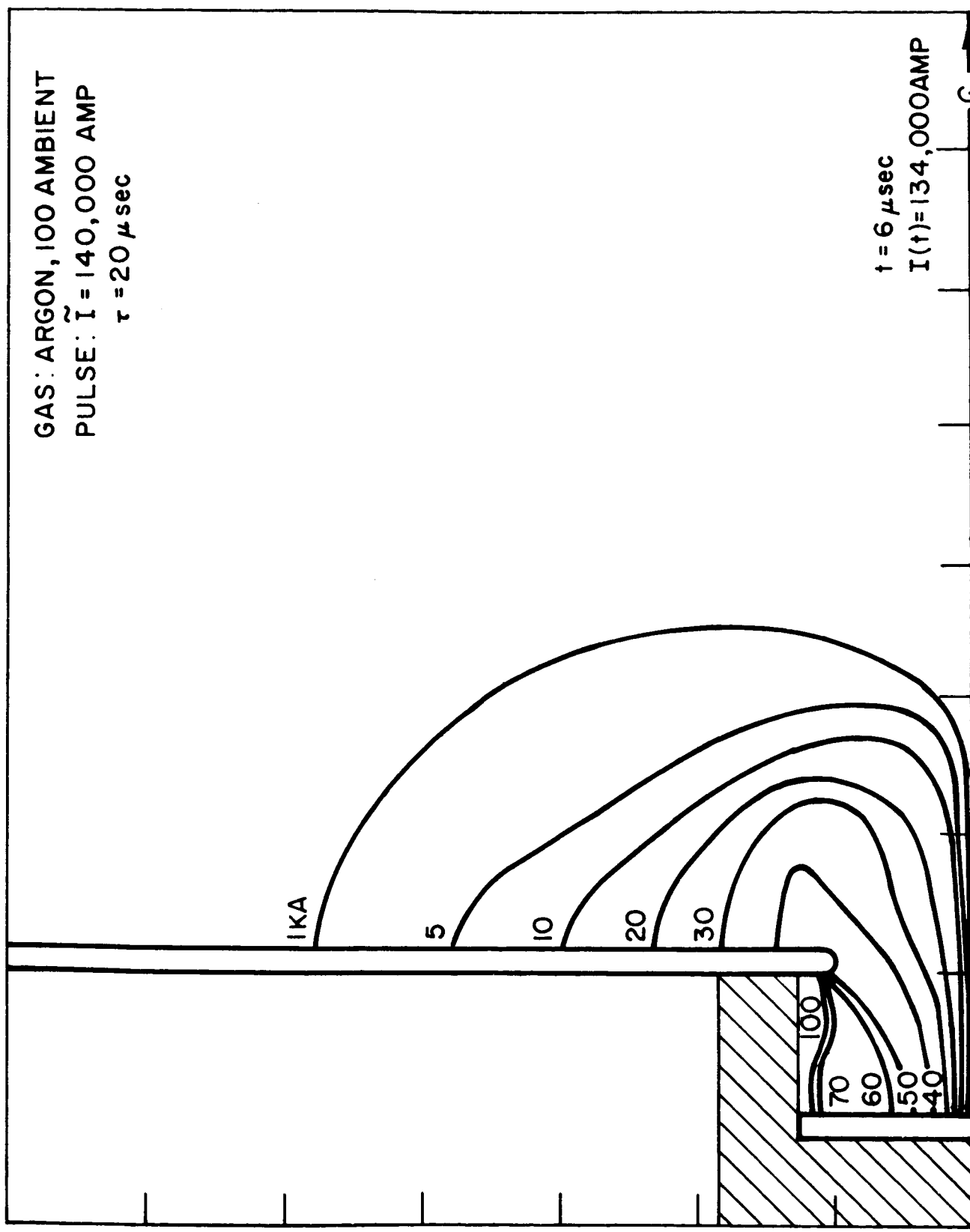

MAP OF ENCLOSED CURRENT

FIGURE 5c

AP25-4207-67

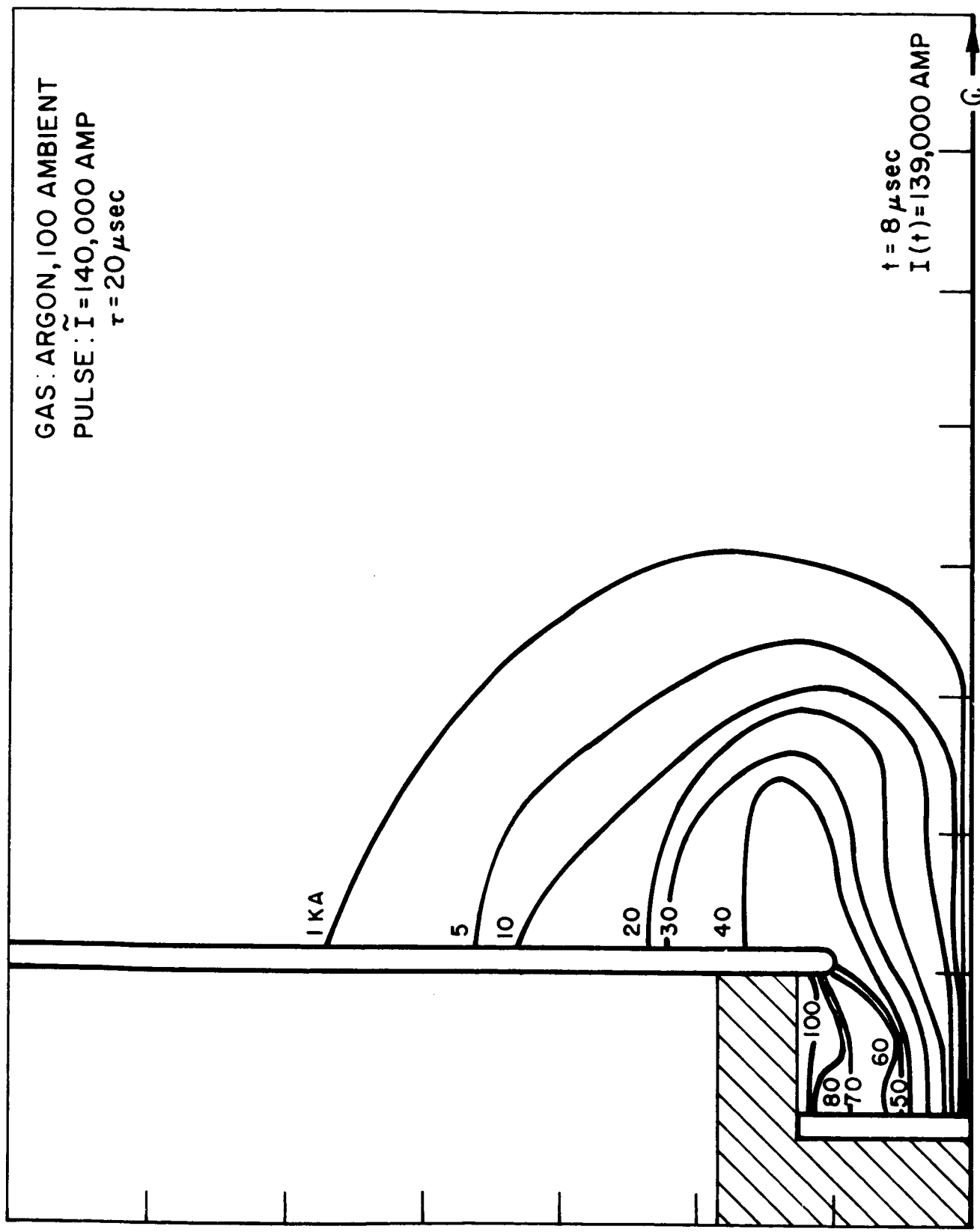

MAP OF ENCLOSED CURRENT

FIGURE 5d

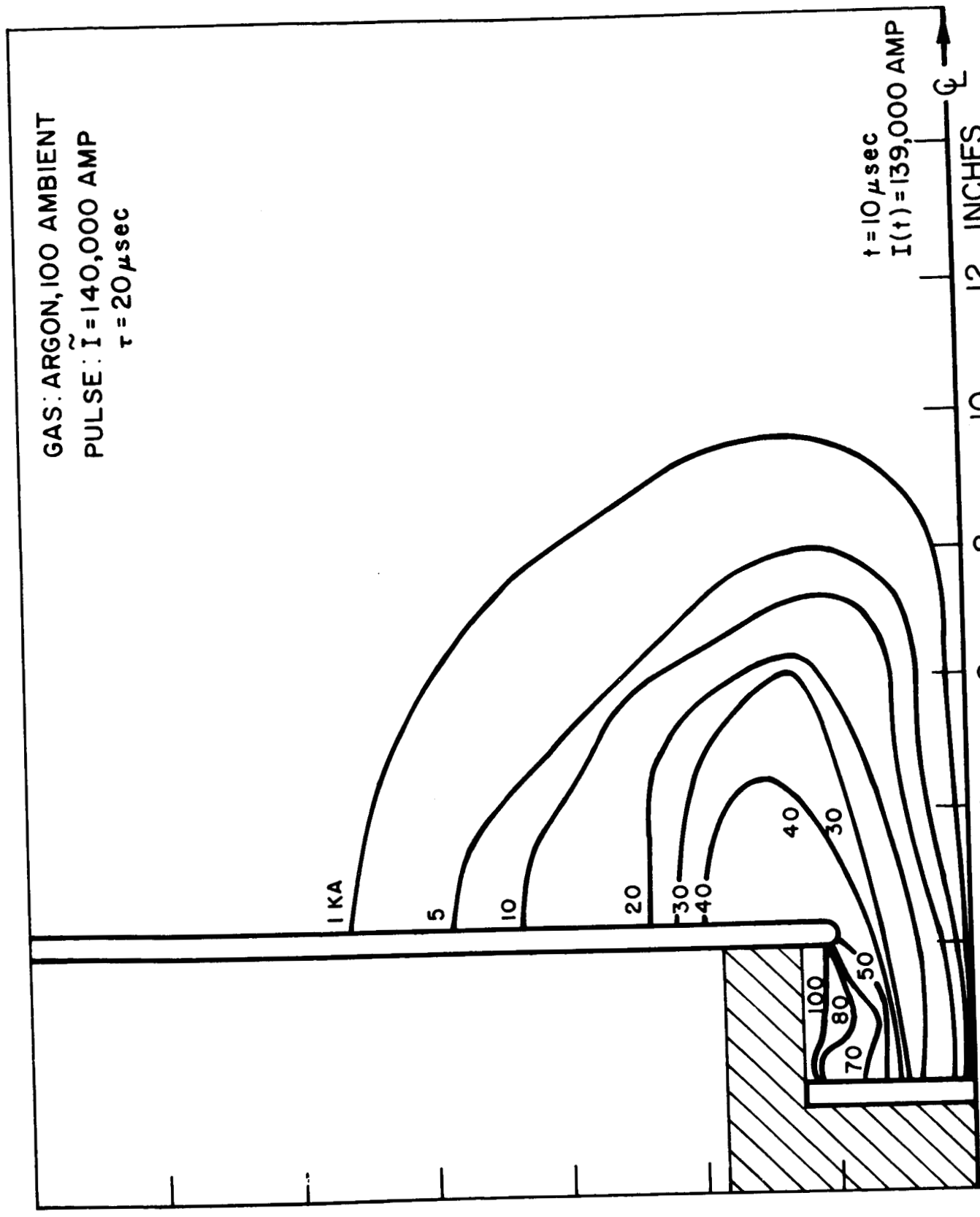

AP 25-4209-67

FIGURE 5e

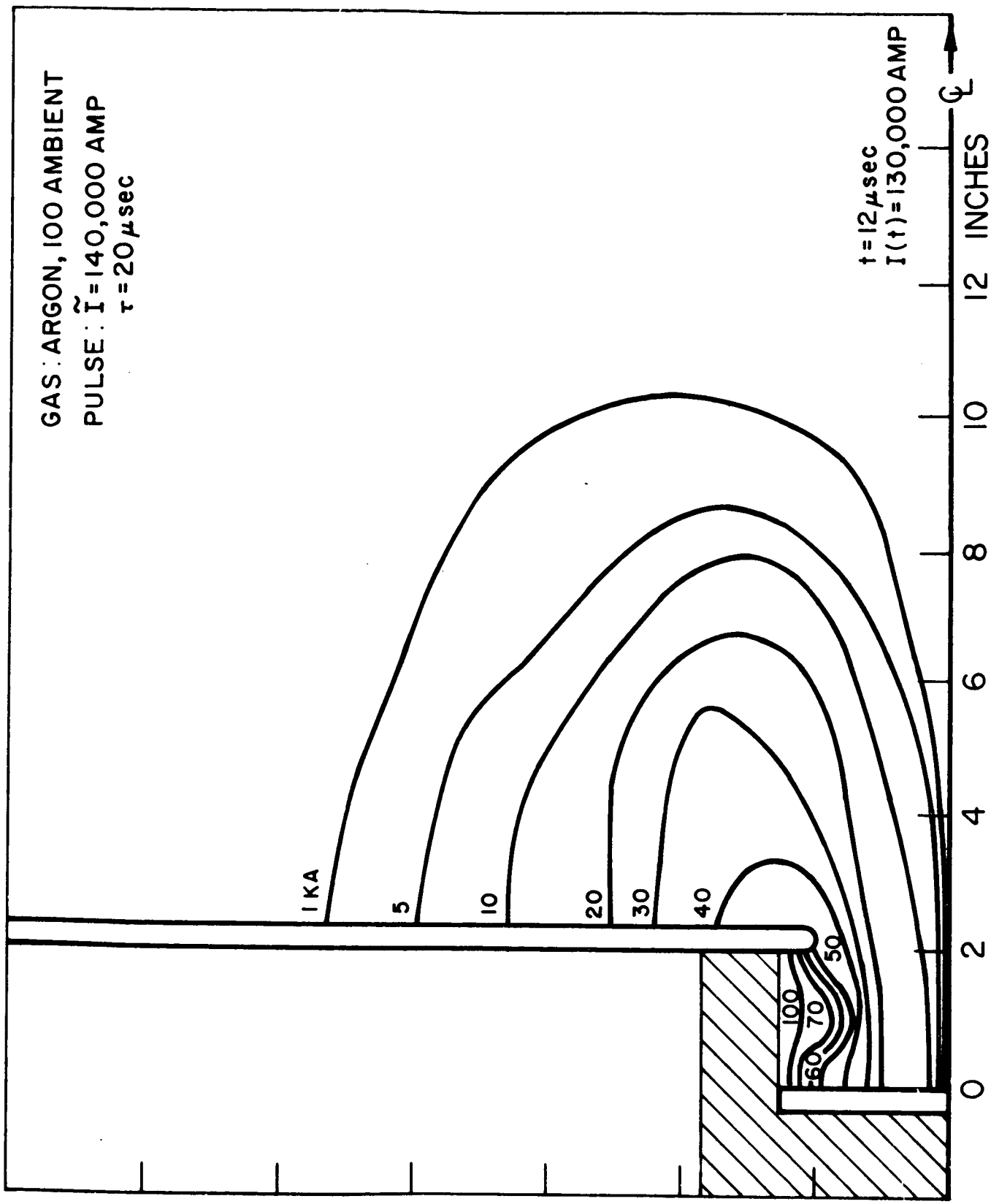
GAS: ARGON, 100 AMBIENT
PULSE: Ĩ=140,000 AMP
τ=20μsec
t=12μsec
I(t)=130,000 AMP
1 KA
5
10
20
30
40
50
70
100
60
0
2
4
6
8
10
12 INCHES
℄
MAP OF ENCLOSED CURRENT

FIGURE 5f

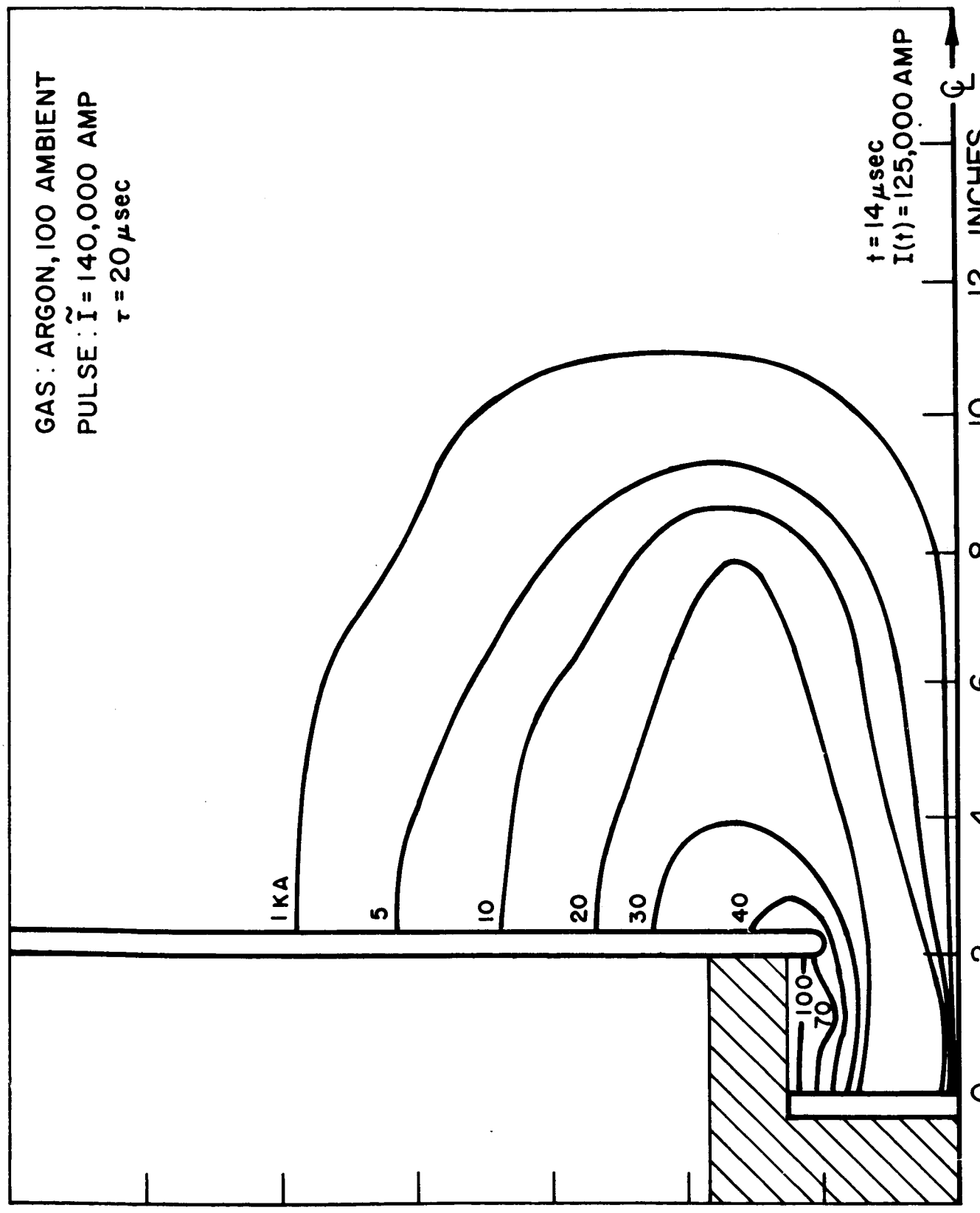

MAP OF ENCLOSED CURRENT

FIGURE 5g

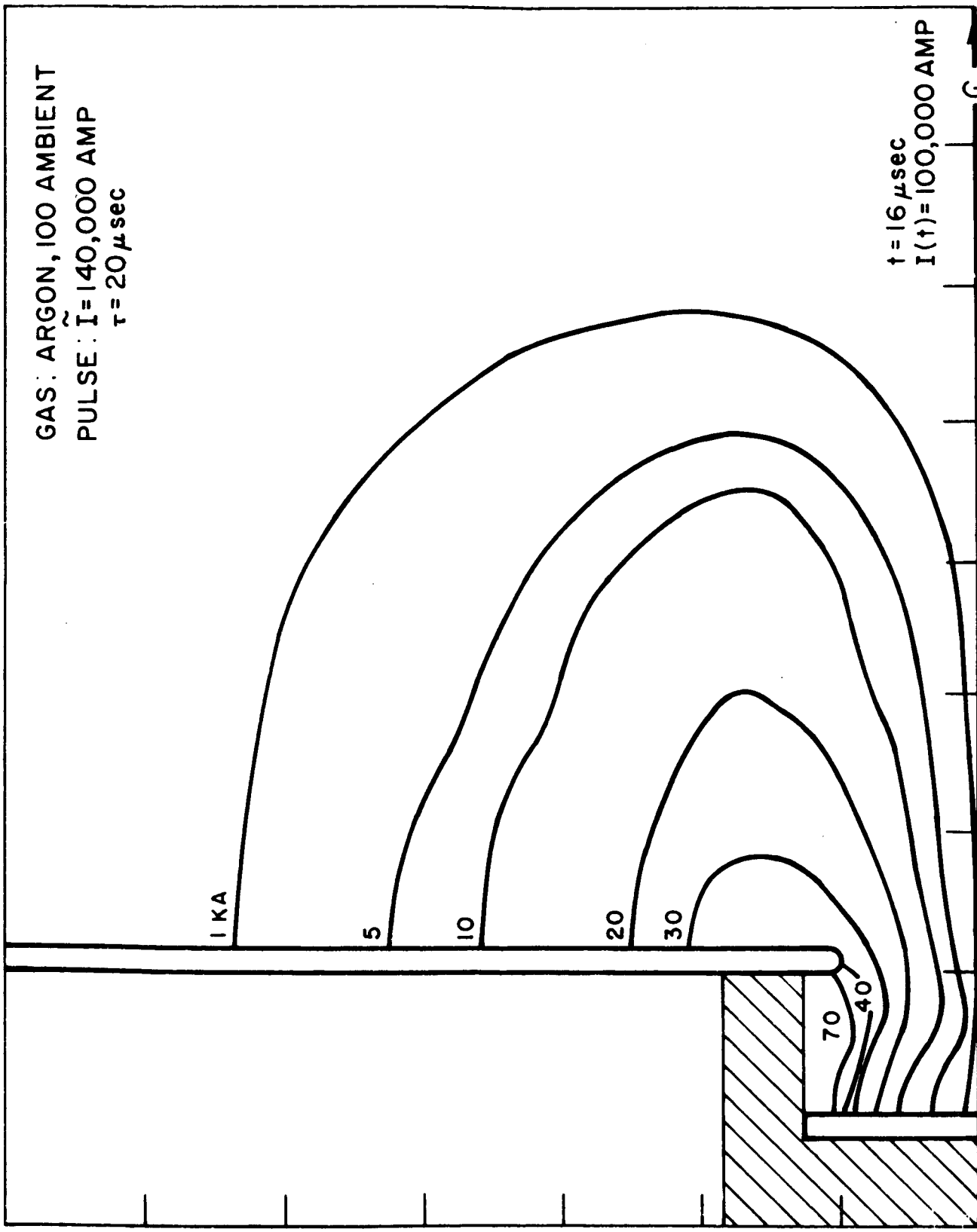
GAS: ARGON, 100 AMBIENT
PULSE: Ĩ = 140,000 AMP
τ = 20 μsec
t = 16 μsec
I(t) = 100,000 AMP
1 KA
5
10
20
30
40
70
0
2
4
6
8
10
12 INCHES
MAP OF ENCLOSED CURRENT

FIGURE 5h

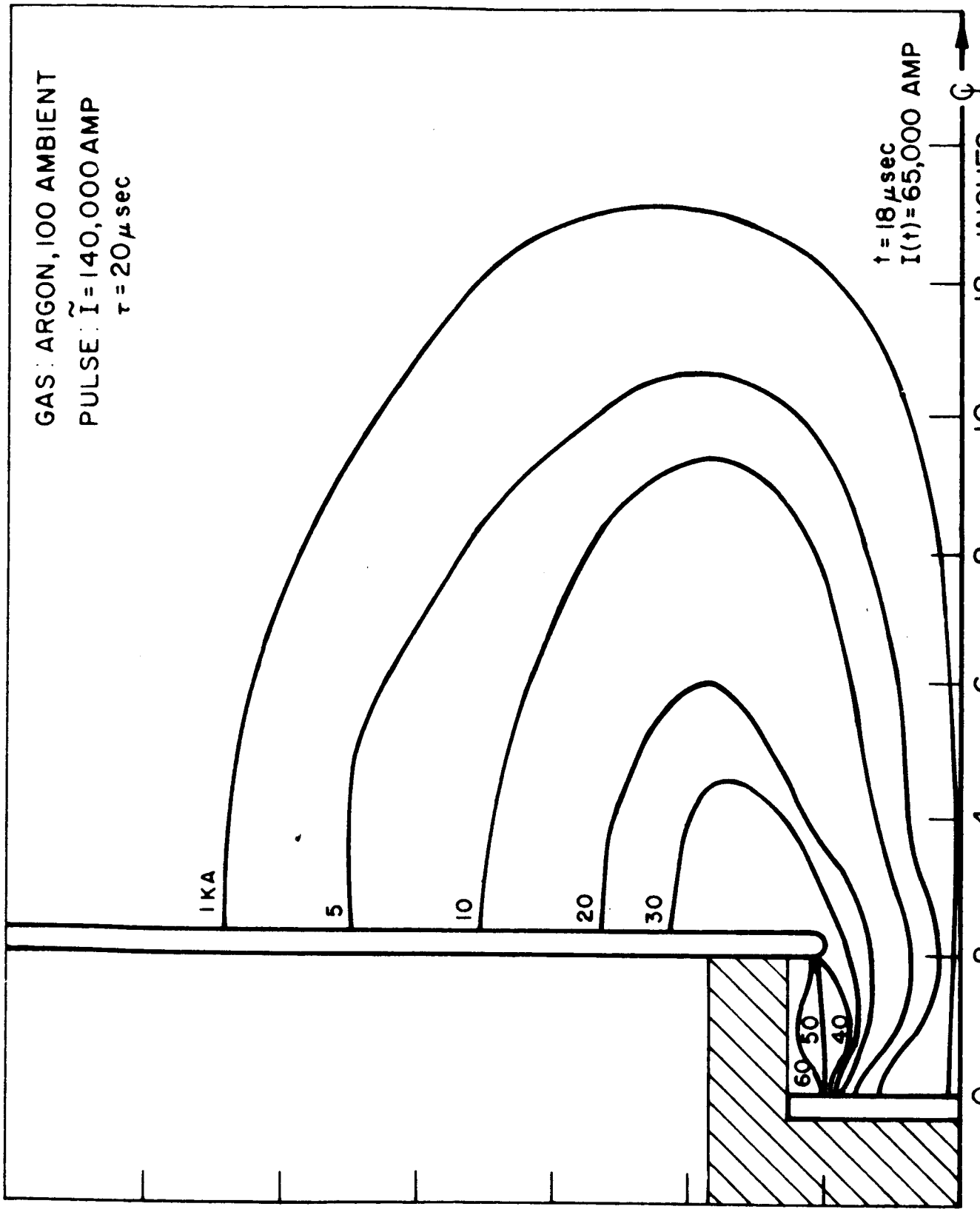
GAS: ARGON, 100 AMBIENT
PULSE: Ĩ = 140,000 AMP
τ = 20 μsec
t = 18 μsec
I(t) = 65,000 AMP
1 KA
5
10
20
30
40
50
60
0
2
4
6
8
10
12 INCHES
MAP OF ENCLOSED CURRENT

FIGURE 5i

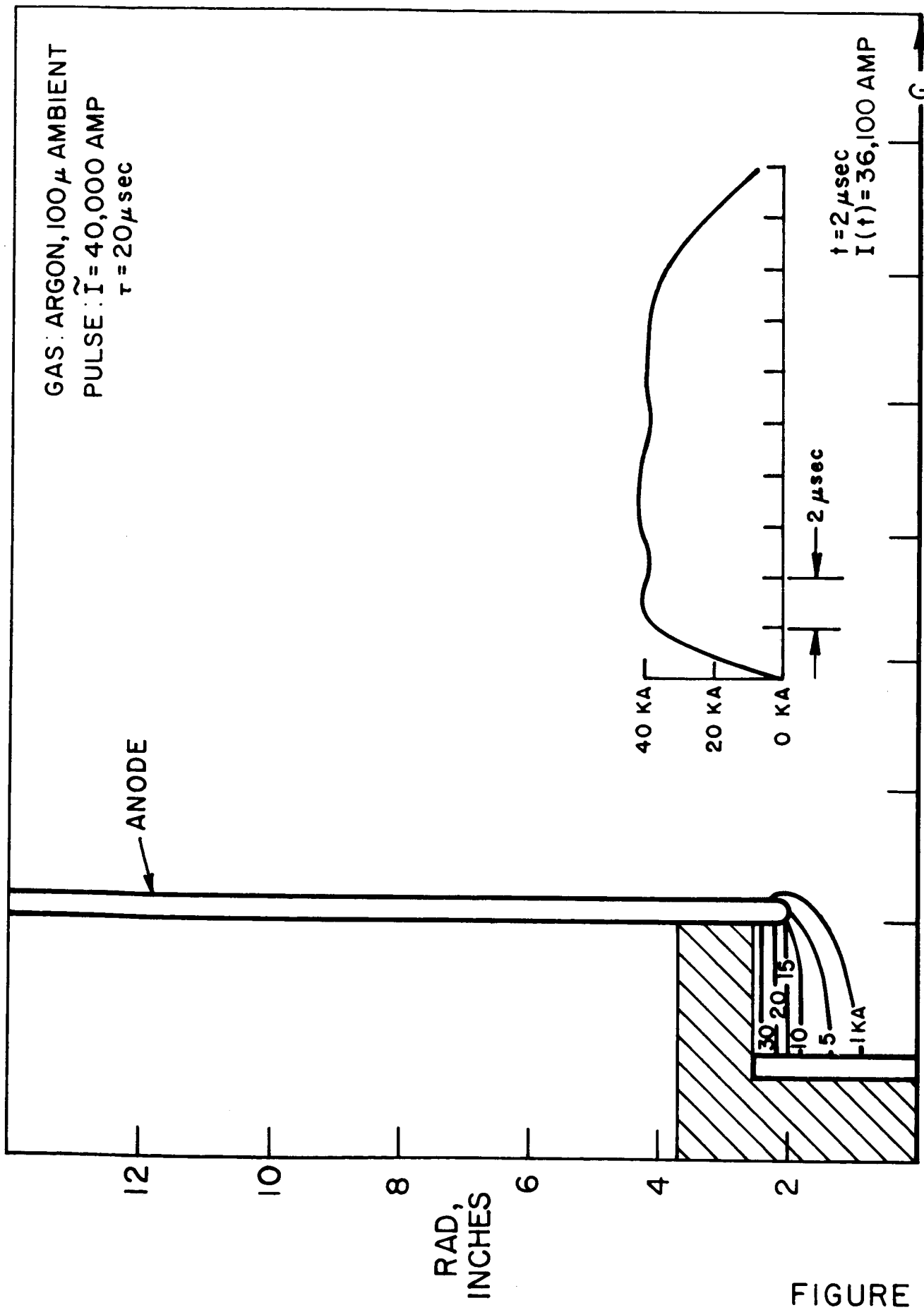

MAP OF ENCLOSED CURRENT

FIGURE 6a

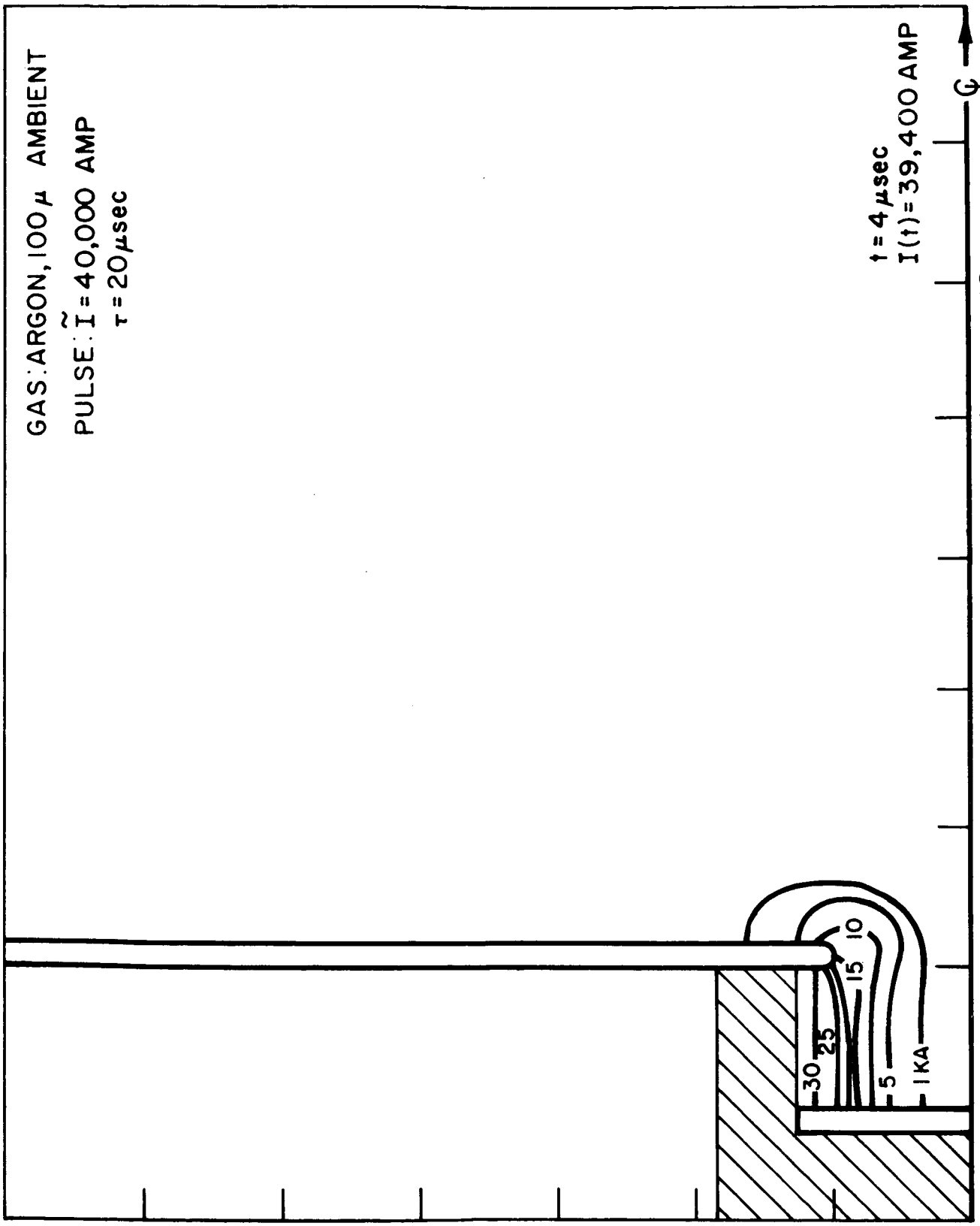

MAP OF ENCLOSED CURRENT

FIGURE 6b

AP25-7015-67

AP25-4216-67

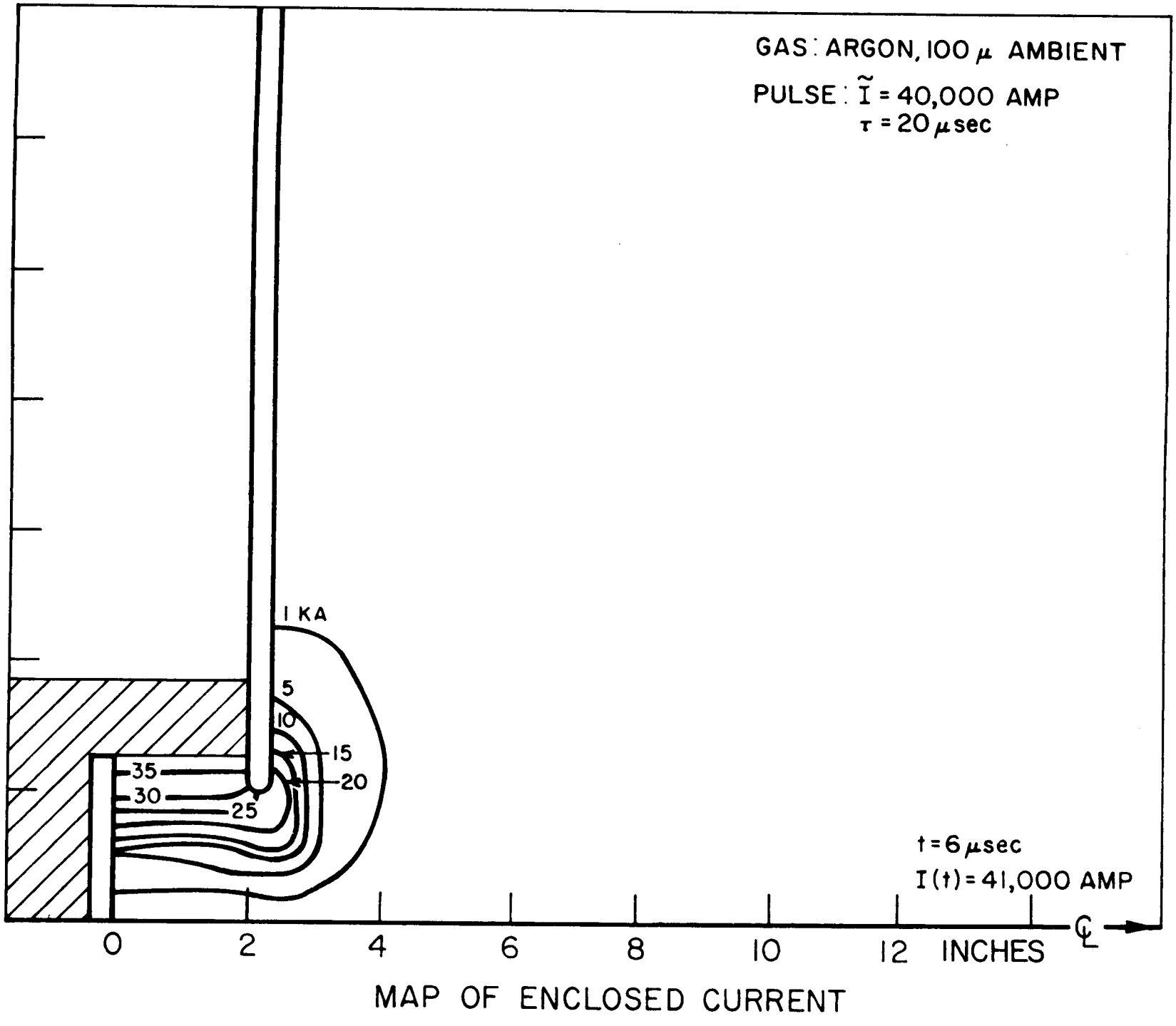

MAP OF ENCLOSED CURRENT

FIGURE 6c

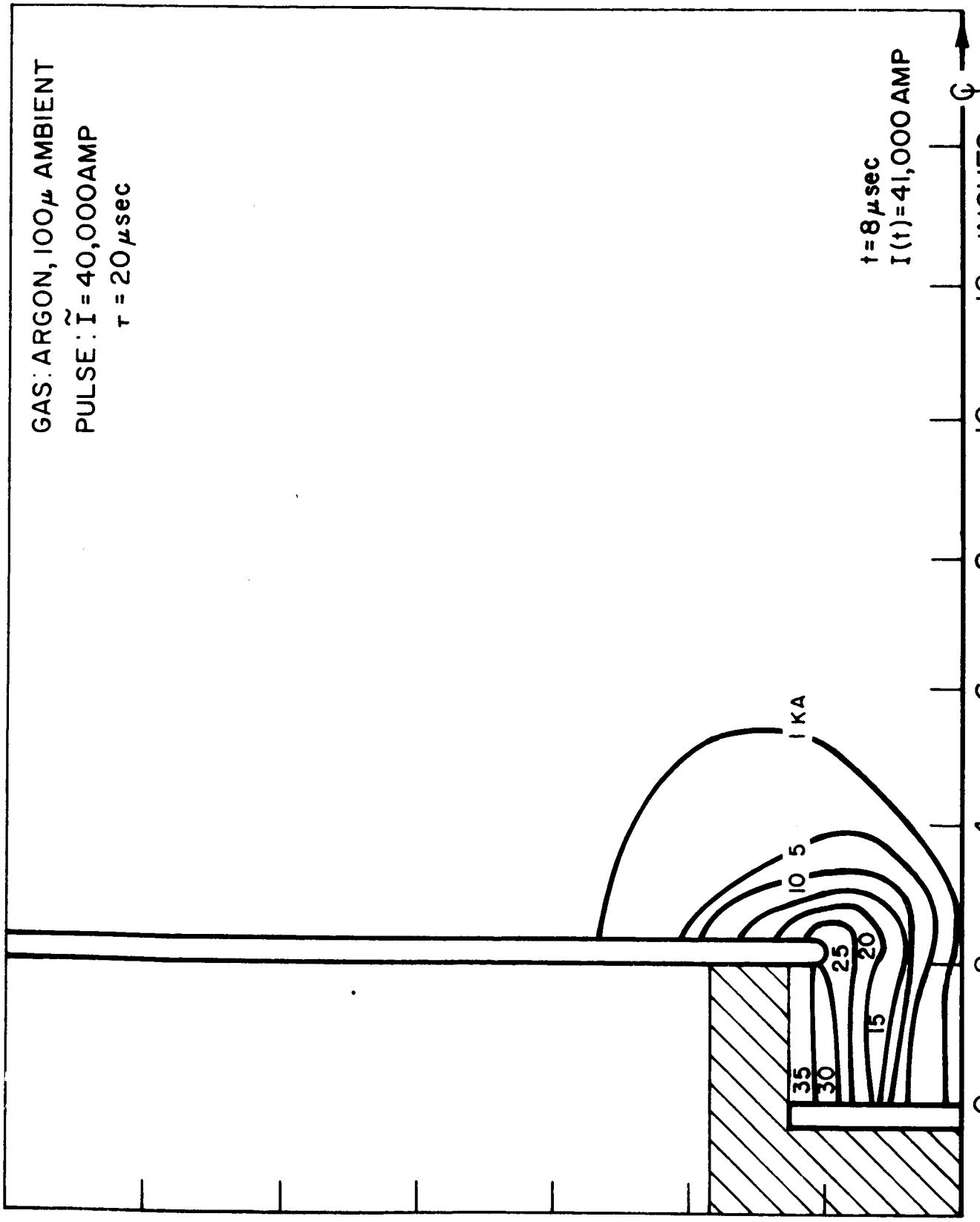

MAP OF ENCLOSED CURRENT

FIGURE 6d

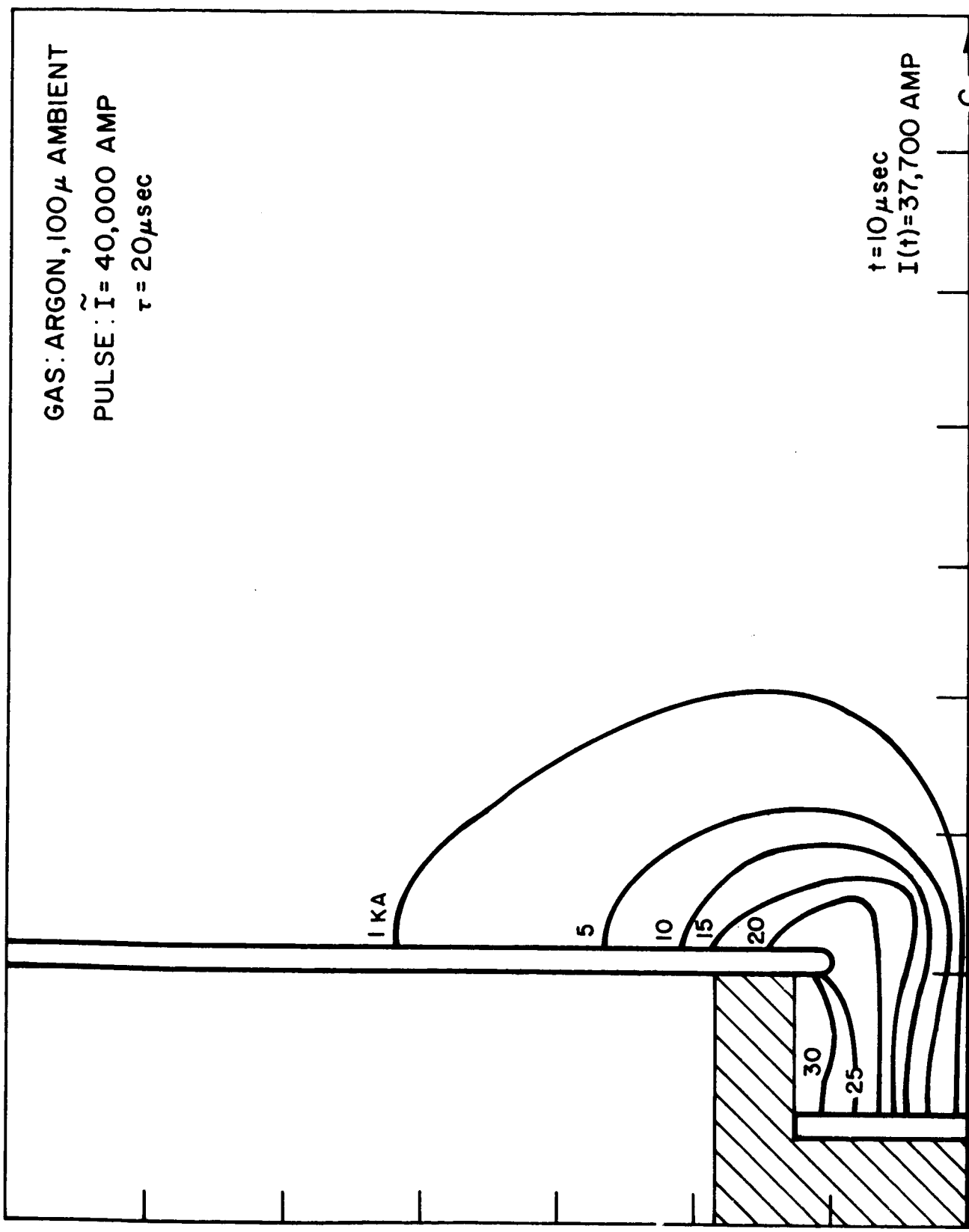

MAP OF ENCLOSED CURRENT

FIGURE 6e

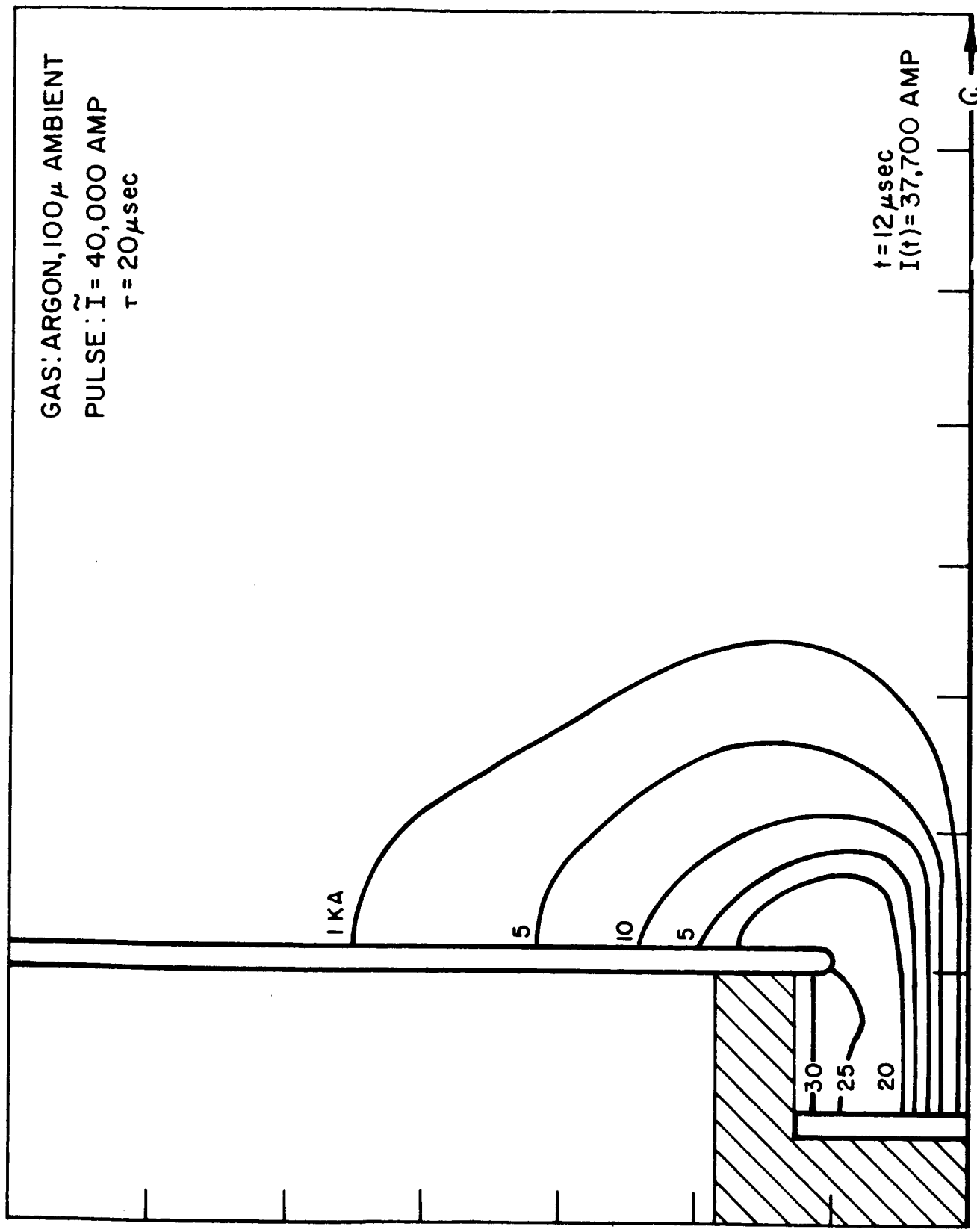

FIGURE 6f

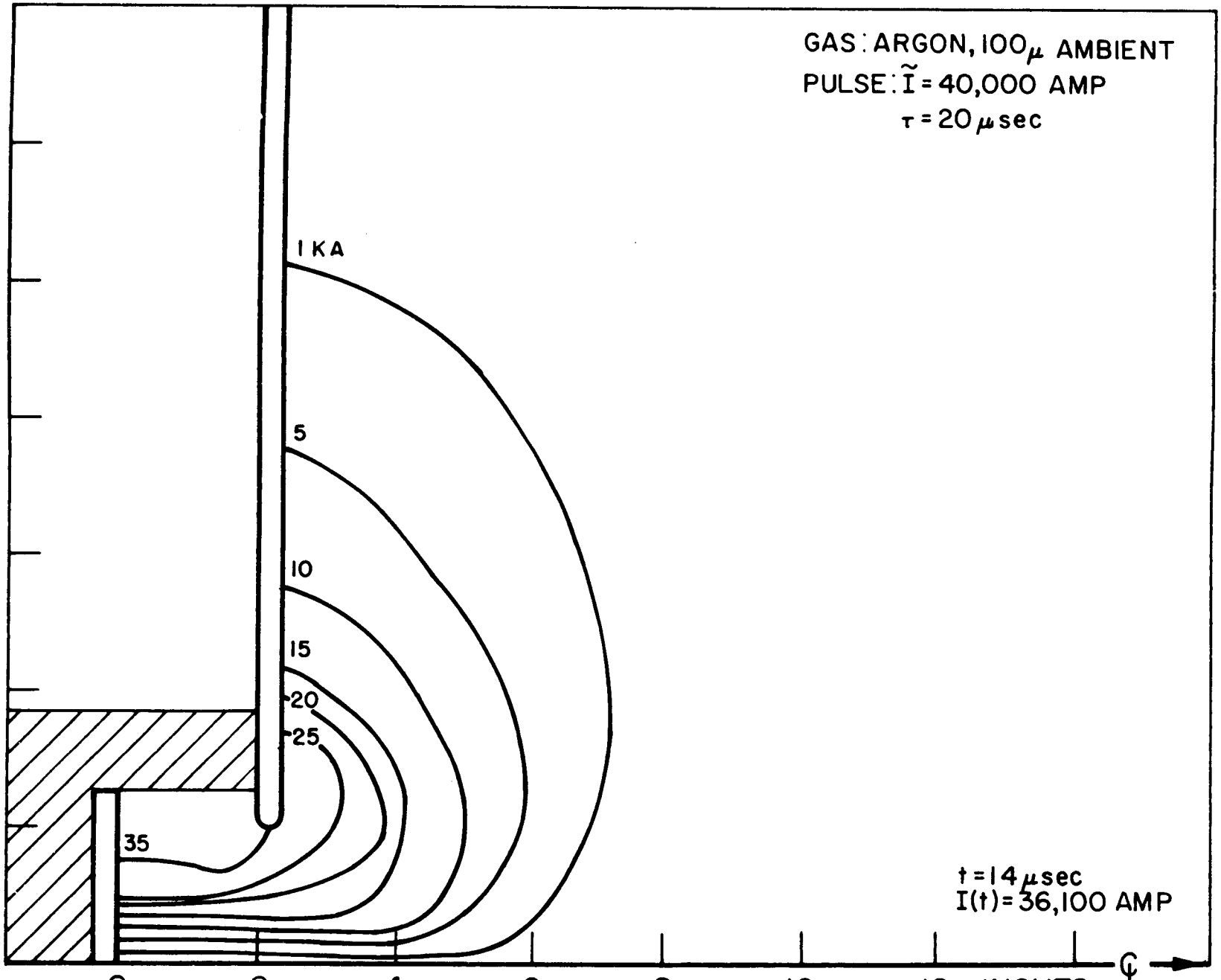

MAP OF ENCLOSED CURRENT

FIGURE 6g

AP-25-4221-67

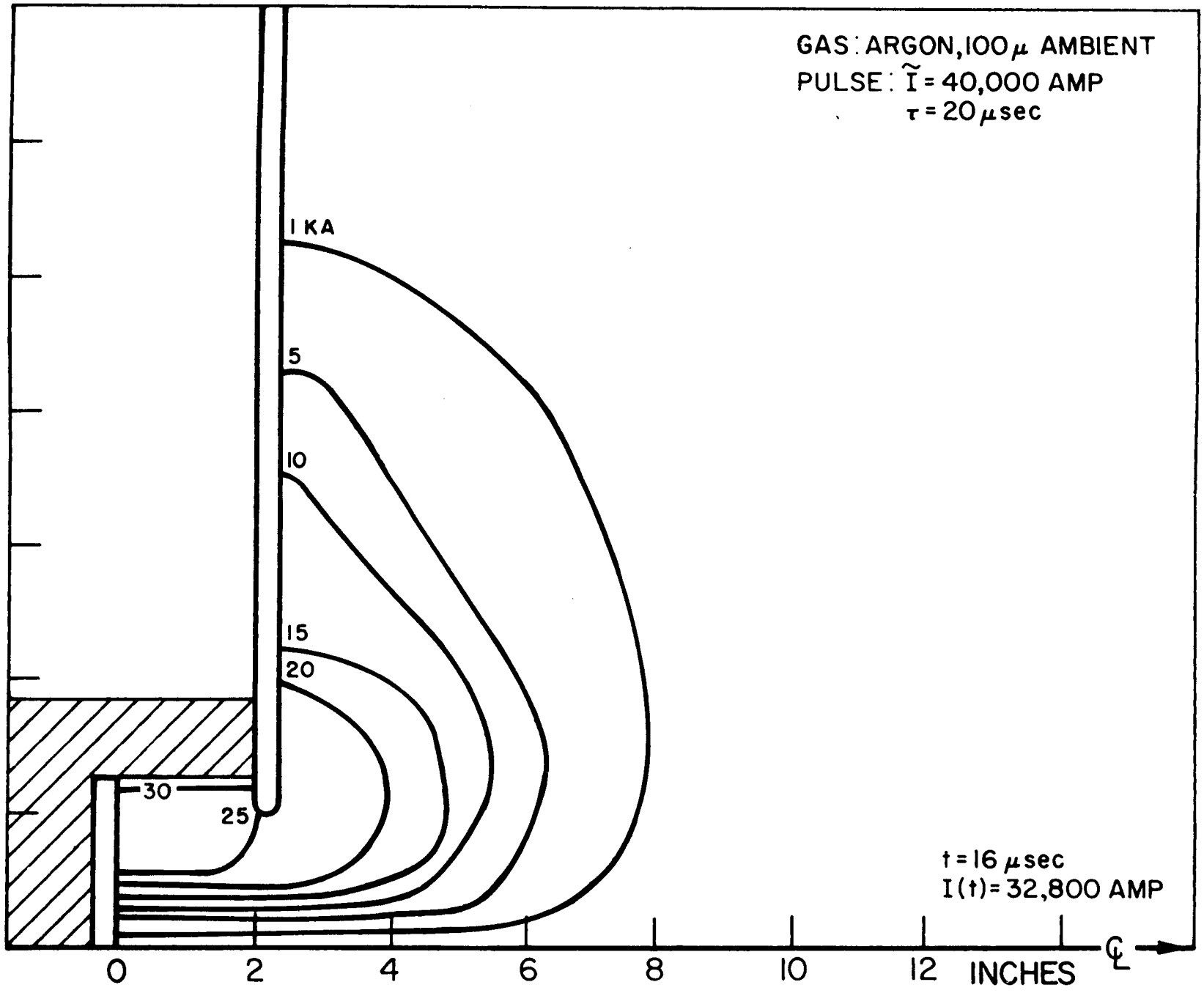

MAP OF ENCLOSED CURRENT

FIGURE 6h

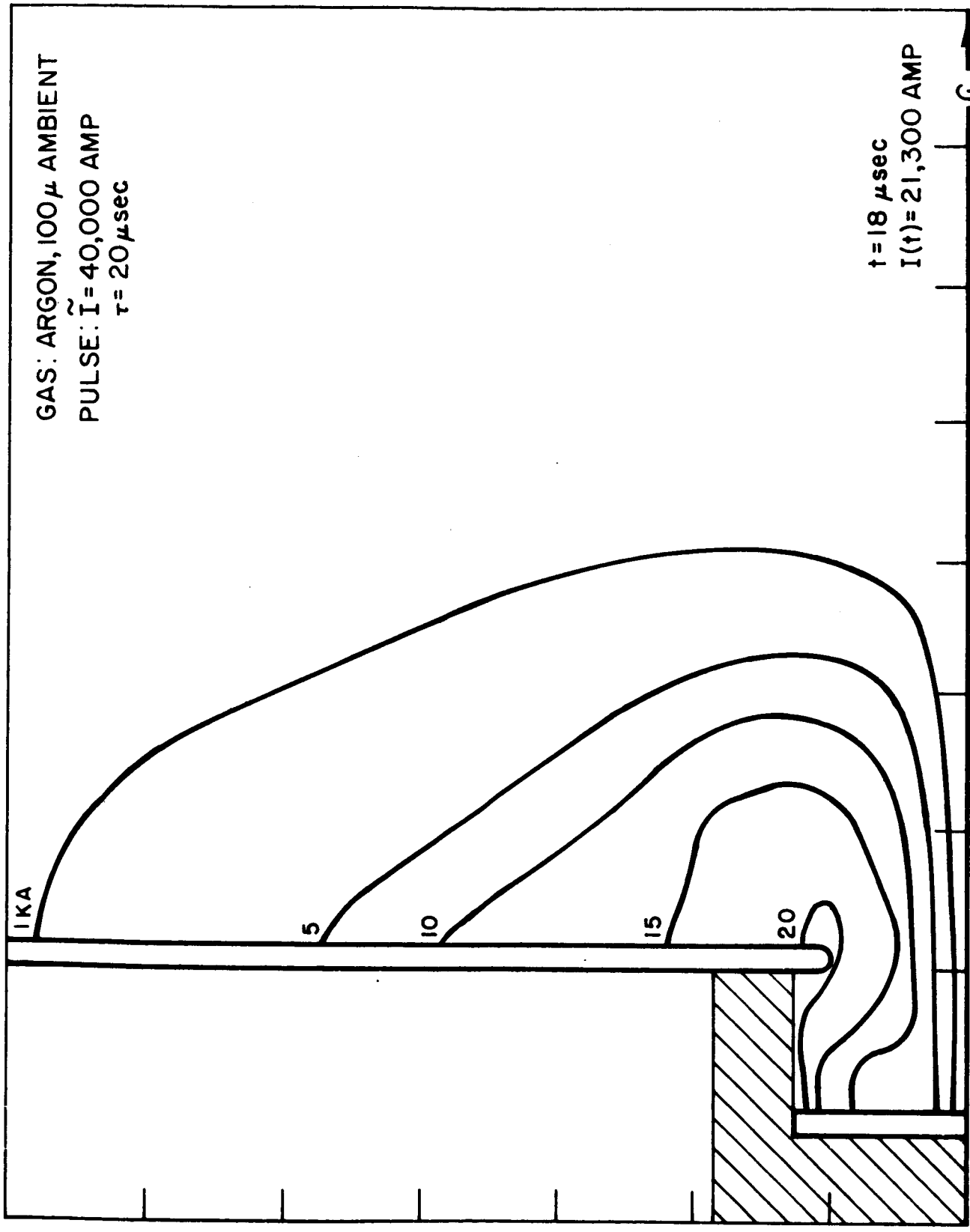

MAP OF ENCLOSED CURRENT

FIGURE 6i

AP25-4222-67

through 7g is found. Again, only about 60% of the current participates in the pinch and then exhausts. As in the first case, radial stabilization occurs, now at about 40 μsec. Unlike the first case, however, axial stabilization also occurs after about 40 μsec. Thereafter the entire pattern remains essentially steady for the remaining 30 μsec of the pulse.

In the low back pressure cases, .05 μ with shock tube injection, a qualitative difference is noticed in the exhaust process. Figs. 8a through 8i show the plume growth for the 140,000 amp - 20 μsec pulse. In comparing these results with those of the first case (same pulse, p_B = 100 μ) it is seen that approximately the same percentage of current participates in the pinch process. However, less current progresses out into the exhaust, and that which does continues to progress both radially and axially throughout the pulse. Part way through the pulse, the higher contours of enclosed current draw back inside the pinch chamber and in so doing break off a torus of enclosed current much like a smoke ring or starting vortex shed from an airfoil.

Meaningful data could not be obtained from the 40,000 amp, 20 μsec pulse with shock tube injection due to the irreproducibility of the data over this time interval. By extending the pulse at the same current level and back pressure from 20 μsec to 70 μsec, however, it was found that this irreproducibility ceased after 20 μsec. Figs. 9a through 9g show the plume development from 20 to 70 μsec. It is apparent that some degree of stabilization exists both radially and axially for times after 40 μsec. Compared to the high current-low back pressure case, the current here appears to be more evenly distributed than before. The results of these surveys are summarized in Table 2.

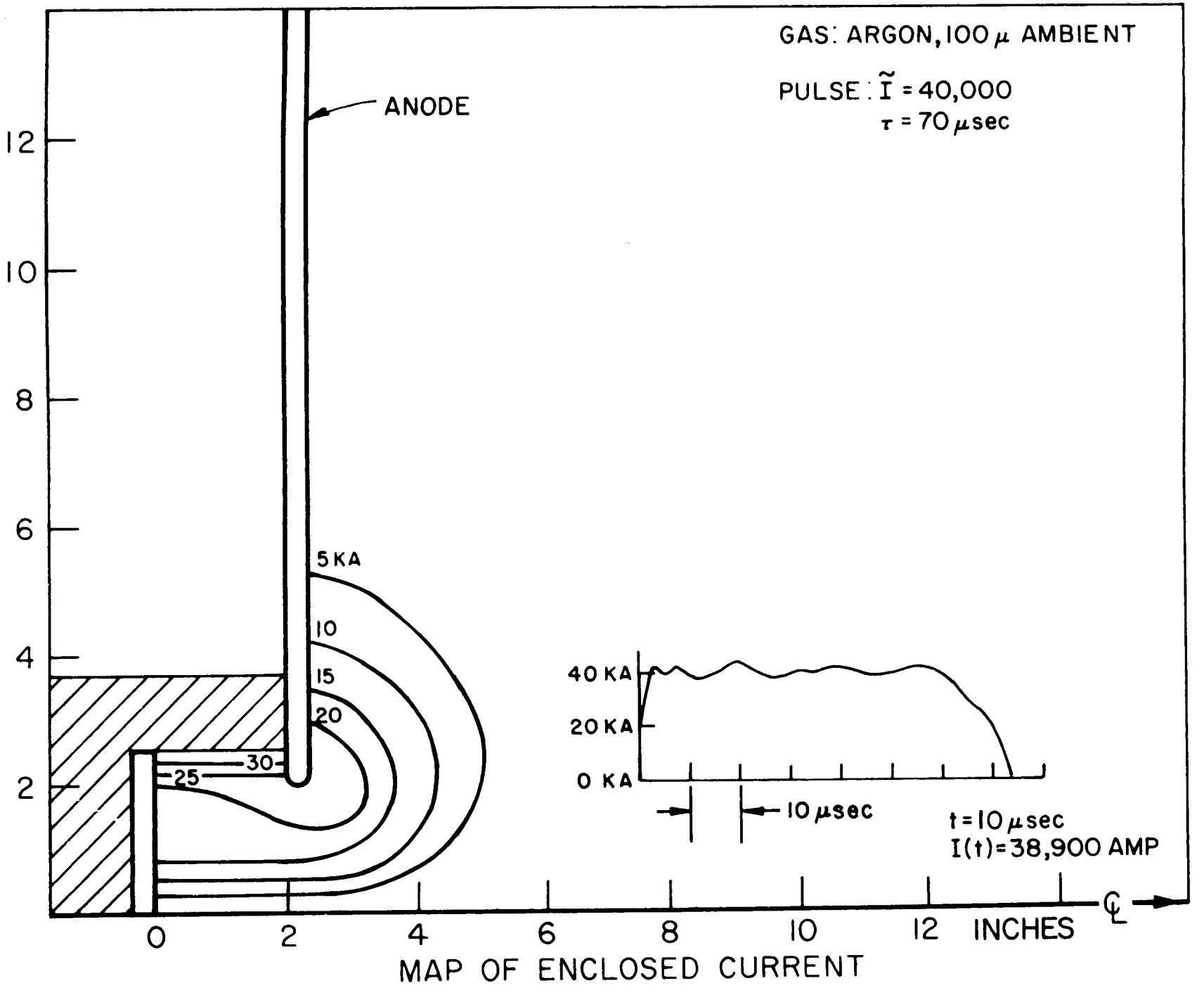
GAS: ARGON, 100 μ AMBIENT
PULSE: Ĩ = 40,000
τ = 70 μsec
ANODE
RAD, INCHES
12
10
8
6
4
2
5 KA
10
15
20
25
30
40 KA
20 KA
0 KA
10 μsec
t = 10 μsec
I(t) = 38,900 AMP
0
2
4
6
8
10
12 INCHES
℄
MAP OF ENCLOSED CURRENT

FIGURE 7a

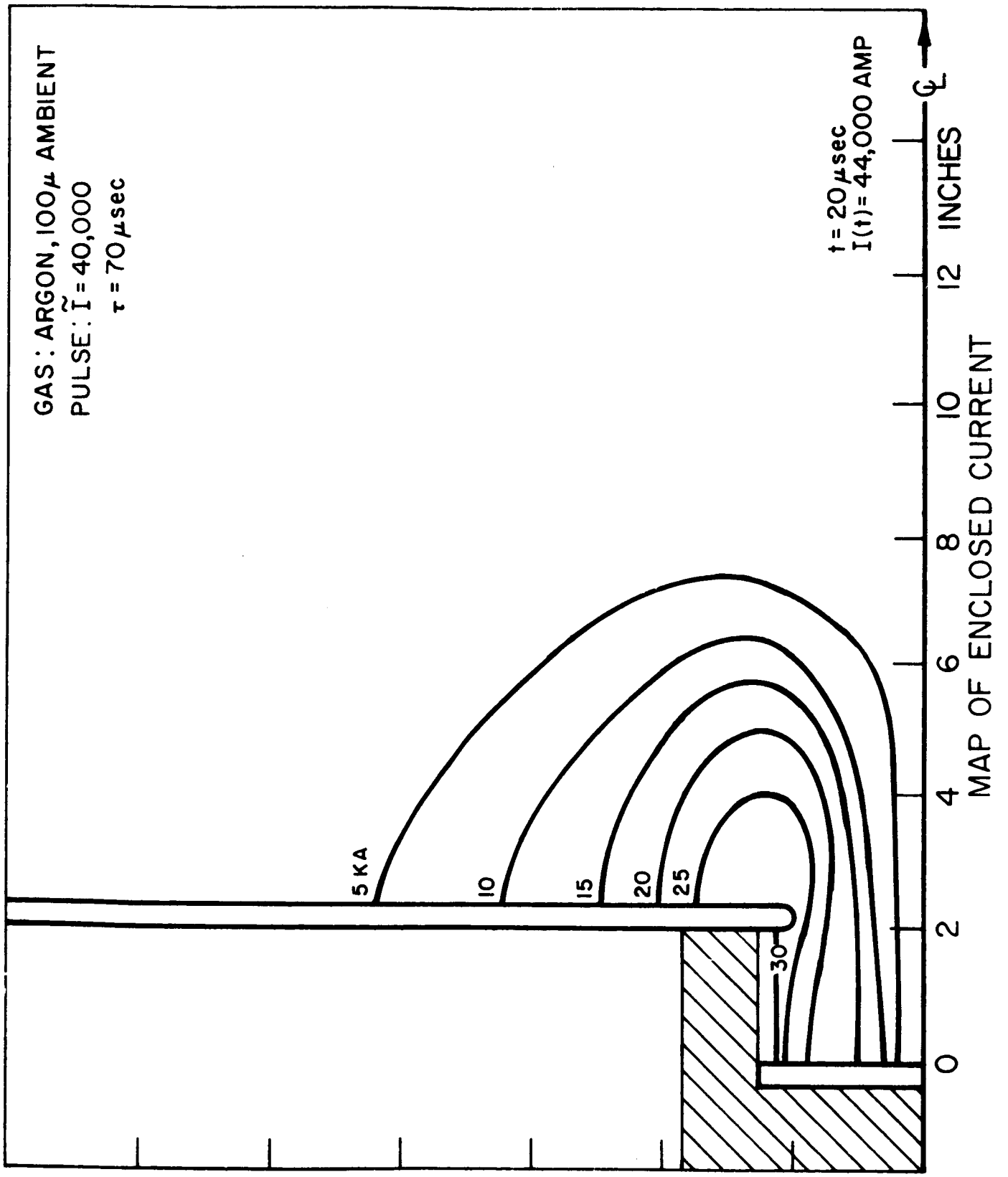

JPR-4231-67

FIGURE 7b

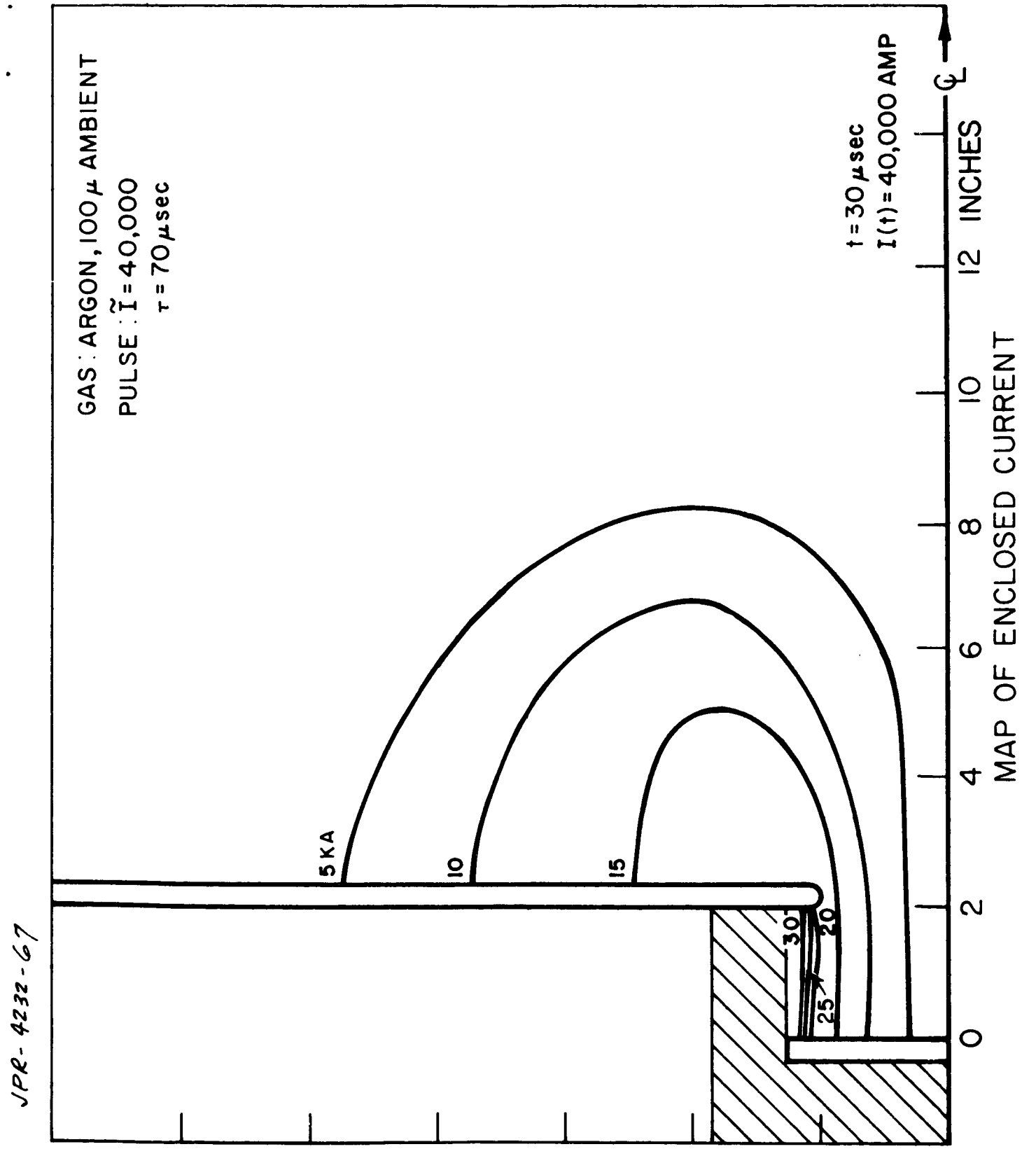
GAS: ARGON, 100 μ AMBIENT
PULSE: Ĩ = 40,000
τ = 70 μsec
t = 30 μsec
I(t) = 40,000 AMP
5 KA
10
15
20
25
30
0
2
4
6
8
10
12 INCHES
℄
MAP OF ENCLOSED CURRENT
JPR-4232-67

FIGURE 7c

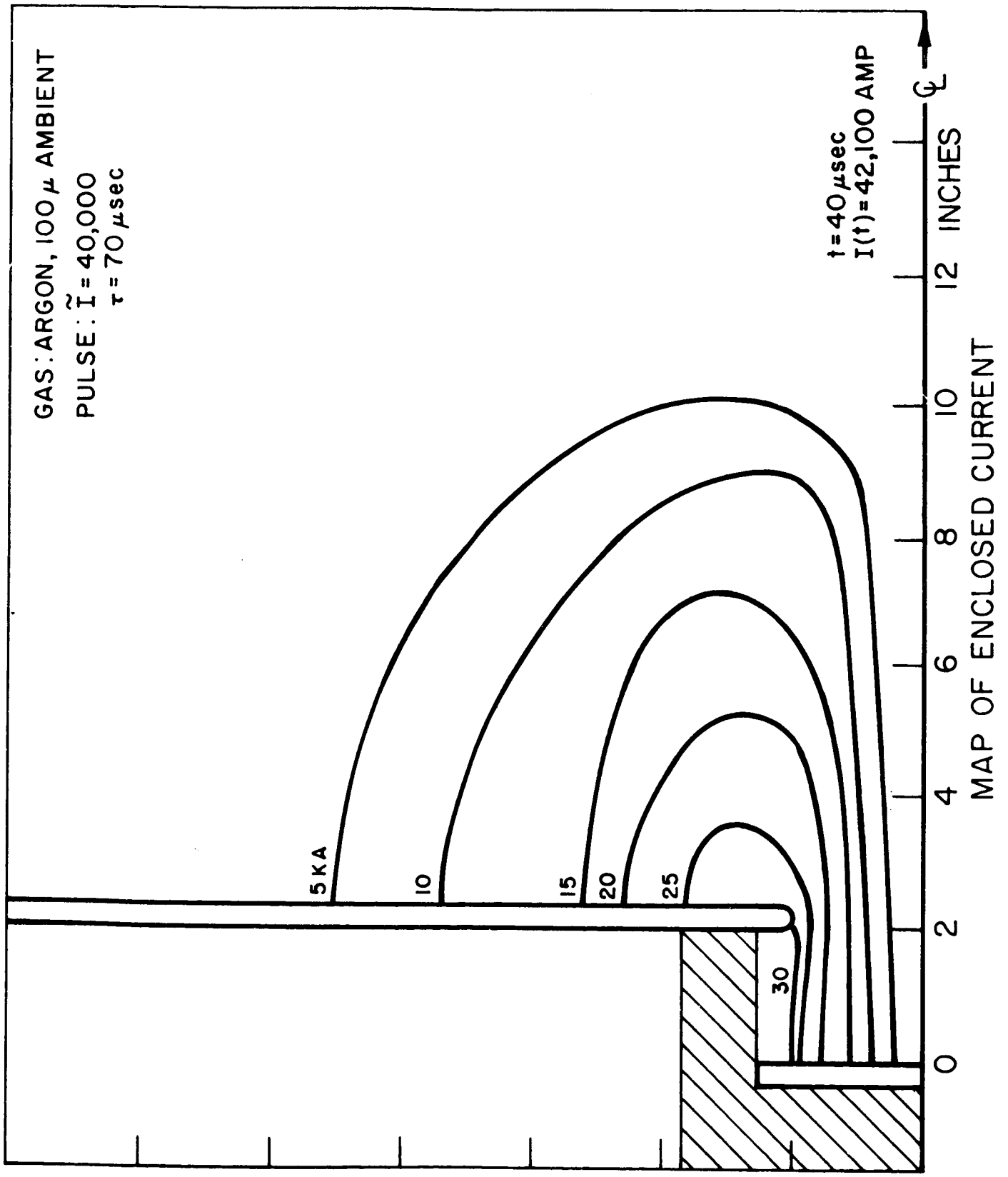

FIGURE 7d

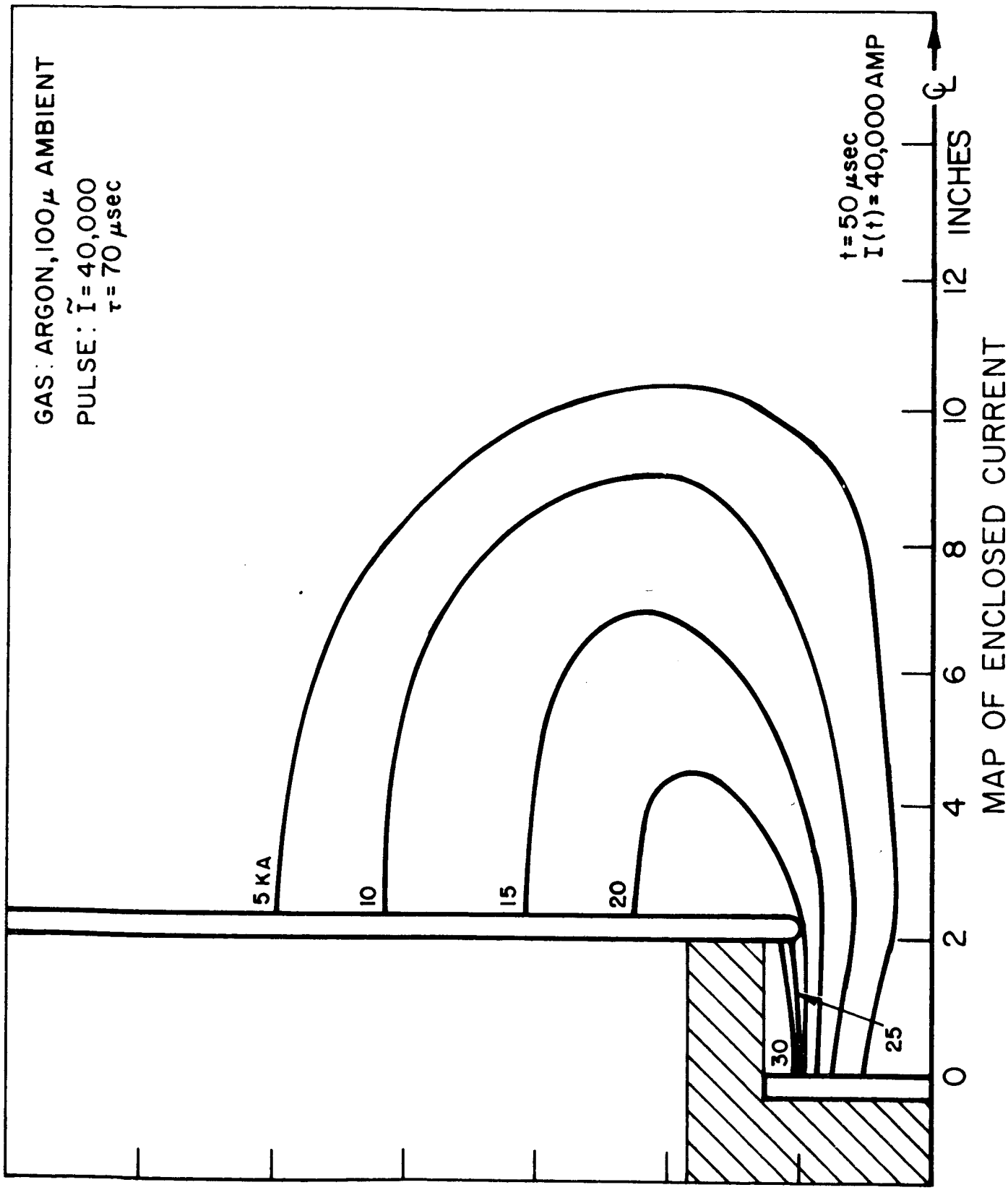

JPR-4234-67

FIGURE 7e

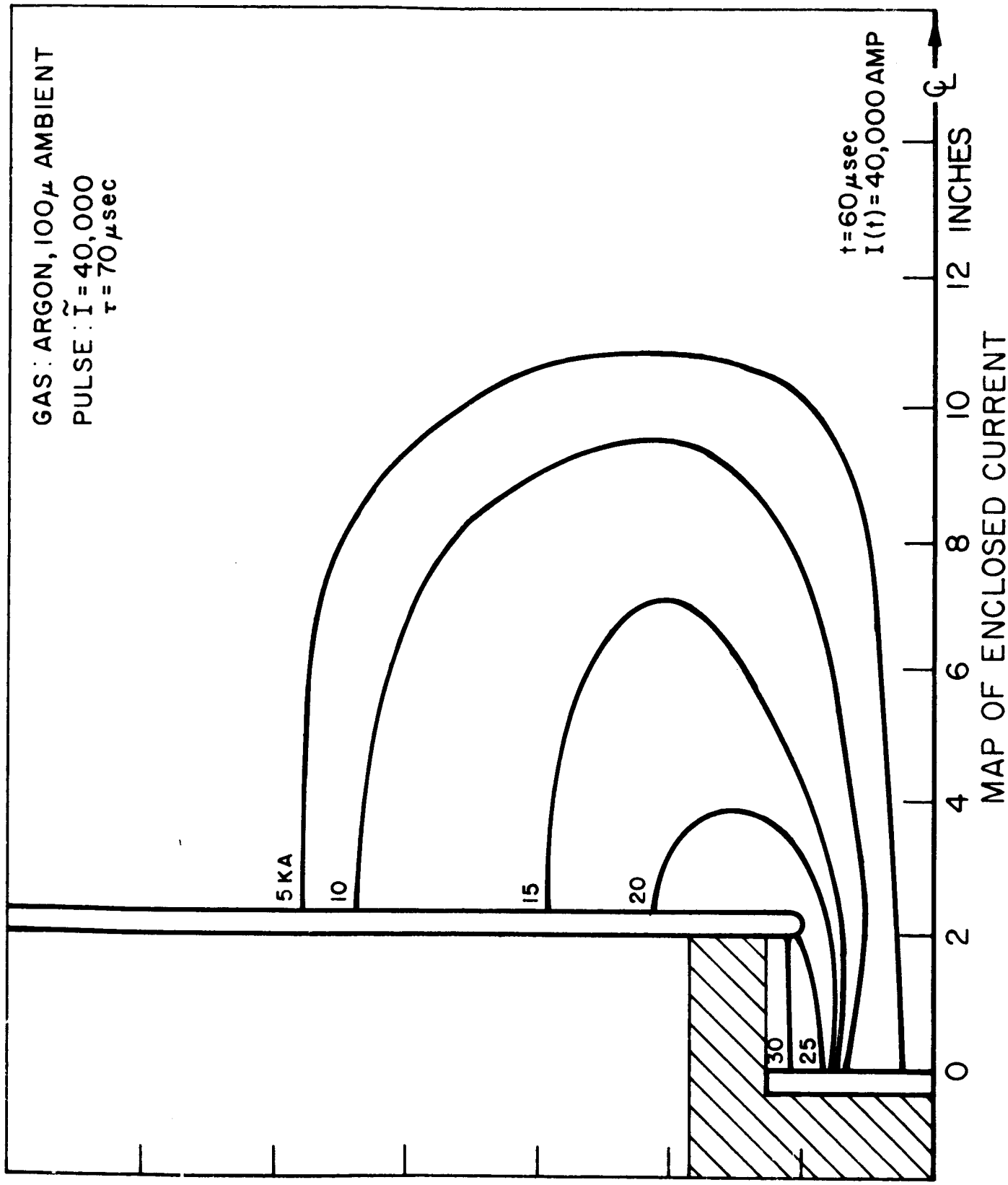

JPR-4235-67

FIGURE 7f

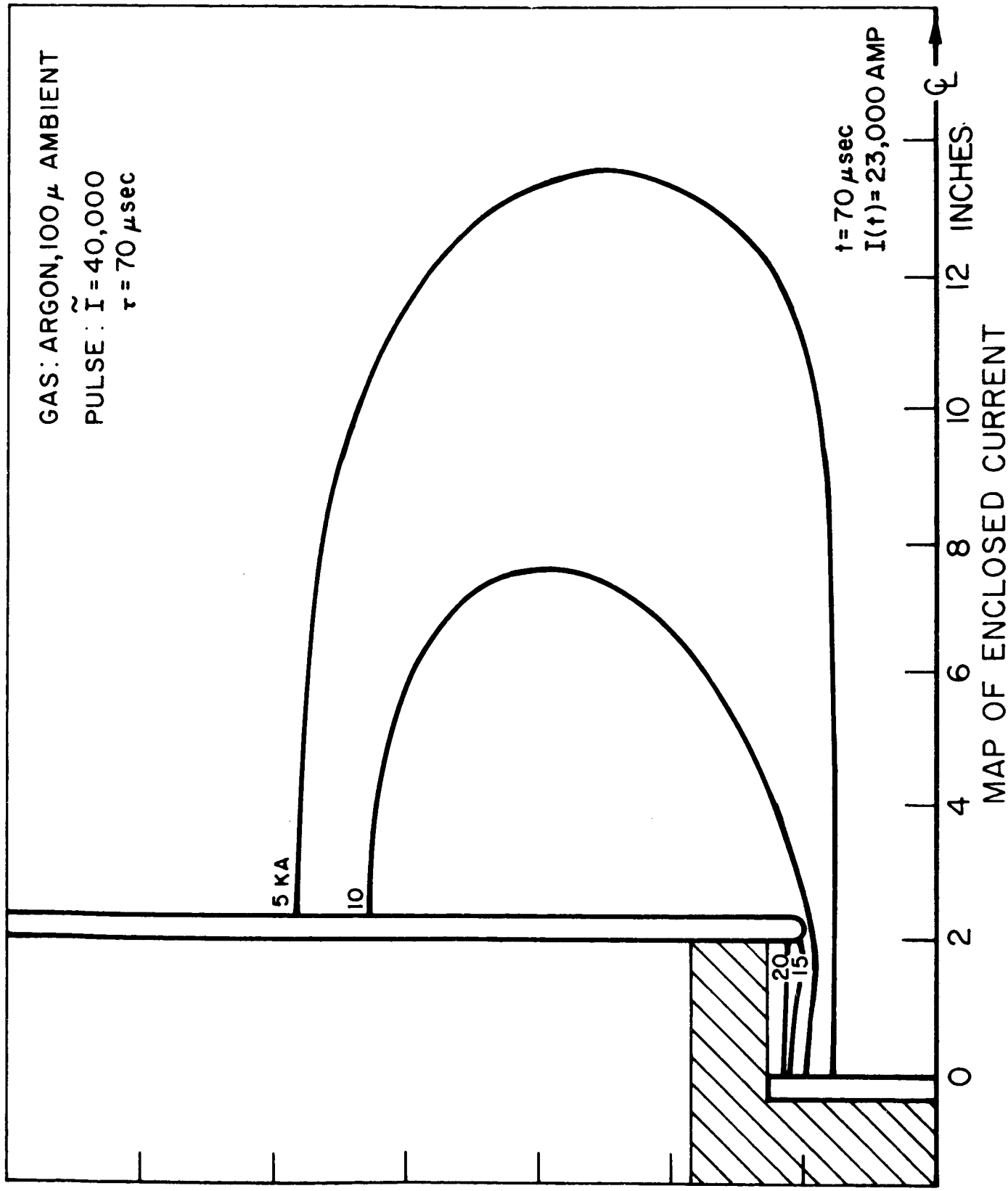

JPR. 9236-67

FIGURE 7g

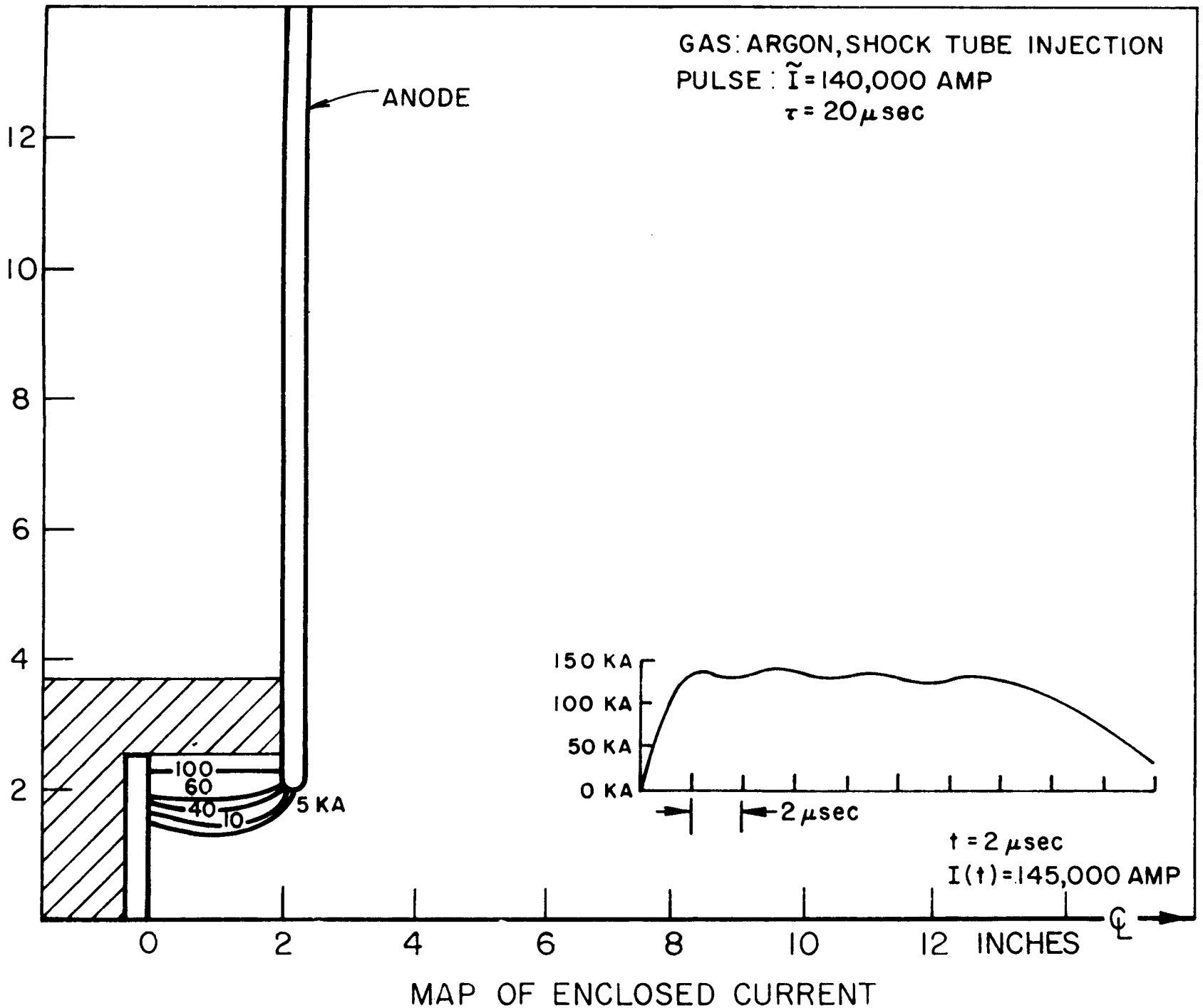
GAS: ARGON, SHOCK TUBE INJECTION
PULSE : Ĩ = 140,000 AMP
τ = 20 μsec
ANODE
RAD, INCHES
12
10
8
6
4
2
100
60
40
10
5 KA
150 KA
100 KA
50 KA
0 KA
2 μsec
t = 2 μsec
I(t) = 145,000 AMP
0
2
4
6
8
10
12 INCHES
℄
MAP OF ENCLOSED CURRENT

FIGURE 8a

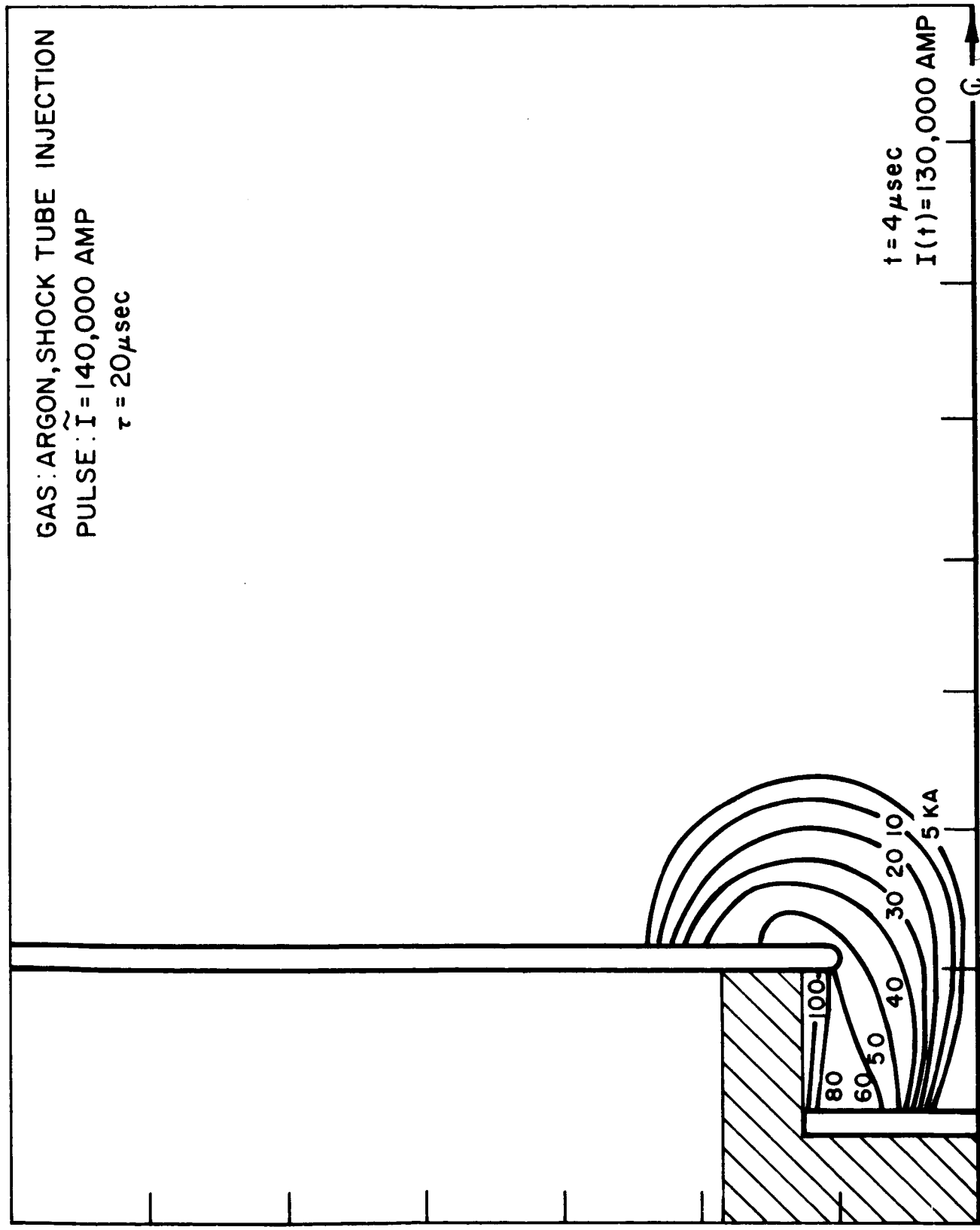

FIGURE 8b

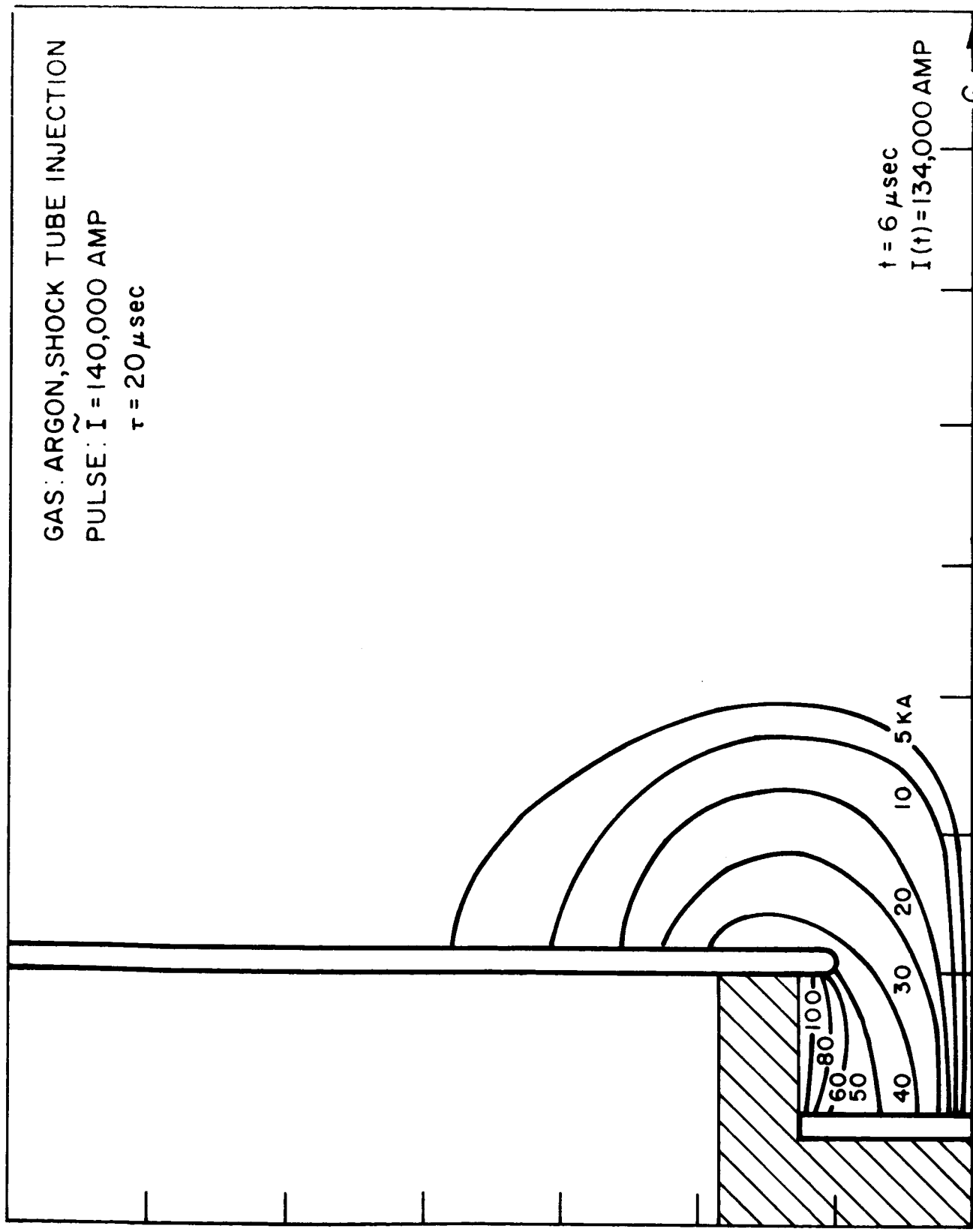

MAP OF ENCLOSED CURRENT

FIGURE 8c

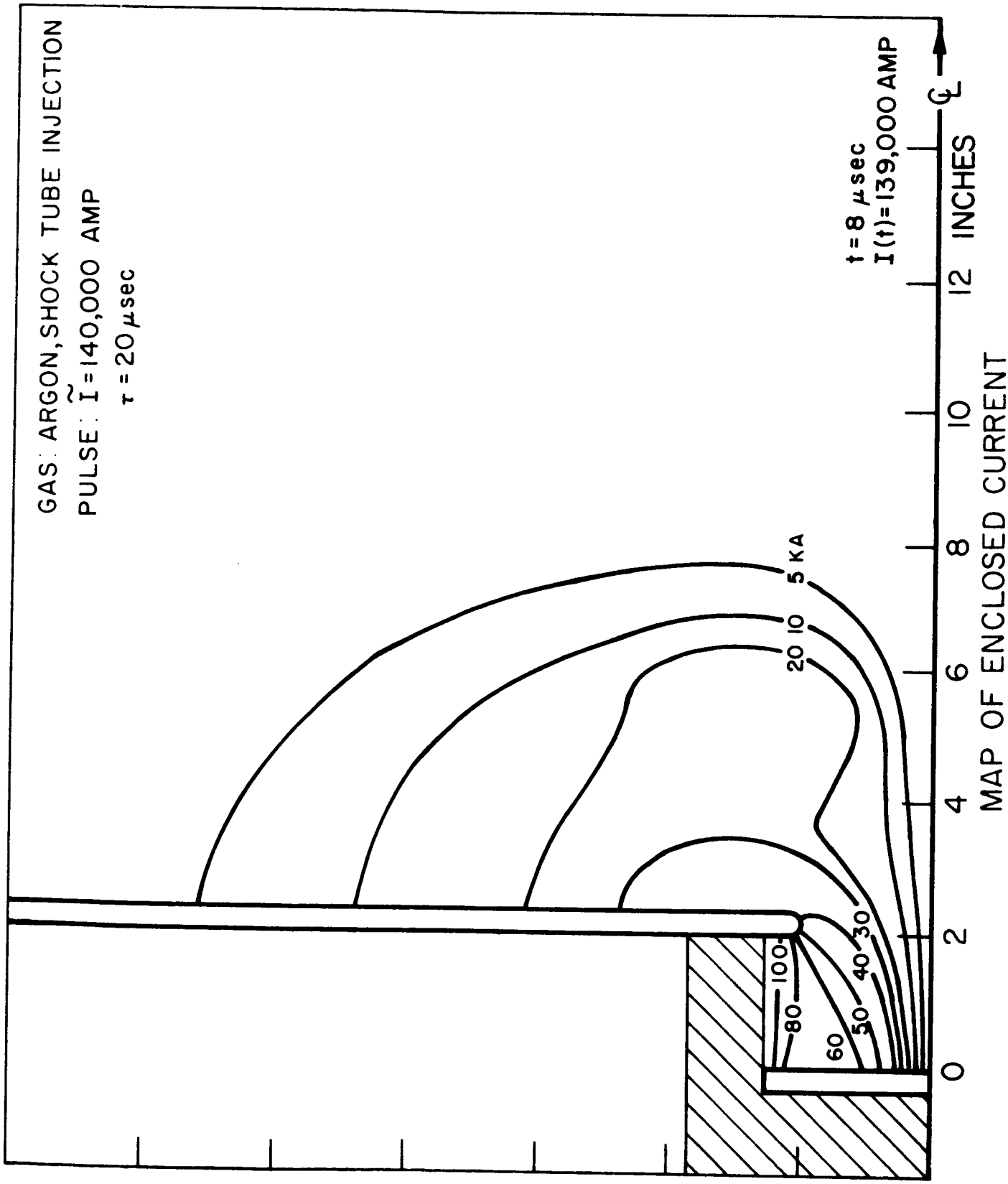

FIGURE 8d

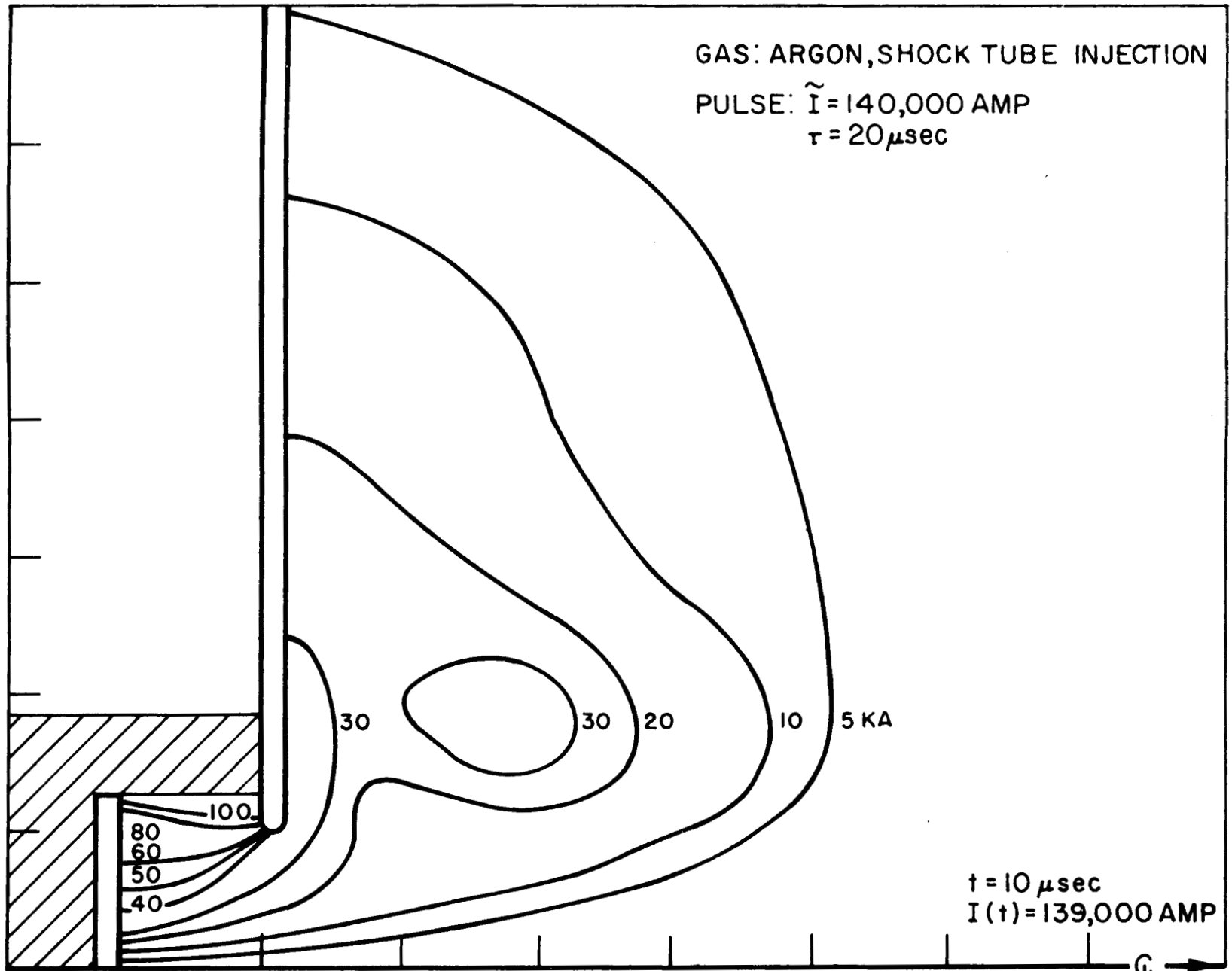

MAP OF ENCLOSED CURRENT

FIGURE 8e

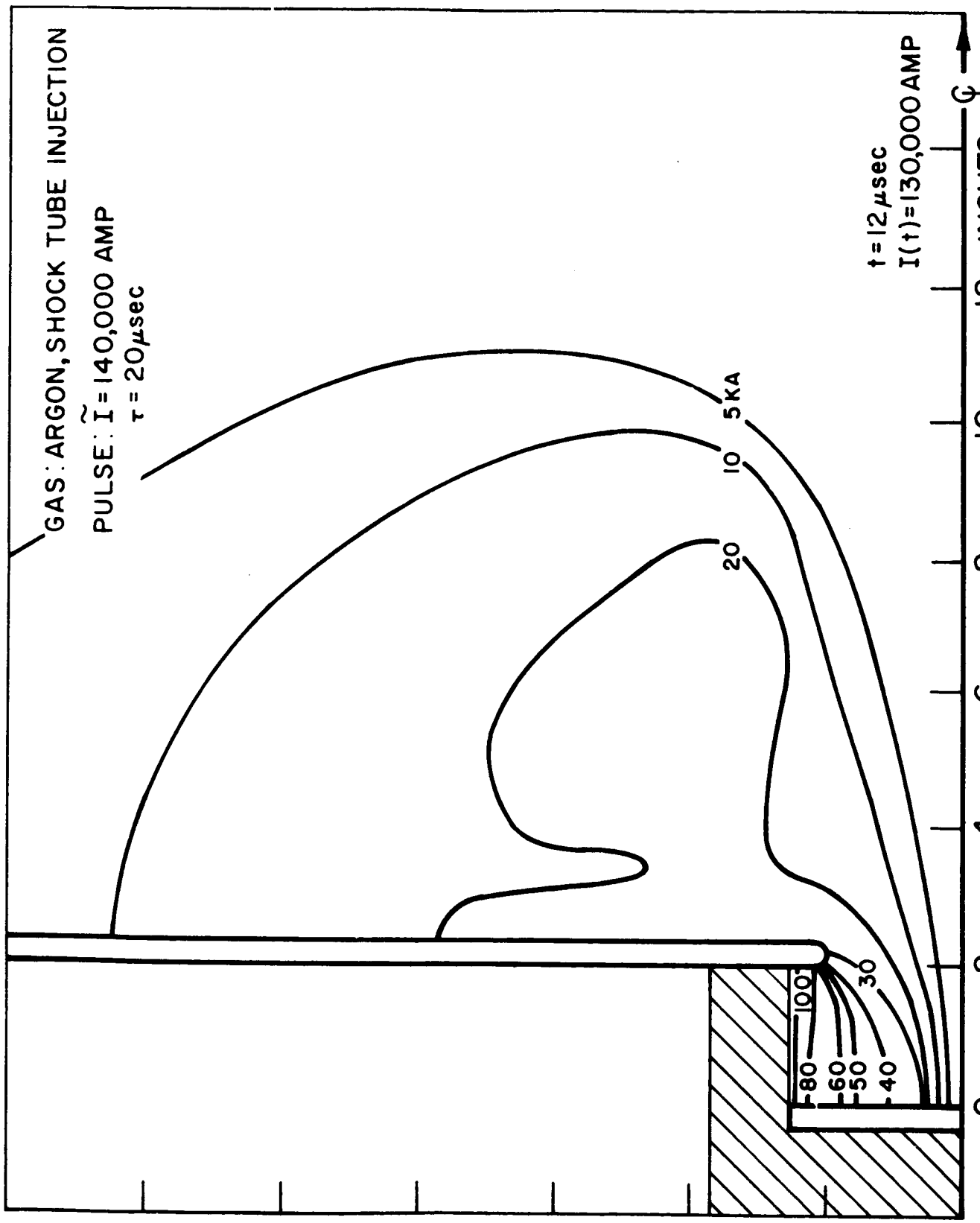

MAP OF ENCLOSED CURRENT

FIGURE 8f

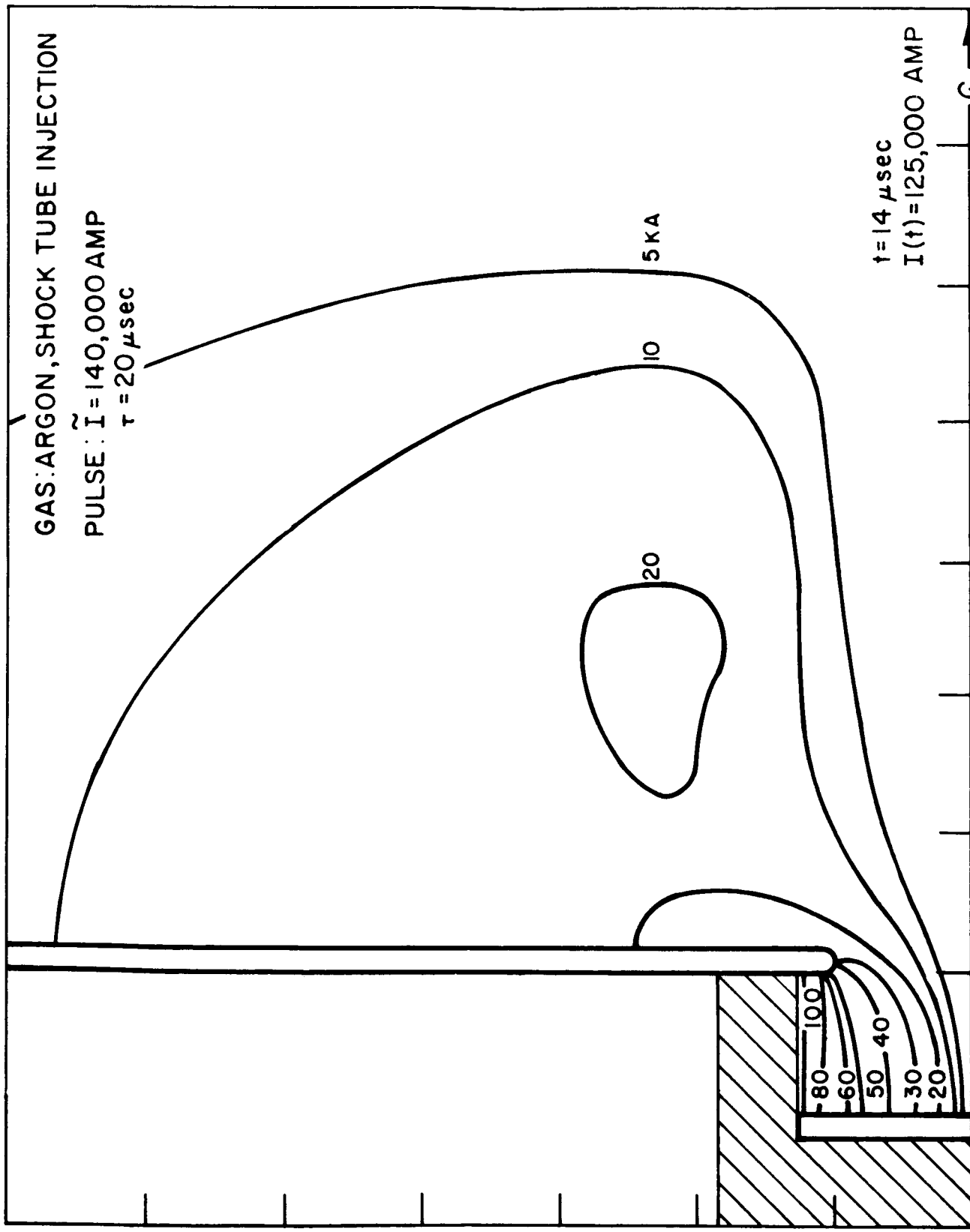

MAP OF ENCLOSED CURRENT

FIGURE 8g

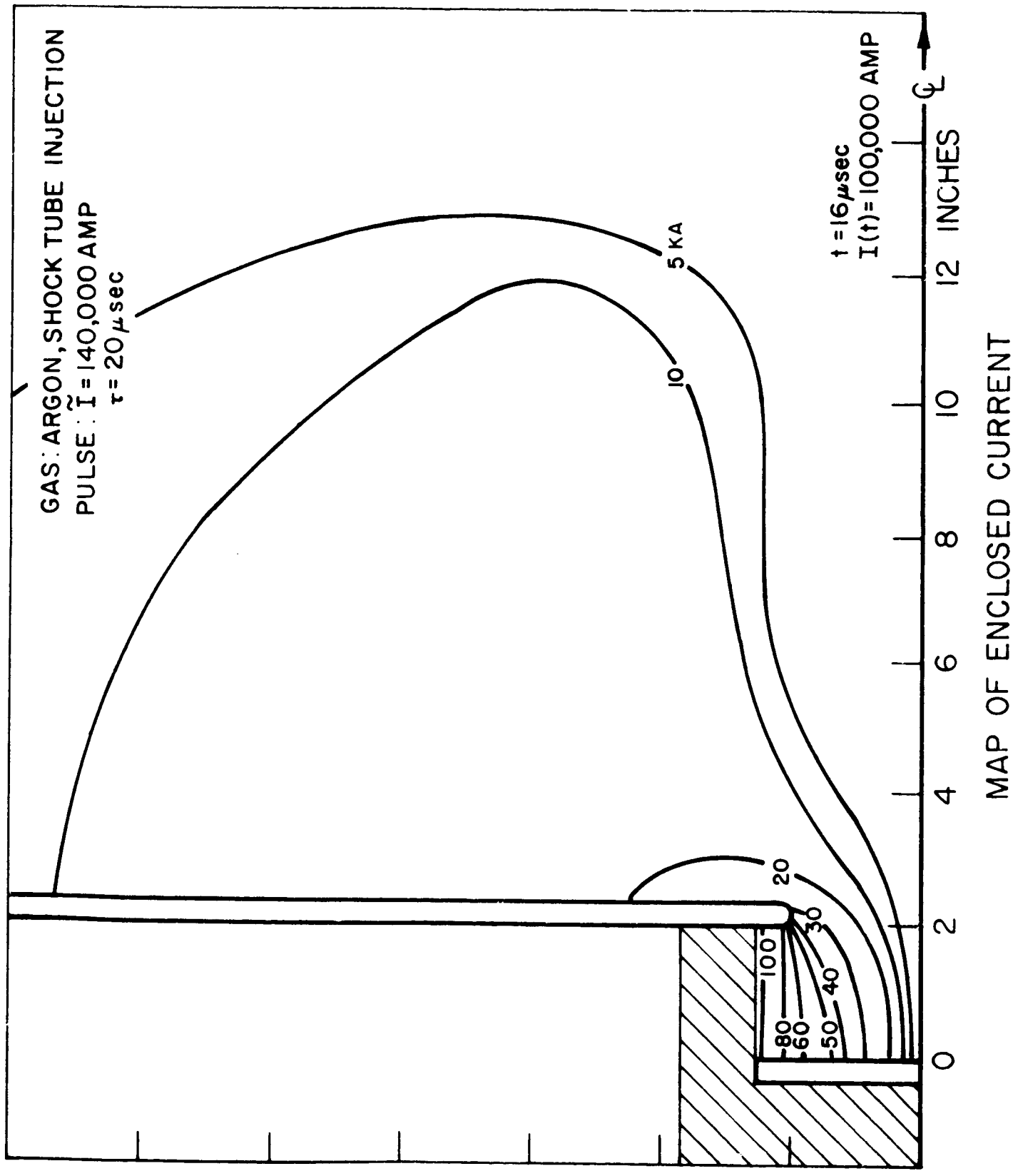
GAS: ARGON, SHOCK TUBE INJECTION
PULSE: $\tilde{I}$ = 140,000 AMP
τ = 20 μsec
t = 16 μsec
I(t) = 100,000 AMP
5 KA
10
20
30
40
50
60
80
100
0
2
4
6
8
10
12 INCHES
℄
MAP OF ENCLOSED CURRENT

FIGURE 8h

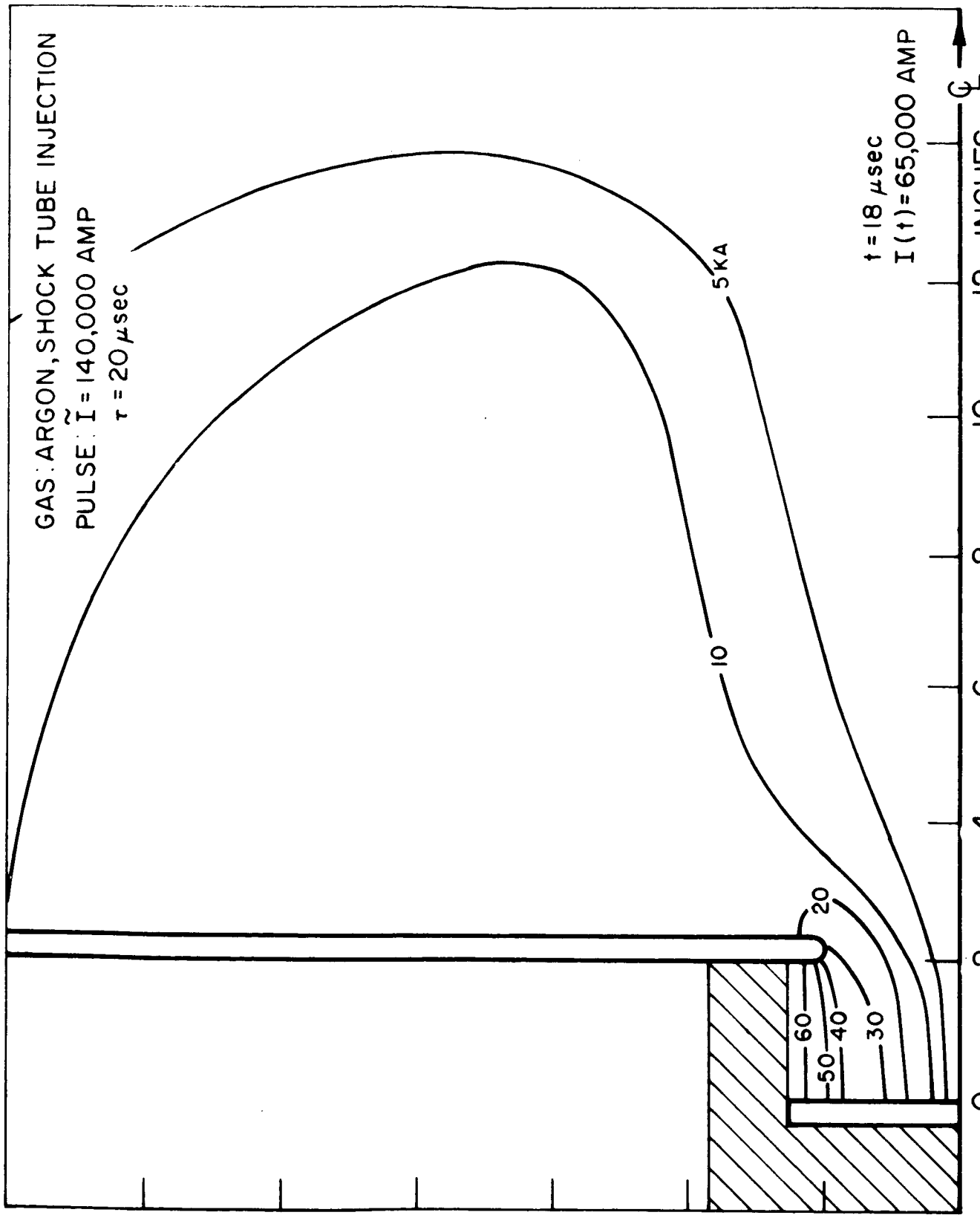

MAP OF ENCLOSED CURRENT

FIGURE 8i

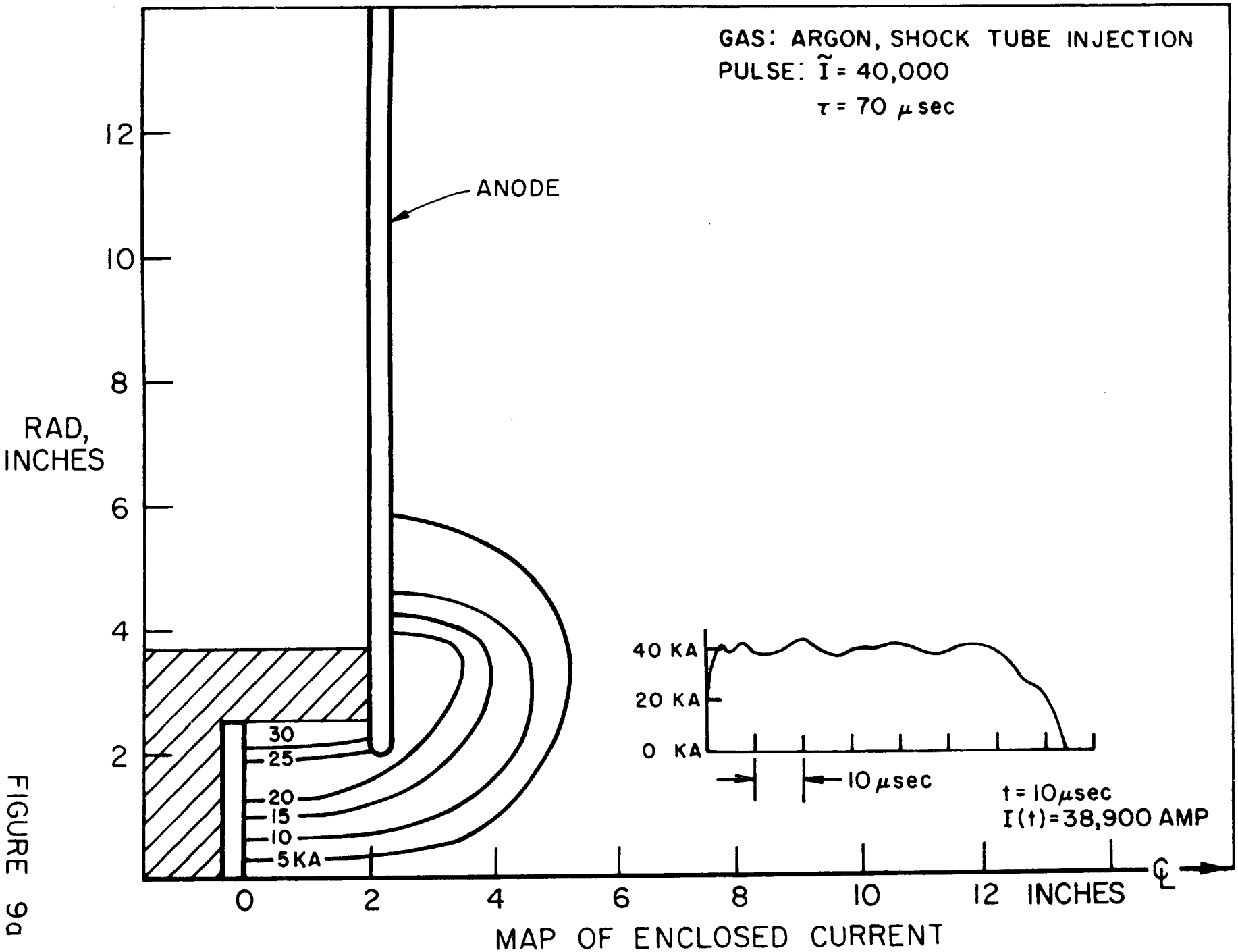

MAP OF ENCLOSED CURRENT

FIGURE 9a

AP 25-4224-67

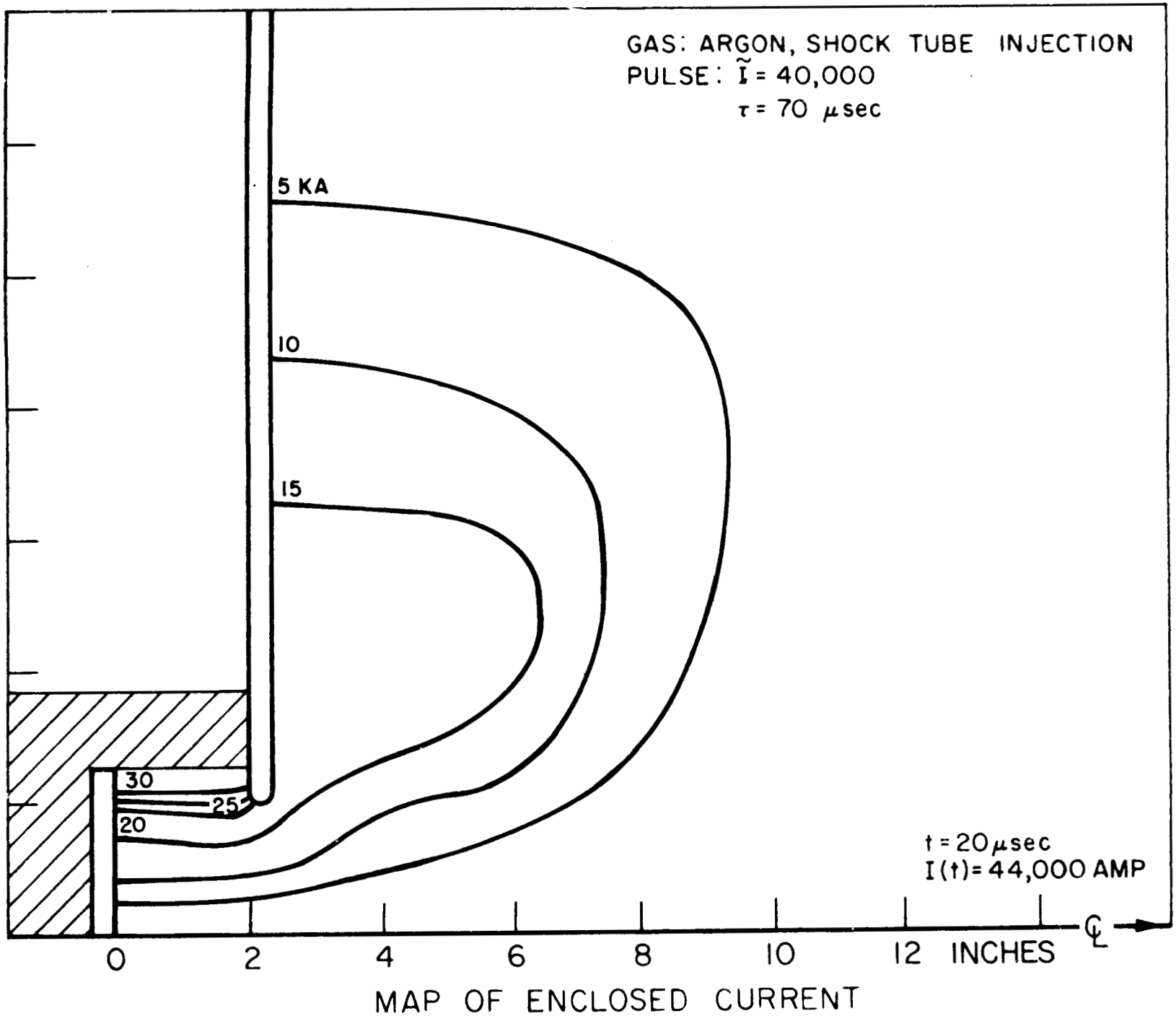

MAP OF ENCLOSED CURRENT

FIGURE 9b

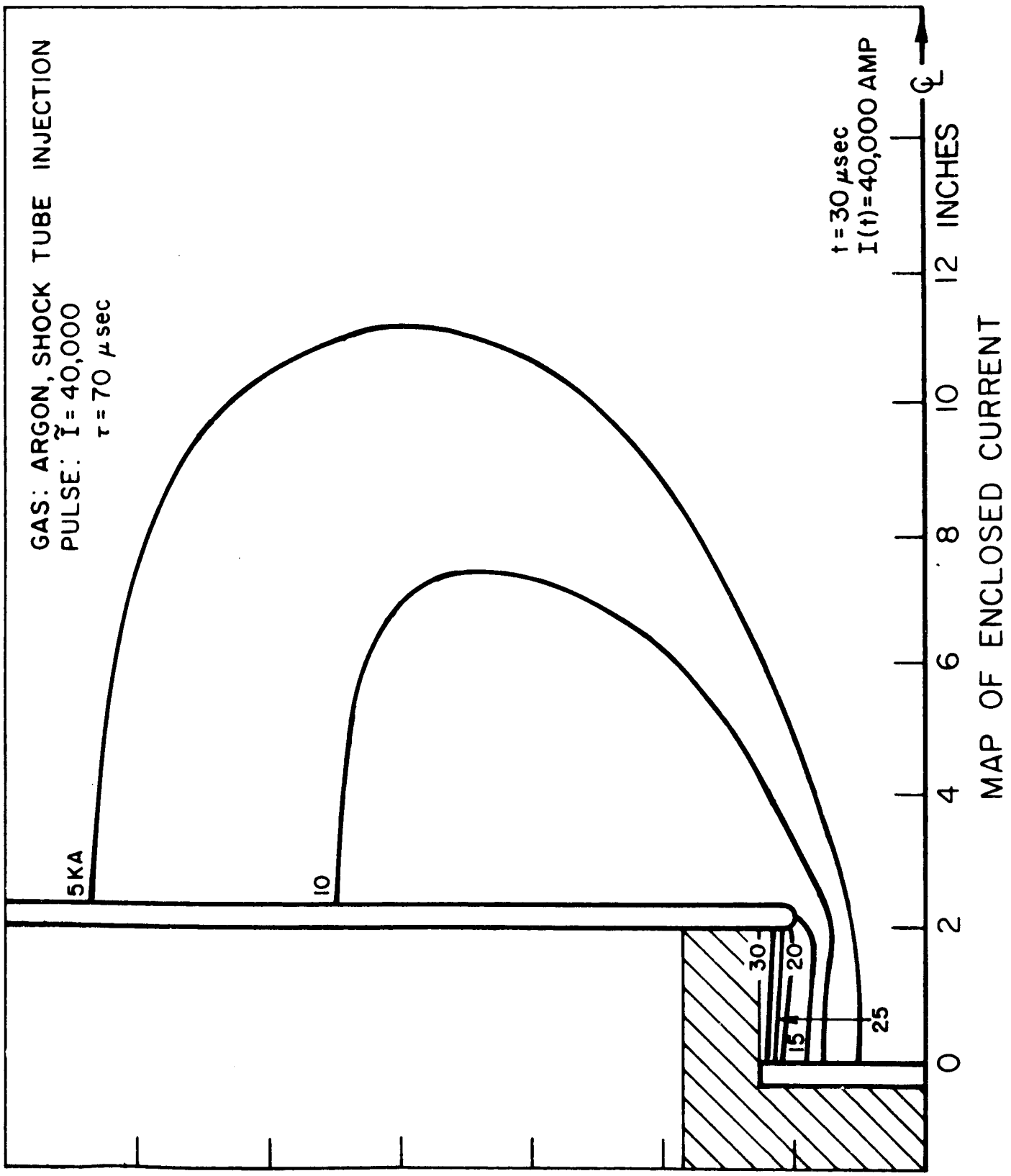

FIGURE 9c

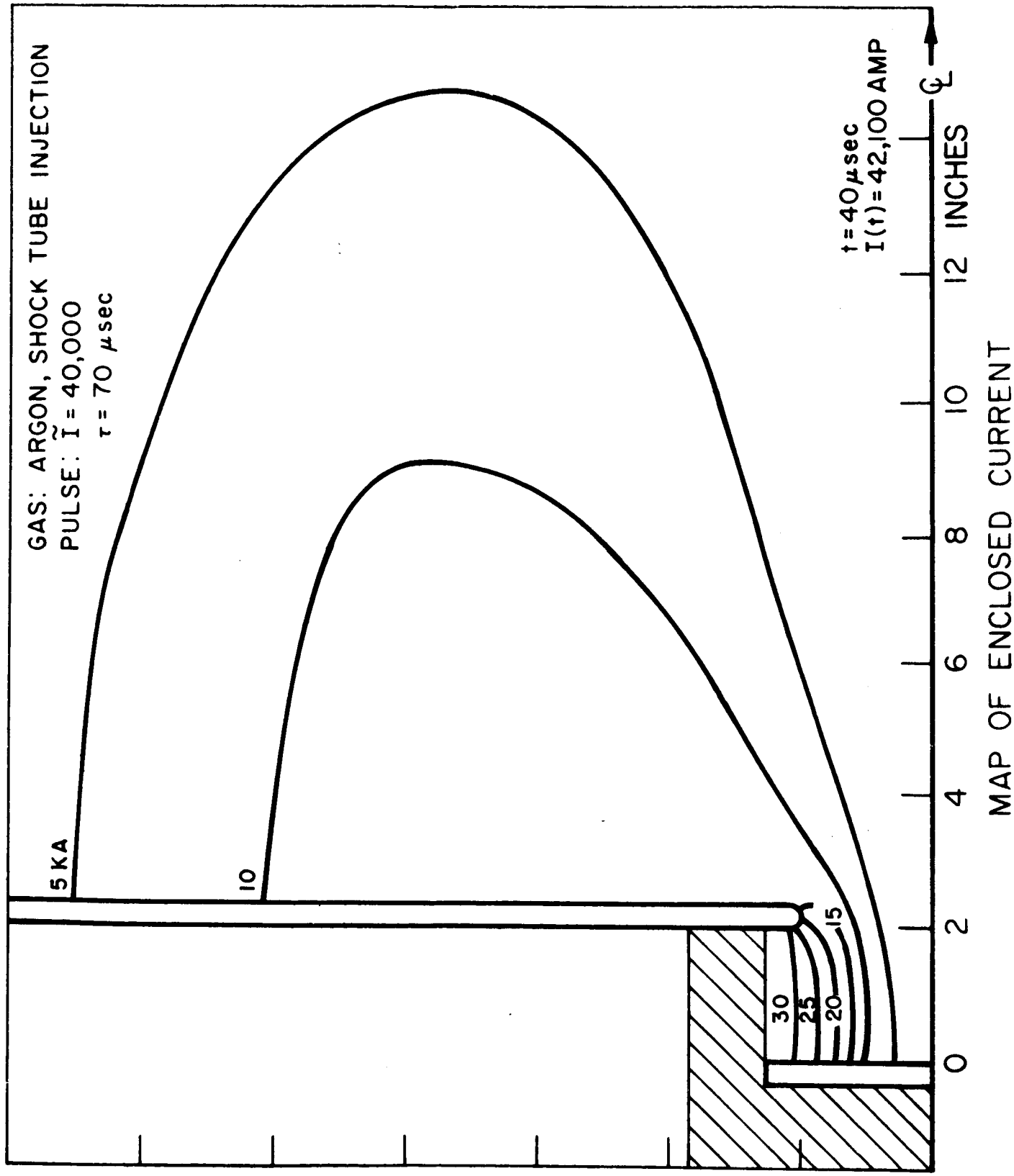

FIGURE 9d

AP25-4226-67

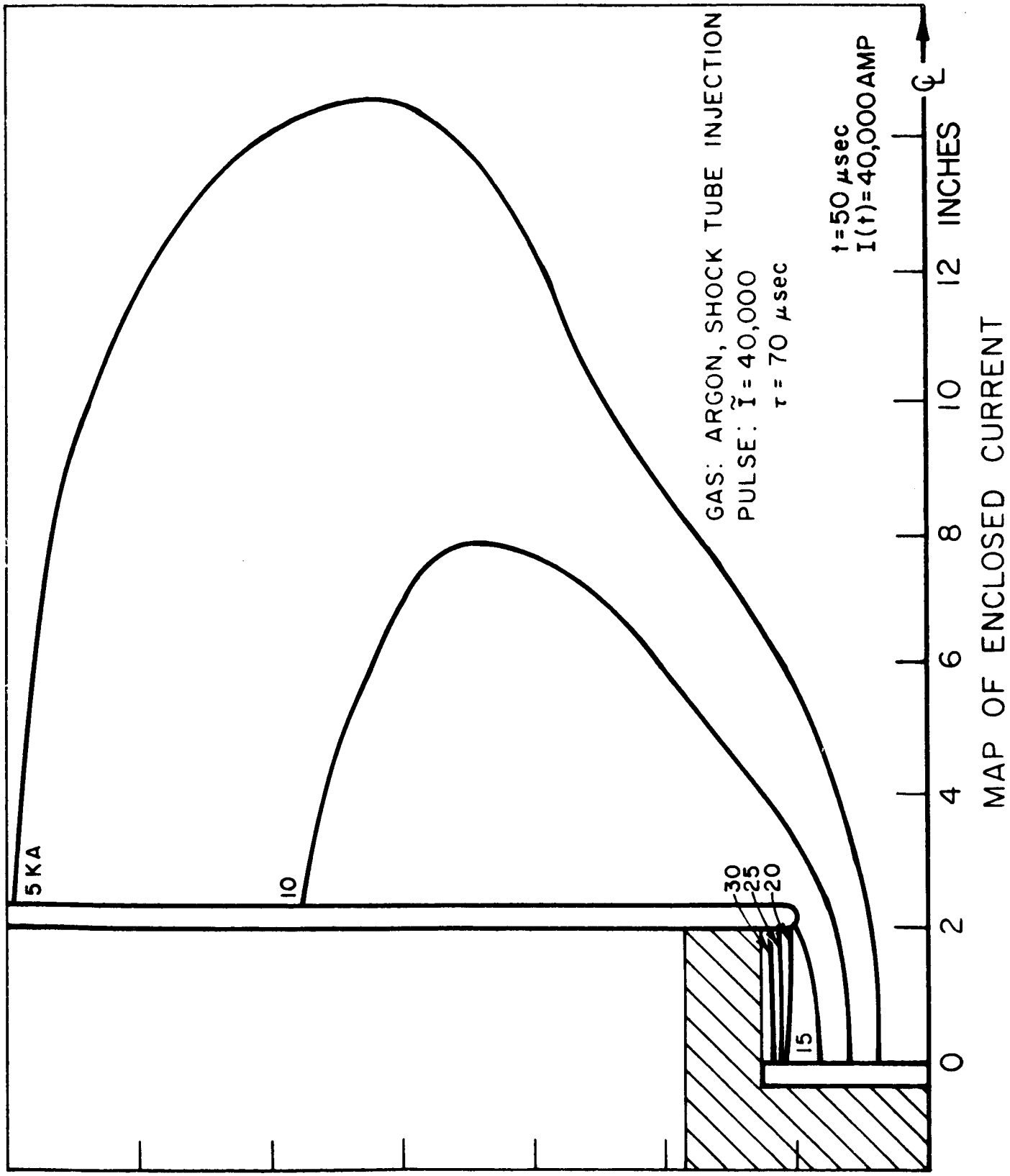

FIGURE 9e

AP25-4227-67

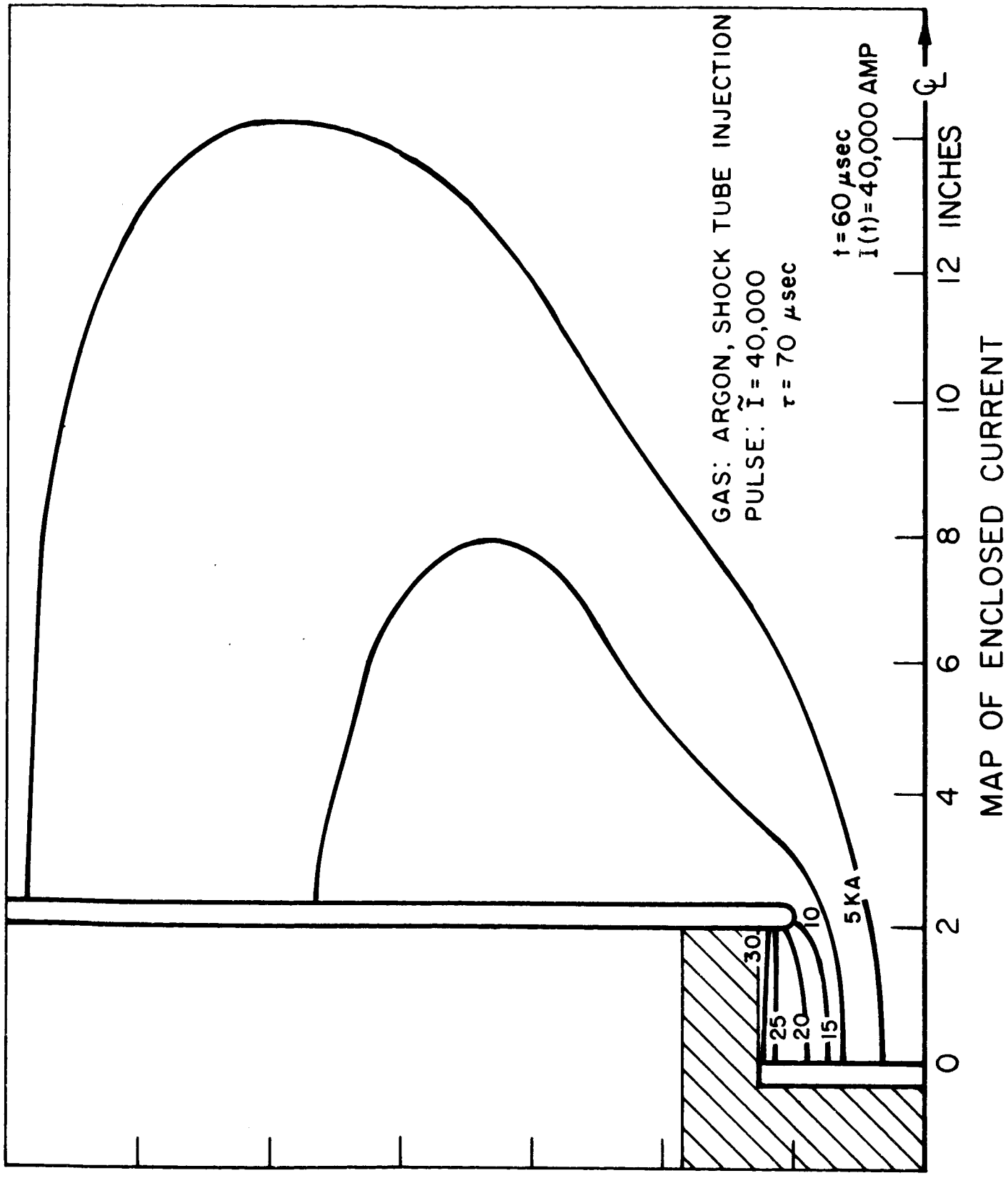

FIGURE 9f

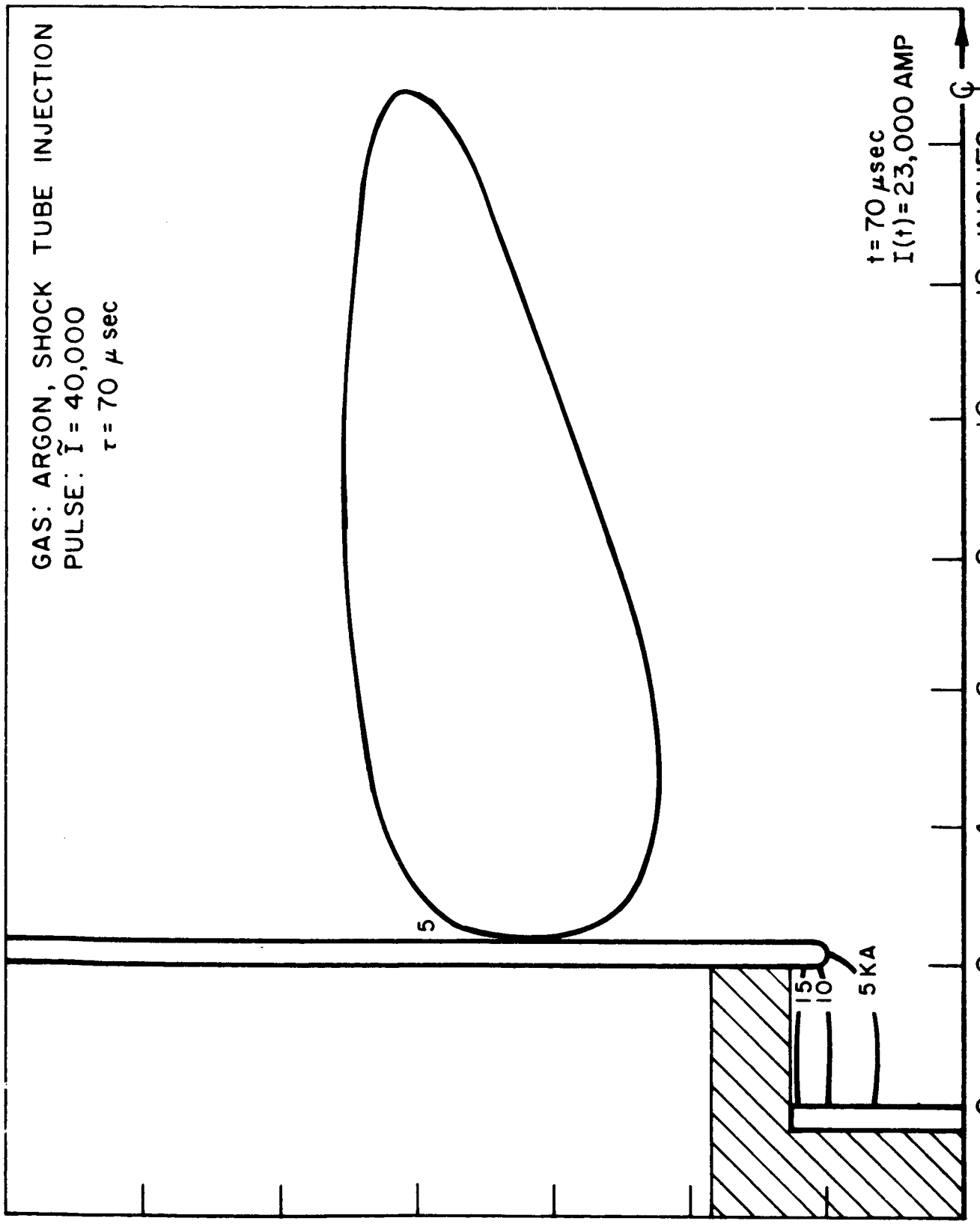

FIGURE 9g

Table 2

Back Pressure	$\tilde{I}$	τ	% $\tilde{I}$ Pinched	% $\tilde{I}$ in Exhaust	Stabilization
100 μ	140,000	20	~ 30	~ 30	Radial, t > 8 μsec
	40,000	20	~ 60	~ 60	None
	40,000	70	~ 60	~ 60	Radial and Axial t > 40 μsec
0.05 μ	140,000	20	~ 30	~ 30 (initially)	None
	40,000	20	Irreproducible data		
	40,000	70	Pinch in irreproducible portion		Radial and Axial t > 40 μsec

The failure of large fractions of the discharge current to participate in the pinch process is somewhat in contradiction with our previous experience with closed chamber discharges at higher current levels. To pursue this point a bit, the interior of the chamber was probed, and current density plots as a function of radius at various axial positions were constructed for times of 1, 2, 3 μsec, and compared with those observed in a closed chamber. These results are shown in Figs. 10, 11, 12. Comparing the two cases, one is able to say that a sheet is formed in each case and that both propagate in to pinch at roughly the same rate. Other than this there is no close resemblance between the two patterns.

Typical voltage measurements across the pinch chamber for the 40,000 amp, 70 μsec pulses at both back pressures are shown in Figs. 13a and 13b. There is little qualitative or quantitative difference in the voltage for the two back pressures. The average voltage across the pinch chamber in the interval from 10 to 60 μsec is approximately 200 volts. Since the average current in this same interval is 40,000 amps, the total power

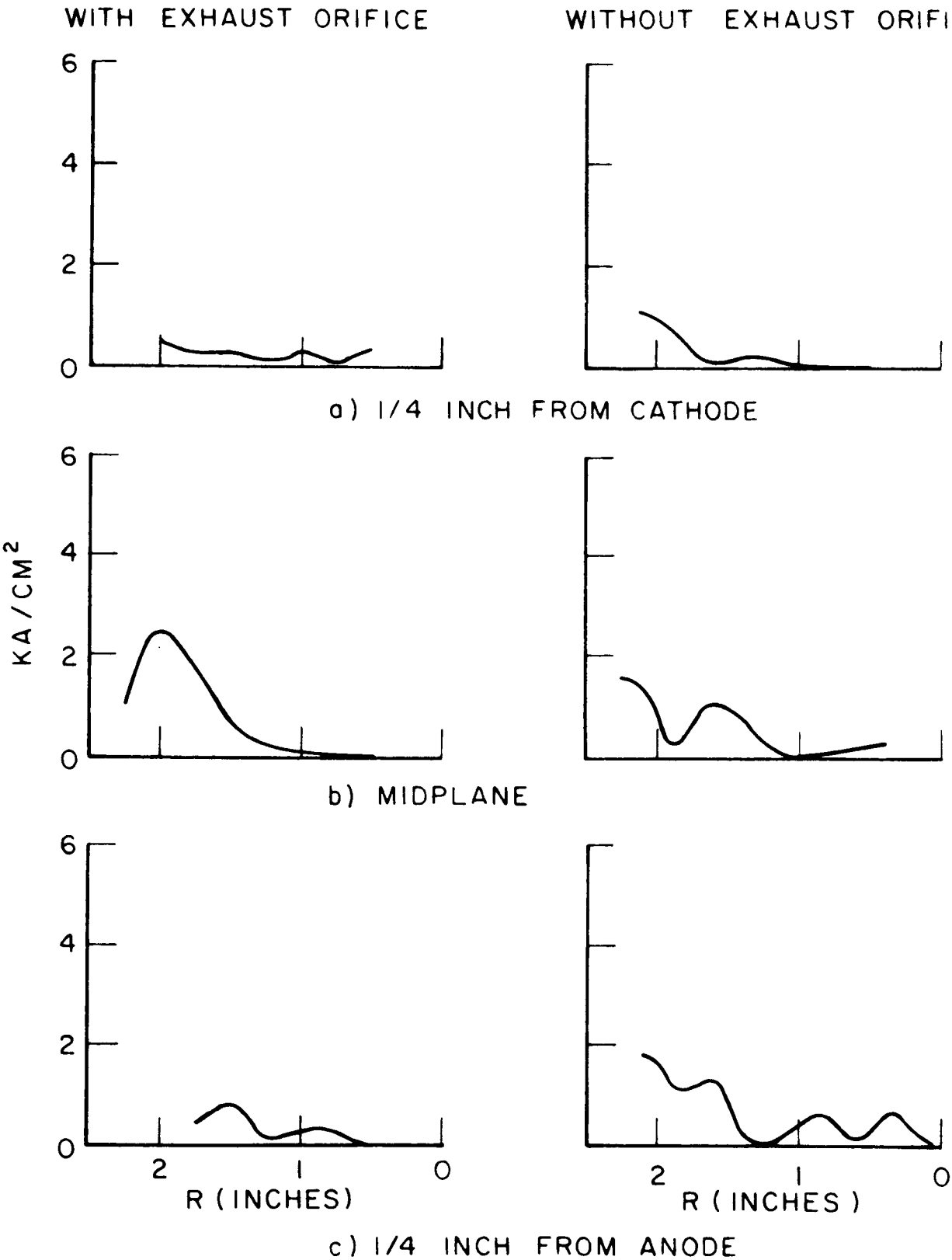

CURRENT DENSITIES FOR 100 μ ARGON INSIDE DISCHARGE CHAMBER FOR 20 μ sec PULSE AT 140 KA, AT 1 μ sec

FIGURE 10

AP25-4248-67

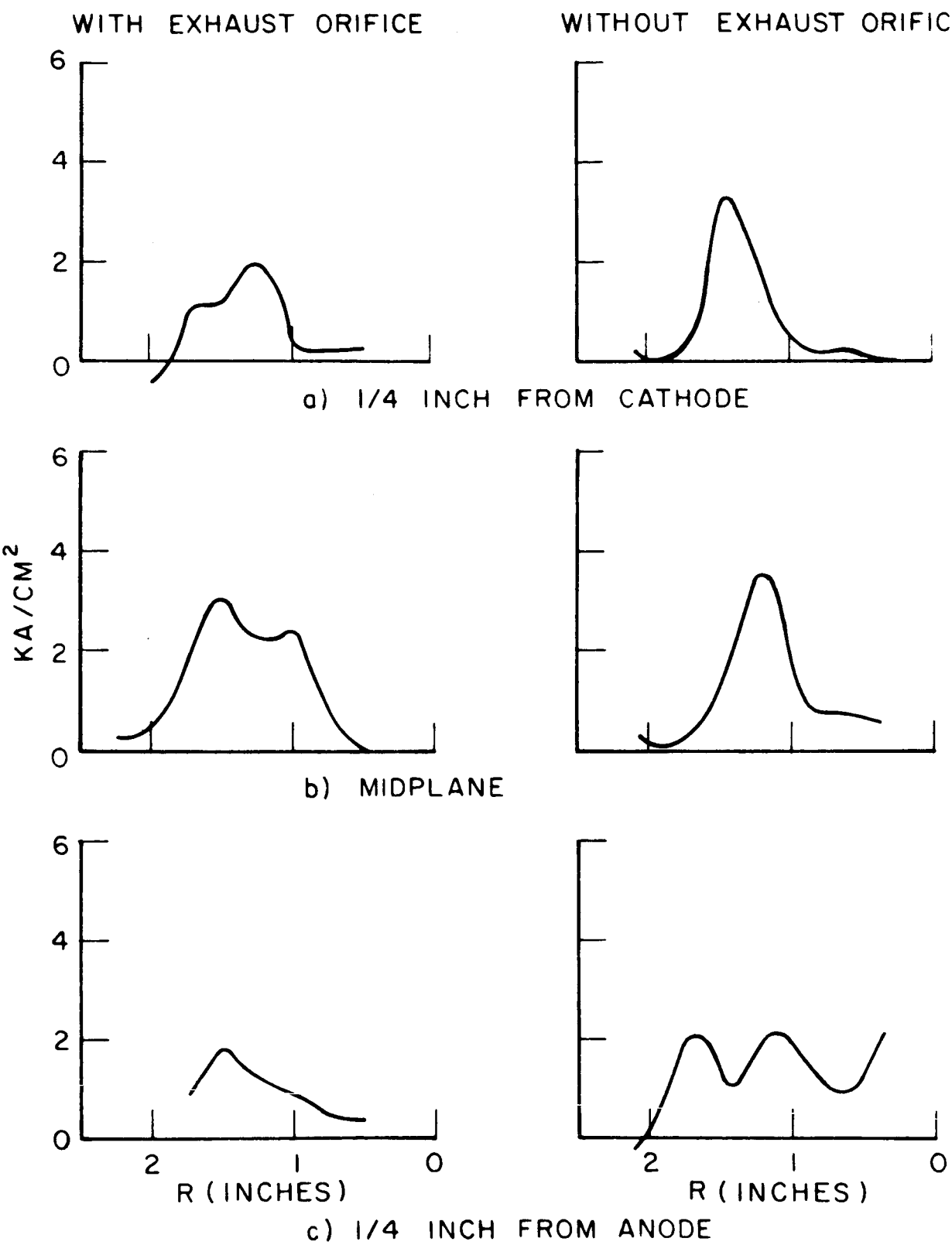

CURRENT DENSITIES FOR 100 μ ARGON INSIDE DISCHARGE CHAMBER FOR 20 μsec PULSE AT 140 KA, AT 2 μsec

FIGURE 11

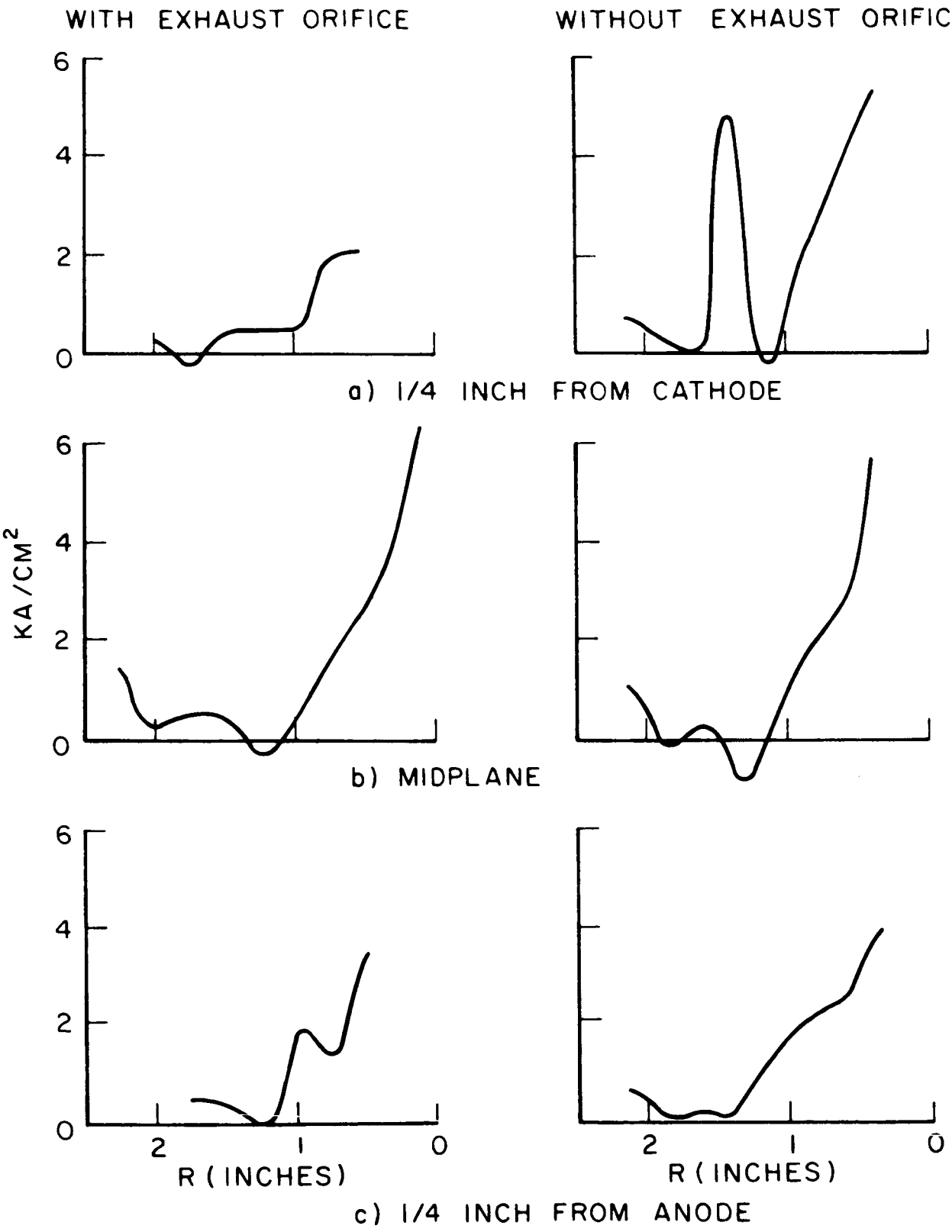

CURRENT DENSITIES FOR 100 μ ARGON INSIDE DISCHARGE CHAMBER FOR 20 μ sec PULSE AT 140 KA, AT 3 μ sec

FIGURE 12

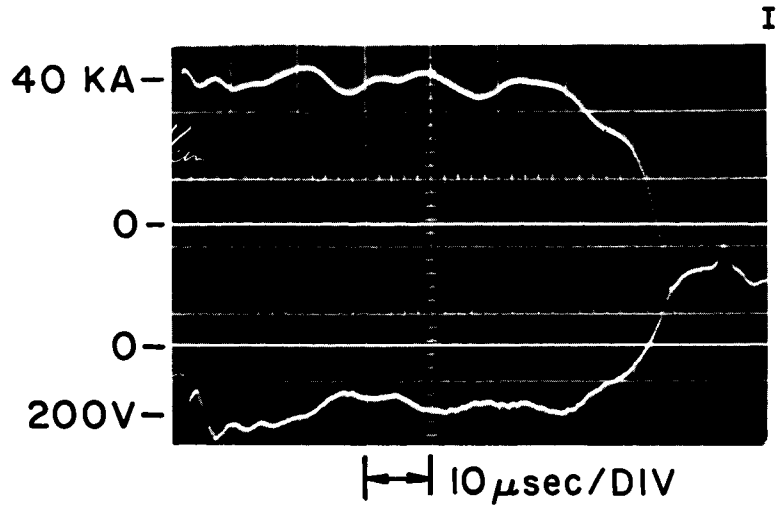

a) AT 40 KA IN 100μ ARGON

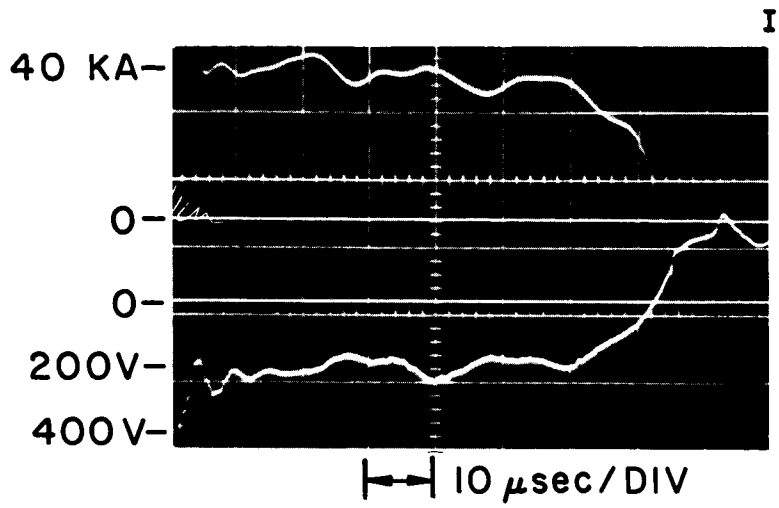

b) AT 40 KA WITH GAS INJECTION

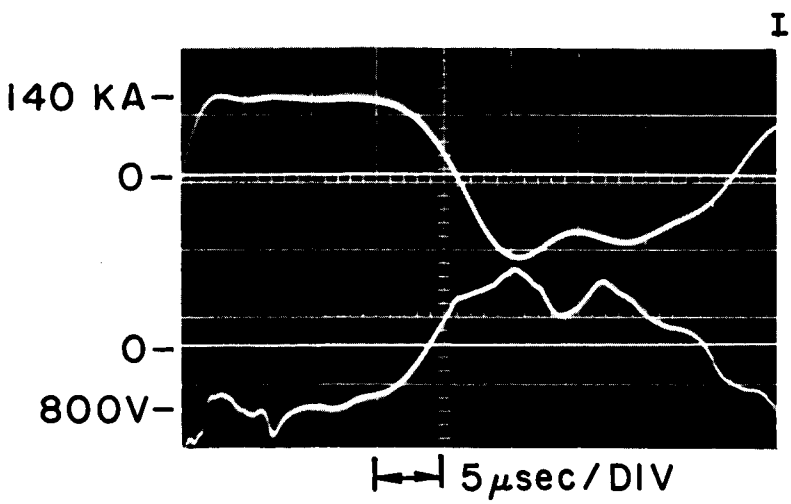

c) AT 140 KA WITH GAS INJECTION

VOLTAGE ACROSS DISCHARGE

FIGURE 13

in the discharge is roughly 8 megawatts. In the case of the 140,000 amp pulse for 20 μsec, we find an average of about 800 volts corresponding to an average power of about 110 megawatts (Fig. 13c).

The foregoing observations of the exhaust patterns suggest certain generalizations:

1) For the selected rectangular waveforms driving the discharge, only a single "sheet" is created and pinched, but this sheet does not contain the total current. A sizeable fraction remains at the outer edge of the pinch chamber.

2) For a given pulse time and current amplitude a greater portion of the arc current appears to flow into the exhaust plume at higher back pressures than at lower back pressures, primarily as a result of the retrograde motion of the high current contours in the latter case. Whether this is truly a back pressure effect or is related to the gas injection velocity and density profiles is not yet known.

3) For a given energy pulse a greater percentage of current flows in the plume for the lower amplitude, longer pulses.

4) If the magnitude of the current is held constant and the length of the pulse increased, the pattern for the longer pulse is the same over the time span of the shorter pulse and the remainder is a continuation of the process from that point on. (This seemingly trivial point demonstrates the insensitivity of the development of the bulk of the pattern to small differences in the early portions of the driving current profile.)

5) The plume development progresses through three phases: a) an initial, unsteady portion with well-defined propagating current zones; b) a transition phase of diffuse but unsteady current patterns; and c) a stabilized or pseudosteady phase with fixed current pattern. The latter phase is not attained in all cases within the testing times available. In particular, pinch time must be considerably less than the driving pulse length if

this is to be possible. In these experiments, complete stabilization is observed only for the 70 μsec pulses, in both ambient and injection conditions. Figs. 14a,b and 15a,b attempt to summarize the development in time of particular enclosed current contours for illustrative cases.

Preliminary work with ion collecting probes has shown that all three of the pattern phases are propulsive in nature; i.e., they accelerate and eject plasma. It has been pointed out in previous reports that using phase (c), the MPD arc may be simulated and studied. Phase (b) is interesting because the microscopic details of the gas acceleration process must be changing, and a study of this transition may lead to a better understanding of the atomic-scale interactions which participate in both mechanisms. At this time, two new accelerators are under design and construction to explore each of these possibilities separately, in more appropriate configurations. The MPD arc simulation device will more closely resemble its steady flow prototype; and the transition study will be made in a simpler, parallel plate geometry.

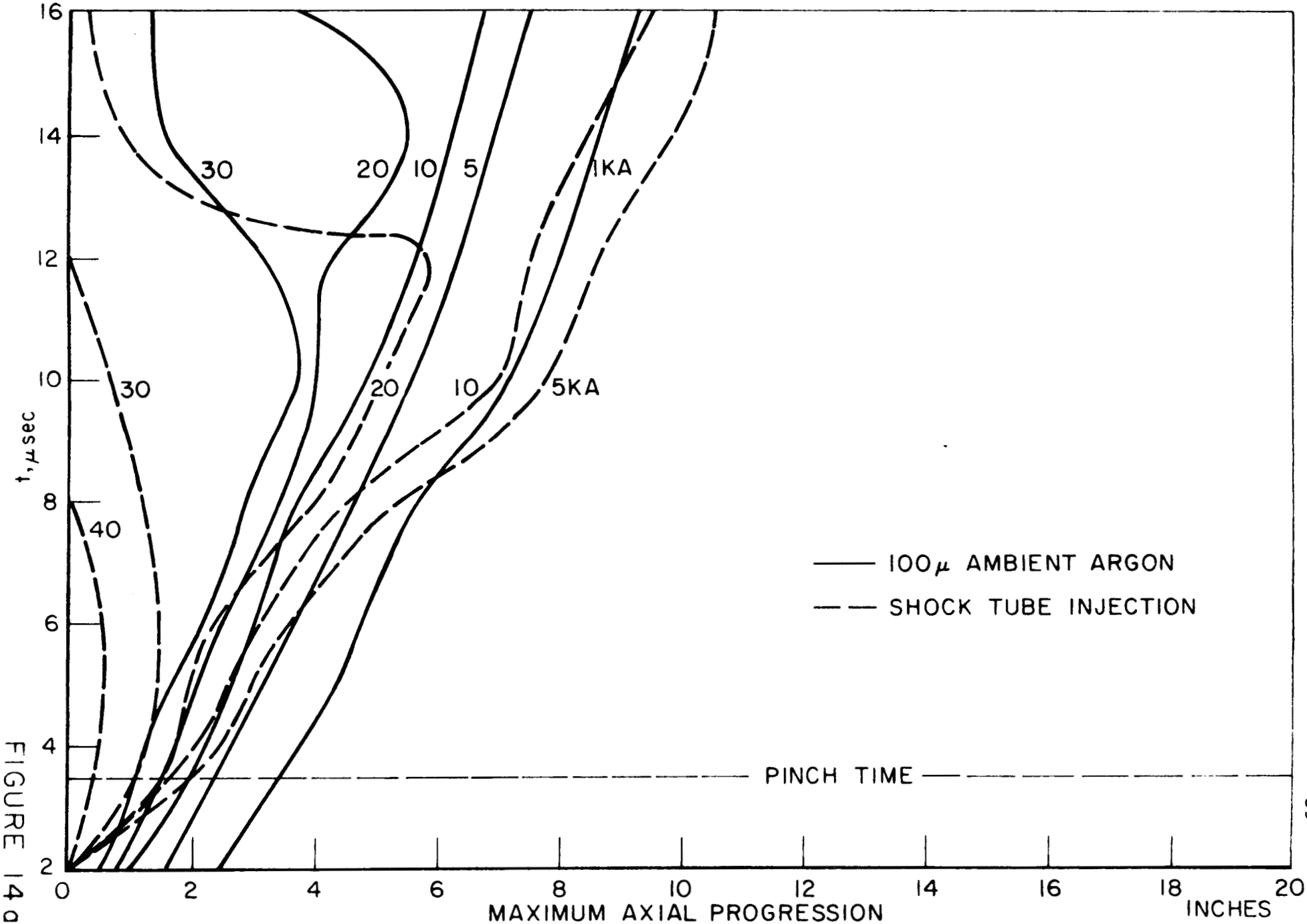

FIGURE 14a

DEVELOPMENT OF ENCLOSED CURRENT CONTOURS FOR 140 KA, 20 μsec PULSE

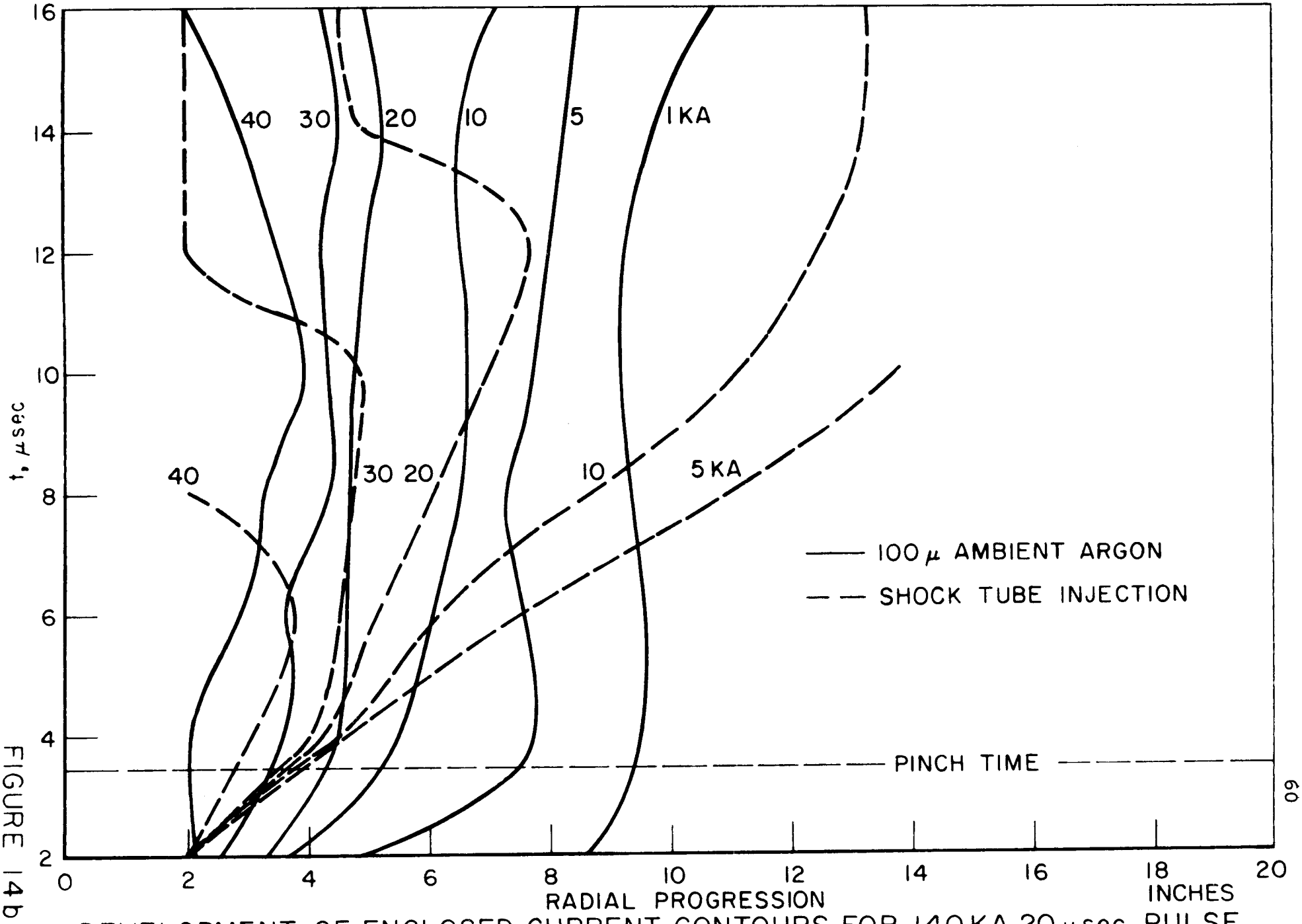

FIGURE 14b

DEVELOPMENT OF ENCLOSED CURRENT CONTOURS FOR 140 KA, 20 μsec PULSE

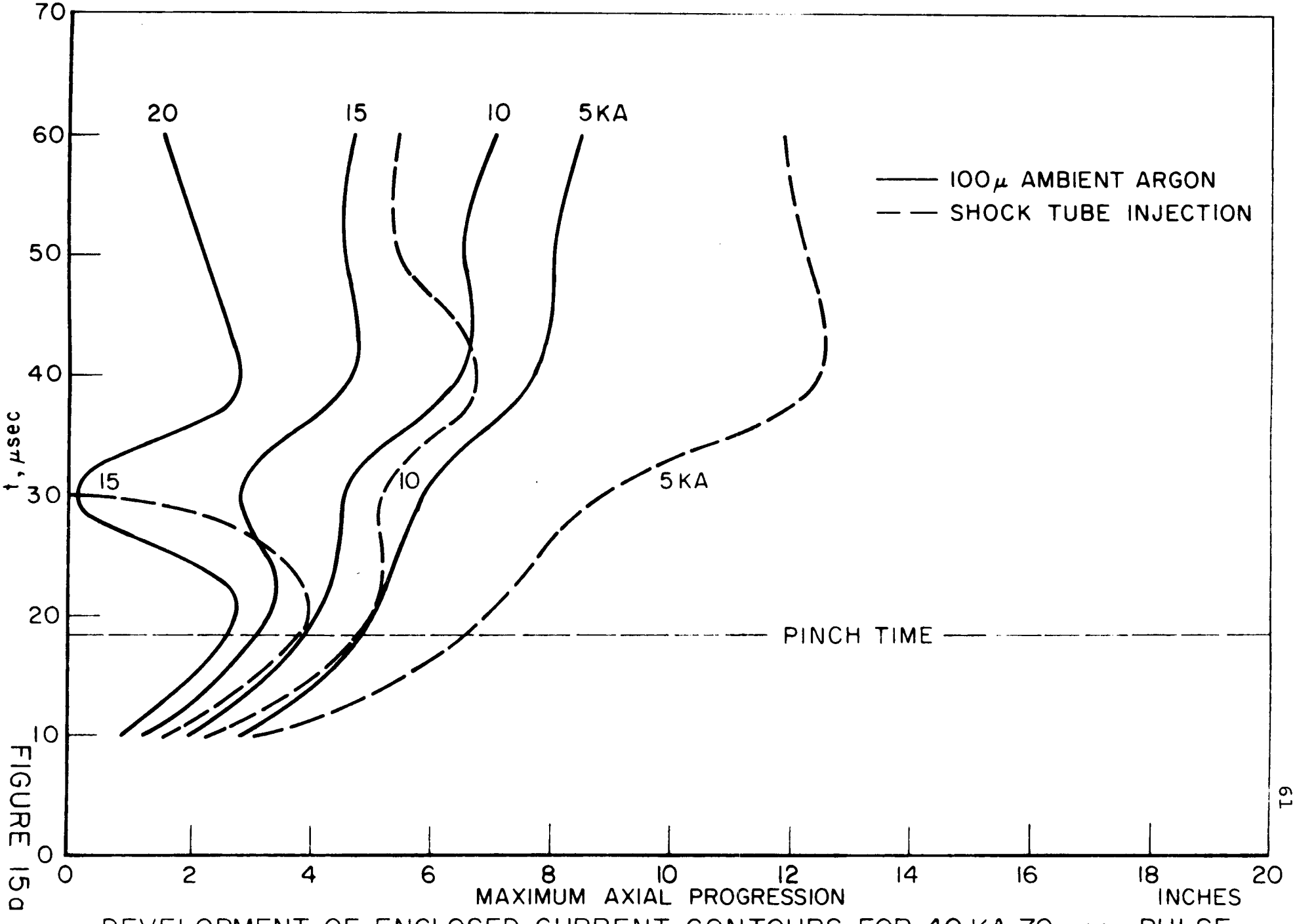

FIGURE 15a

DEVELOPMENT OF ENCLOSED CURRENT CONTOURS FOR 40 KA, 70 μsec PULSE

AF 23 7246-61

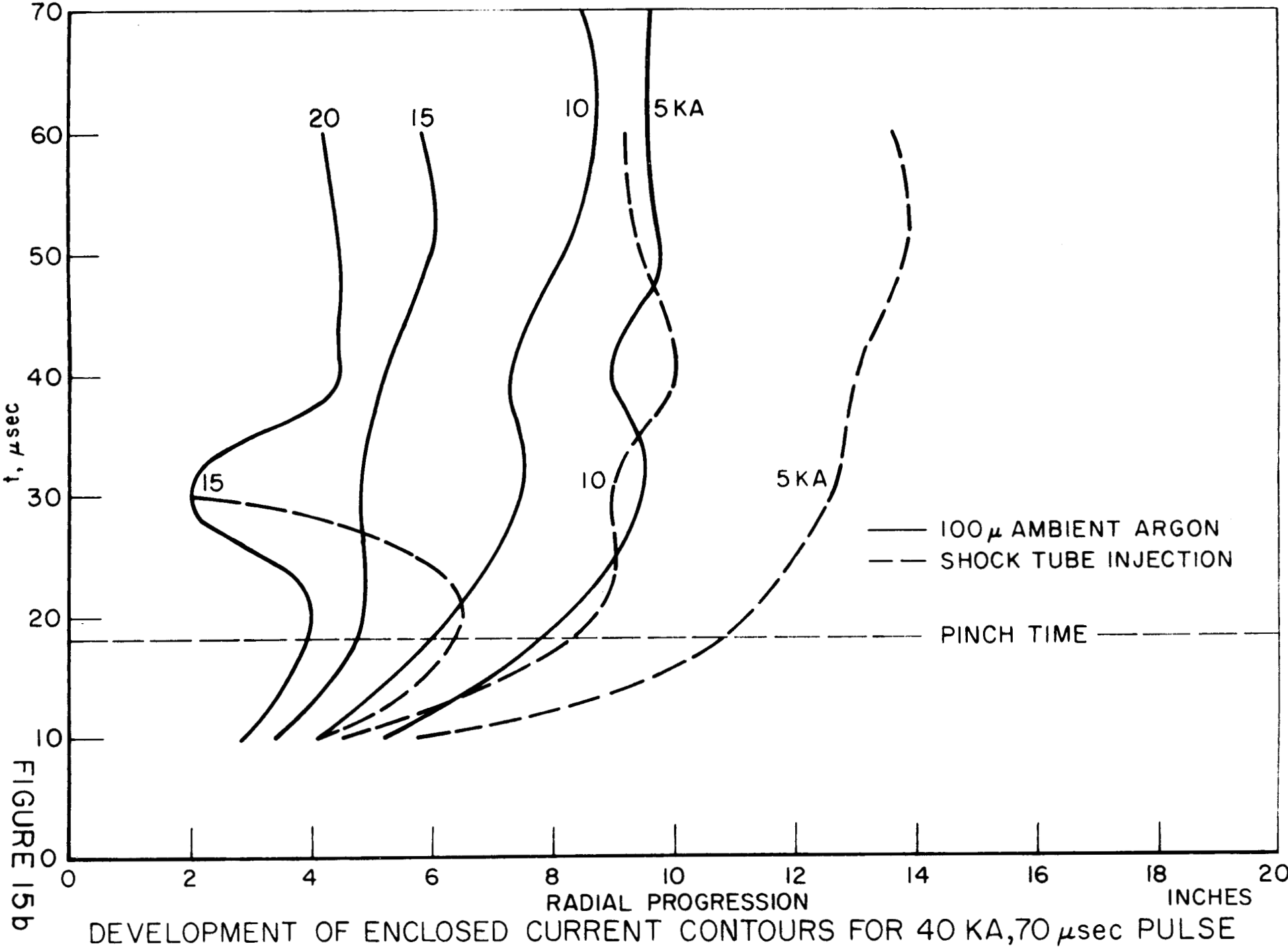

FIGURE 15b

DEVELOPMENT OF ENCLOSED CURRENT CONTOURS FOR 40 KA, 70 μsec PULSE

III. Closed Chamber Probe Studies (Ellis, Turchi)

In addition to the exhaust studies, much attention continues to focus on closed chamber discharges. The basic goal in these studies is to wed precise experimental measurements of the basic plasma parameters and fields with a self-consistent theoretical model of the gas acceleration mechanism. The physical events which participate in the processes of current conduction and gas entrainment are most accessible to detailed investigation in closed chamber discharges, due to the higher shot-to-shot reproducibility and the reduced number of experimental variables.

Typically, probes to measure magnetic flux, electric field, electron density, etc., are mounted inside the cylindrical discharge vessel at some given position r, θ, z. The output of these devices is then displayed on oscilloscope traces as a function of time. The most troublesome data to obtain has been the distribution of free electron density within the current sheet. For this purpose a rather sophisticated microwave probe was developed, and previous progress reports have dealt in some detail with this device [14,21,32,43]. Theoretical methods of interpreting the response of this probe in terms of electron density, temperature, and collision frequency have also been previously discussed [32,43]. During this reporting period these plasma properties have been obtained in the 8" T-machine, at a selected position in the chamber, as a function of time under carefully controlled conditions.

Similarly, simultaneous records have been obtained of the electric and magnetic field components as a function of time, under identical conditions. To insure precise correlation, new electric field probes and magnetic probes have been developed specifically for these complementary measurements. The glass envelopes which had previously been used to protect the probe tips from the discharge and to provide a vacuum seal have been replaced with nylon sleeves. Nylon makes the probes much more adaptable, in a mechanical sense, and in addition has proved to

be an excellent vacuum material. Thin coats of epoxy and radio cement are used to protect the probe tips and to provide electrical insulation, thereby presenting a much smaller energy sink to the plasma than did the bulky glass enclosures. In addition, the braided shielding has been replaced with coaxial brass rods which both improve the signal-to-noise ratio and add structural rigidity. All the probes used in these experiments have a spatial resolution of about 2 mm (Fig. 16).

These three probing devices have provided data from which maps of many plasma properties throughout the current sheet can be obtained. These include the electron number density, n_e; electron-ion collision frequency, ν_{ei}; electron-neutral collision frequency, ν_{en}; electron temperature, T_e; the electrical conductivity of the plasma to the applied electric fields, σ ; the Hall parameter, Ω ; the magnetic field components B_r, B_θ, B_z; the electric field components E_r, E_θ, E_z, both applied and induced; the current densities J_r, J_θ, J_z; and the distribution of body forces, $\vec{J} \times \vec{B}$. Insertion of these measured values into various theoretical models commensurate with the sophistication of the measurements [37,42], permit predictions to be made about certain details of the current sheet structure, such as which zones of the sheet carry predominantly electron or ion current, which regions exhibit primarily scalar or Hall conduction, etc.

This work will be fully detailed in a Ph.D. thesis to be submitted shortly [45].

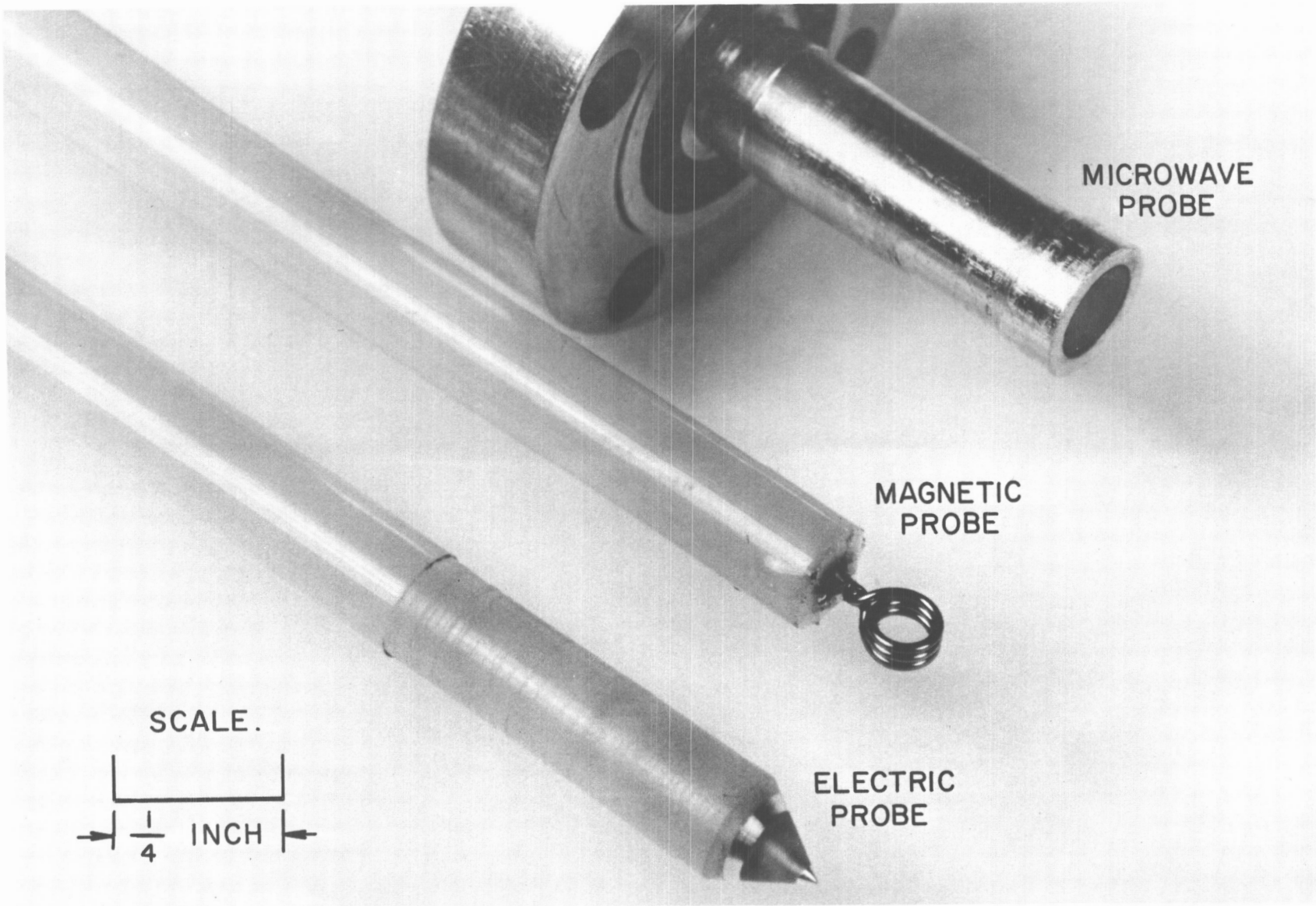

FIGURE 16

MICROWAVE PROBE, MAGNETIC PROBE AND ELECTRIC PROBE USED IN 8" MACHINE CLOSED CHAMBER EXPERIMENTS

IV. Gas Laser-Interferometer Studies of Electron Densities (Cooke, von Jaskowsky)

Following the completion of a series of preliminary studies with a borrowed laser which established the feasibility of the laser interferometer concept for mapping free electron densities in closed-chamber discharges [43], a more serviceable instrument was purchased for the detailed development of this technique. This is an Optics Technology Helium-Neon Gas Laser, Model 70, which emits coherent light at 6328 Å in the visible red. Using this new device, the earlier results of frequency response to 50 megacycles using a rotating mirror to modulate the optical path were reproduced.

Before attempting to use the laser to probe a discharge, a neutral gas expansion chamber was constructed as a calibration device for the proposed interferometer arrangement. As shown in Fig. 17, a cylindrical chamber with plexiglas ends was provided with a diaphragm-covered orifice in its sidewall. This chamber was placed axially in the optical path of the interferometer, filled with room-temperature argon at various pressures above atmospheric, and the diaphragm then ruptured. The resulting sudden reduction in gas density, which is linearly proportional to the change in its index of refraction, was thus monitored as a changing optical path by fringe shifts in the interferometer. From the measured argon pressures before and after the diaphragm was ruptured, the anticipated fringe shifts could be calculated from the known dimensions, wavelength, and refractivity of argon, and these values then compared with the experimental results.

Sample oscillographs from this experiment are shown in Figs. 18a,b. The upper trace of each displays the entire modulation interval, and the lower trace is a tenfold expansion of a portion of the upper trace to facilitate estimation of the total number of interference fringes. Despite the excessive number of fringes provided by this crude experiment, the value estimated from these data are within ten percent of the total

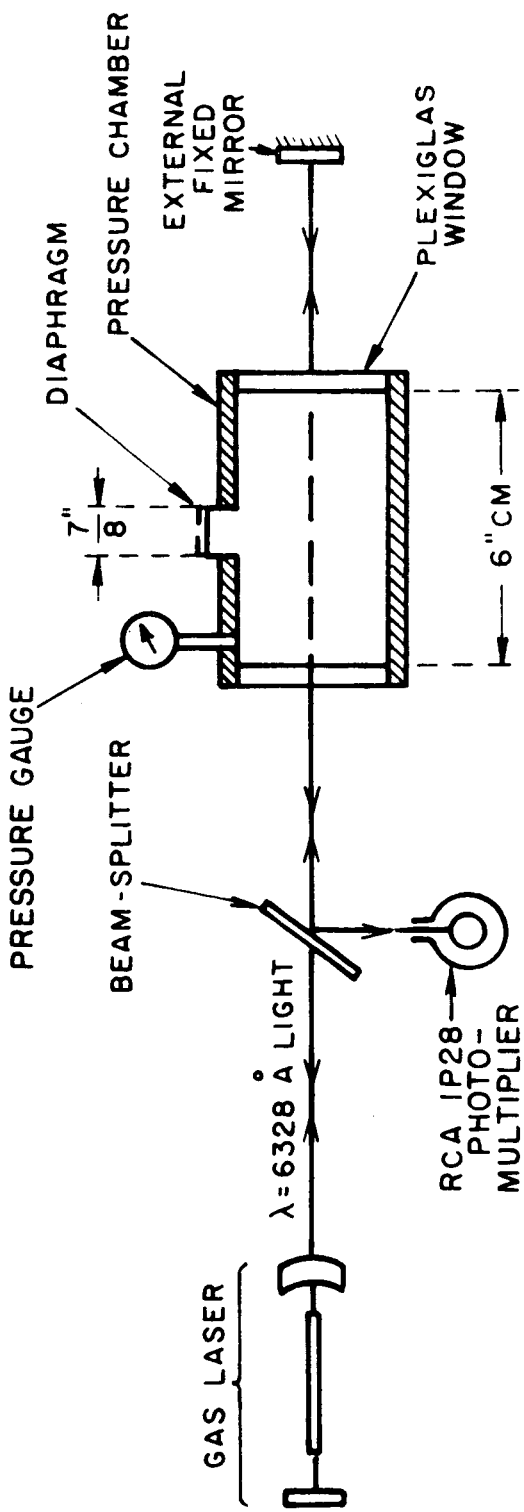

PRESSURE CHAMBER MODULATION EXPERIMENT
(SCHEMATIC)

JP25-4240-67

FIGURE 17

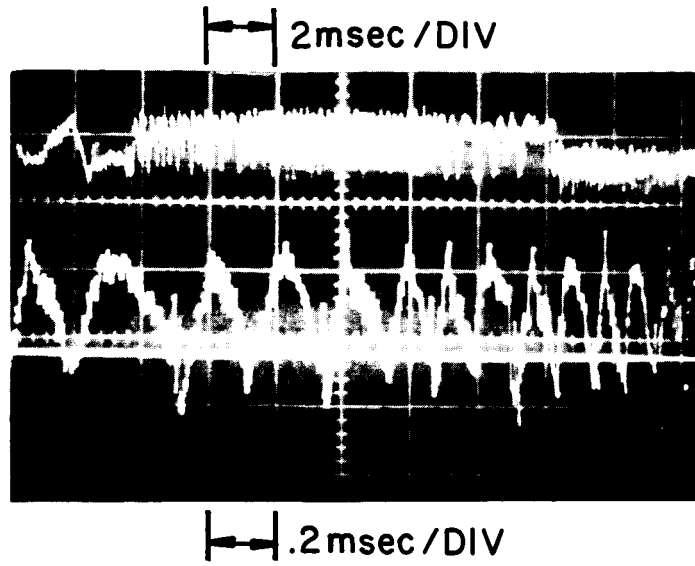

a) PRESSURE CHANGE: 8 PSIG TO 0 PSIG

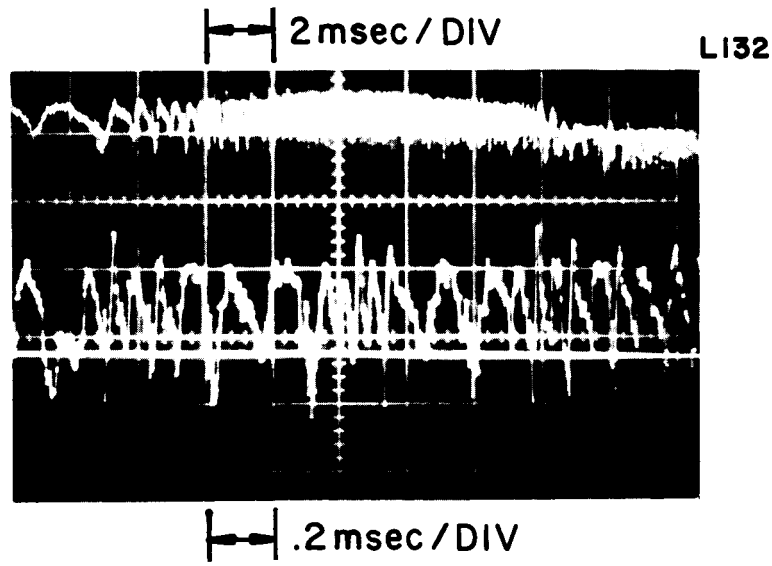

b) PRESSURE CHANGE: 14 PSIG TO 0 PSIG

INTERFEROMETER RESPONSE TO CALIBRATION EXPERIMENT

FIGURE 18

fringe shift calculated from the initial and final pressures in the chamber. Bearing in mind that the magnitude of the contribution of the bound electrons in such a neutral gas is more than an order of magnitude lower than that of the anticipated free electrons in the vicinity of the current sheet in the plasma, we may infer that our device should have ample sensitivity for the proposed application, and that the bound electrons will not significantly affect the accuracy of the free electron density measurements.

Having established that the laser interferometer would respond appropriately to changing refractive index in a fixed-dimension chamber, it was installed on the original 8" pinch machine [2,3,12] with the laser beam parallel to the axis of the discharge chamber (Fig. 19). The anode used was originally designed for Kerr-cell photography, and has a 6" diameter circular glass insert. Through this the laser beam may be passed axially at any desired radial and azimuthal position. A small mirror is attached to the lower electrode (cathode) to assure that the reflected light is unidirectional and uniphase. Suitable masks and red-cutoff filters limit the magnitude of the discharge radiation admitted by the photomultiplier to a small fraction of the magnitude of laser light admitted. Samples of preliminary oscillographs obtained at a chamber radius of 1-5/16" ($R/R_o = 0.33$) and pressures of 120 and 535 μ in argon are shown in Figs. 20a,b. In both oscillographs the topmost, flat trace is the photomultiplier zero-signal; the second trace is the pinch radiation signal and is seen to be quite flat and of relatively small magnitude; the third trace is the modulated laser signal indicative of the development of the free-electron density within the discharge; the lowest trace is the integrated Rogowski coil signal, indicating total discharge current. The onset of the modulation patterns at 5.4 and 13 μsec for the 120 and 535 μ Hg cases, respectively, agree well with the arrival times of the luminosity fronts seen in streak [4,14] and Kerr-cell [5,14] photographs, and with the current sheets detected by magnetic probes. Because of the multiple current

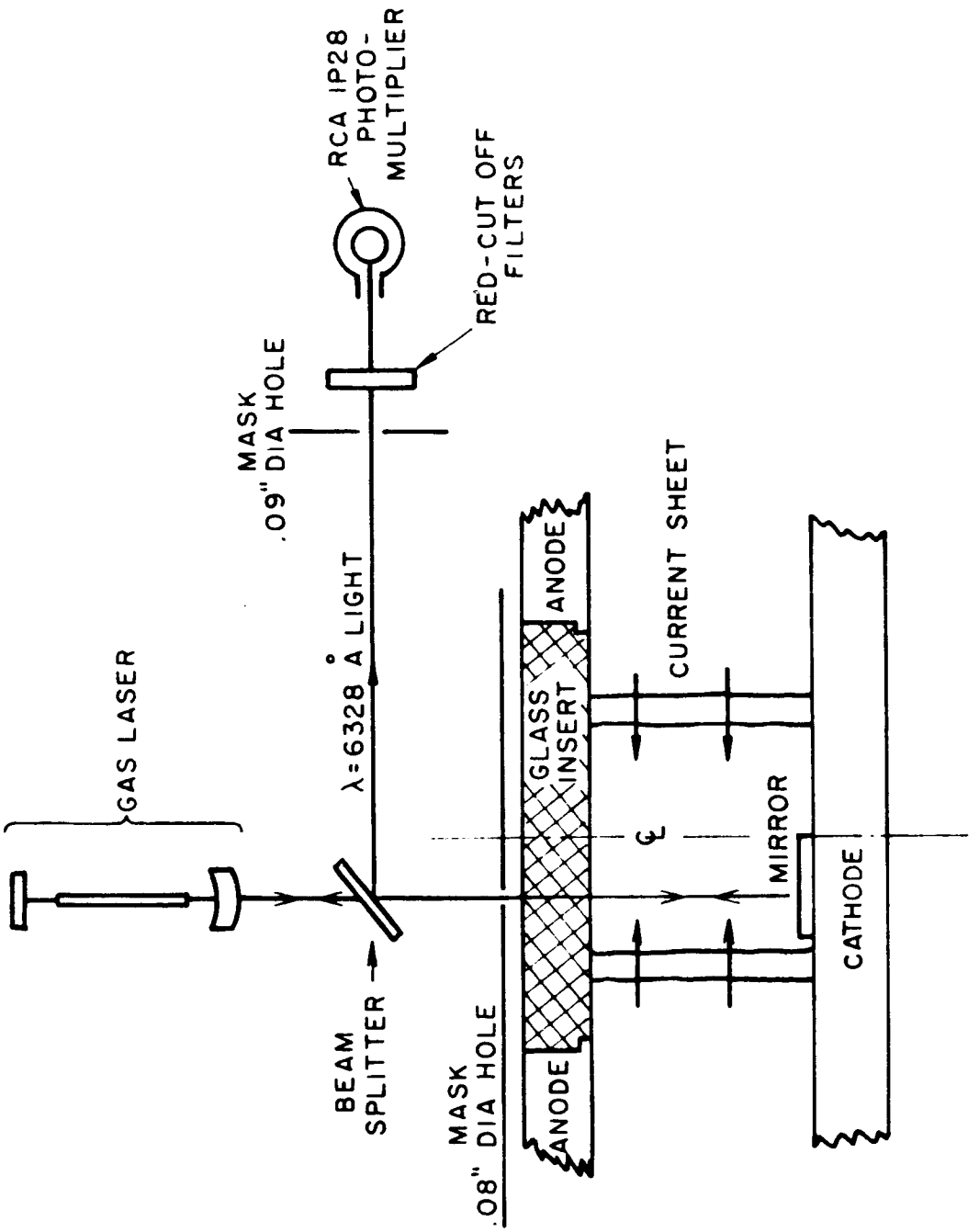

LASER INTERFEROMETER INSTALLED ON 8" PINCH DISCHARGE CHAMBER
(SCHEMATIC)

FIGURE 19

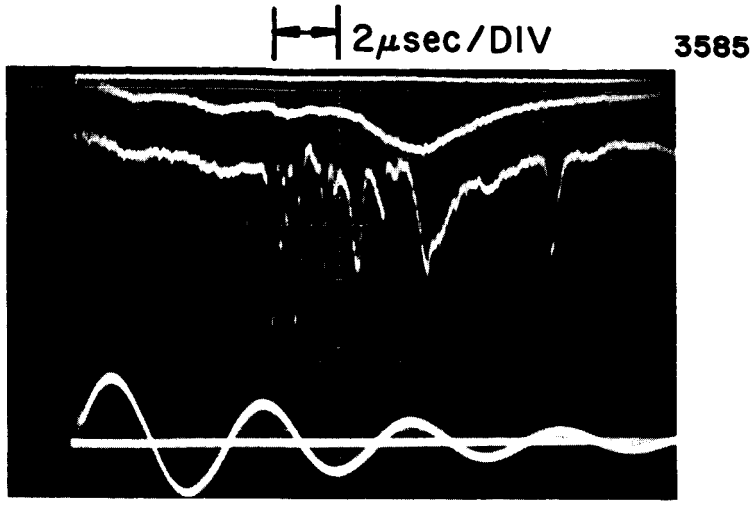

a) 120μ ARGON

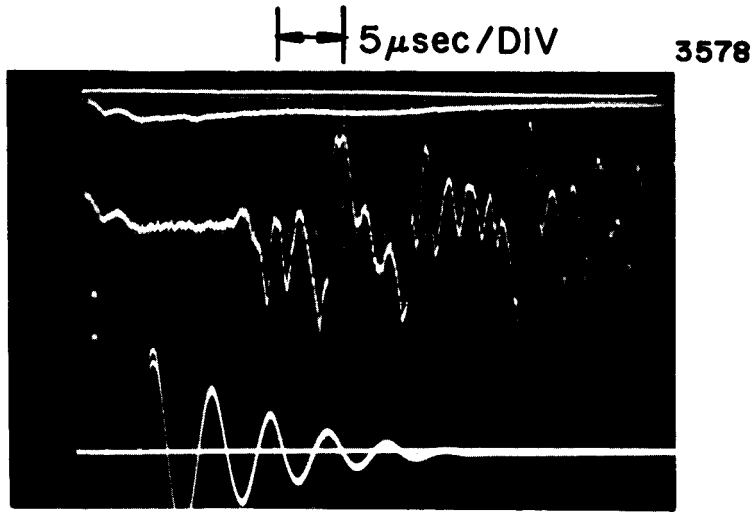

b) 535μ ARGON

INTERFEROMETER RESPONSE TO CLOSED CHAMBER DISCHARGE IN ARGON AT $R/R_0 = 0.33$

FIGURE 20

sheets prevailing with this particular machine [12], and because of the difficulty of identifying reversals of slope of the free electron density, the oscillographs cannot presently be translated unambiguously into time-dependent electron densities, but these problems will presumably be overcome by simultaneous use of an infrared wavelength with the present visible system, or by examining a geometrically less complex discharge pattern driven by our pulse-forming network.

V. Pressure Measurements in Closed Chamber Discharges (York)

Previous semi-annual reports have dealt with general state-of-the-art piezoelectric probe construction and performance [32] and have detailed the development and performance of a high speed piezoelectric probe with improved time-history response [43]. In the latter, some data was presented of simultaneous pressure and magnetic probe response to conditions at the cathode surface of a closed chamber discharge driven by a pulse-forming network. As outlined below, work has continued along these same lines in an attempt to determine the distribution of pressure throughout the chamber during the dynamic pinch process.

The cathode data reported earlier, although reproducible, was achieved with some difficulty because of the sensitive coupling of the electrical insulation and acoustic distortion problems. In order to improve insulation reliability and to allow for more flexible probing, a new probe was constructed that incorporated a significantly thinner (1/64") brass mounting shell, making the mylar tape covering more effective (Fig. 21). The interaction of the thin shell with other probe components resulted in the appearance of a significant low frequency oscillation which fortunately did not degrade the short-time ($< 5\ \mu$sec) calibration in the shock tube; the probe thus was satisfactory for the qualitative survey of interest.

This transducer, like some of its predecessors, is equipped with a magnetic probe unit precisely positioned so that simultaneous measurements of pressure and local magnetic field may be obtained on each current sheet. With this binary probe, data was taken in the 8" T-machine with a 100 μ argon discharge driven by a 5 μsec rectangular current pulse. For a given radial position, the probe was placed at various axial locations: sensing surface flush with cathode (W-C); inserted through cathode but midway between electrodes (M-C); inserted through anode but midway between electrodes (M-A); flush with anode (W-A). A series of shots indicating typical behavior is

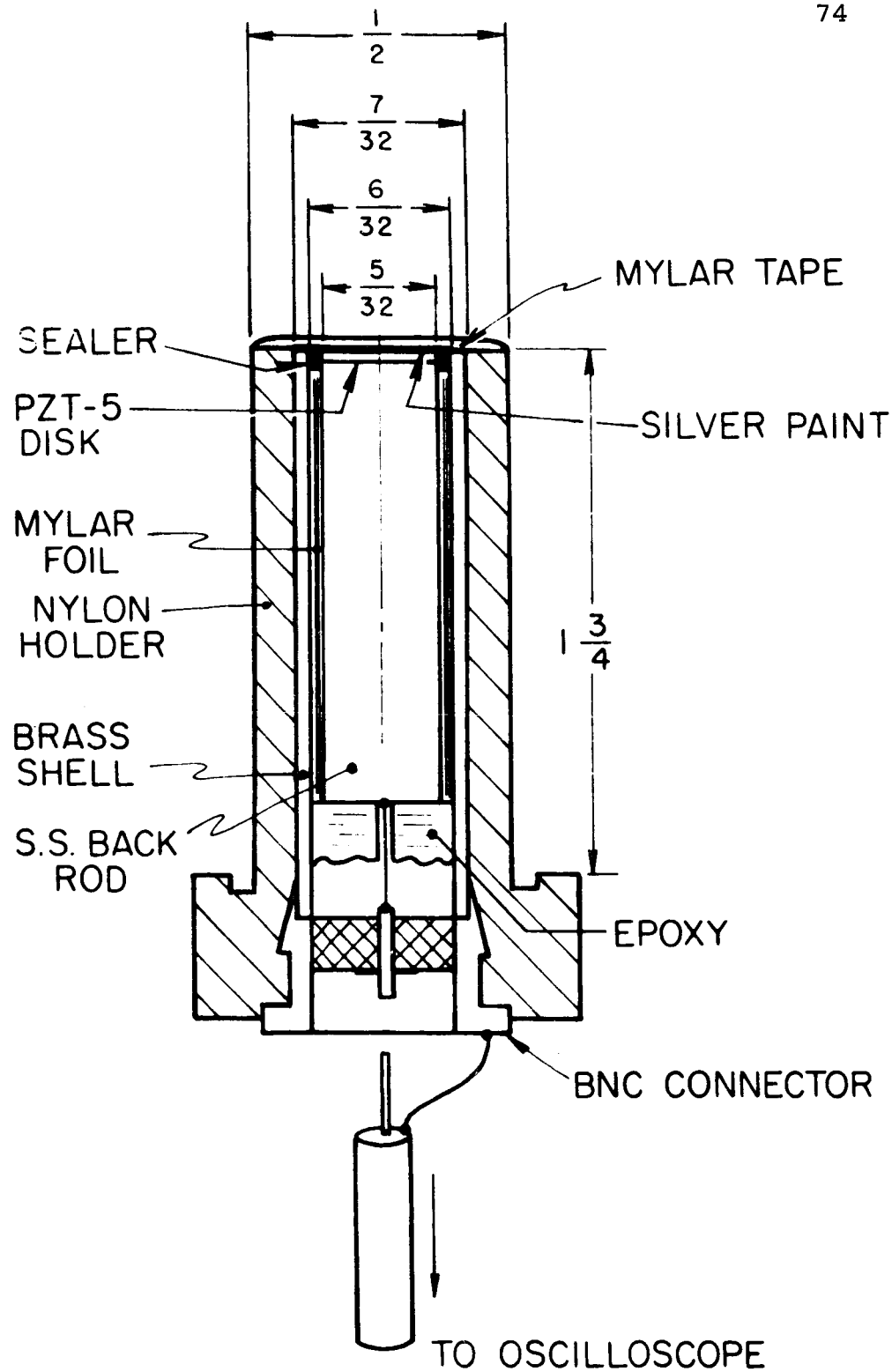

SCHEMATIC OF PIEZOELECTRIC PRESSURE TRANSDUCER

FIGURE 21

presented in Fig. 22. Several features may be noted: a) pressure profiles at W-C and M-C are similar, with the exception of a "negative" pressure portion which may indicate a gasdynamic interaction with the probe structure; b) although probe orientation M-C and M-A are at the same axial position, the sensing surface is facing in opposite directions. The observed differences in response thus indicate an anisotropy in the sheet structure, which may provide information on the current conduction process; c) profiles of both pressure and $\dot{B}_\theta$ are quite diffuse on the anode. There are also indications of a general anode to cathode asymmetry in the magnitude of probe output; this has been noted more clearly at other radial positions, for example, an axial survey of pressures at pinch radius (R = 0) are presented in Fig. 23. At this position, $\dot{B}_\theta$ behavior is quite anomalous, presumably because of the current singularity at the center, but a strong reproducible asymmetry does exist in the pressure probe response.

It is of interest to compare these experimental results and earlier luminosity studies with snowplow theory for the current profile. Using data recorded at location M-C yields the results shown in Fig. 24. Within experimental error, the luminosity, $\dot{B}_\theta$, and pressure fronts coincide, but slightly lead the snowplow trajectory. Similar discrepancies have been observed and discussed in earlier experiments [12].

Similar surveys of pressure and $\dot{B}_\theta$ profiles made for 150 μ and 50 μ argon discharges displayed similar behavior. It now remains to refine the probe technique to the point that detailed pressure profiles may be traced throughout the gas acceleration zone, from which some assignment of local particle density distributions hopefully may be made.

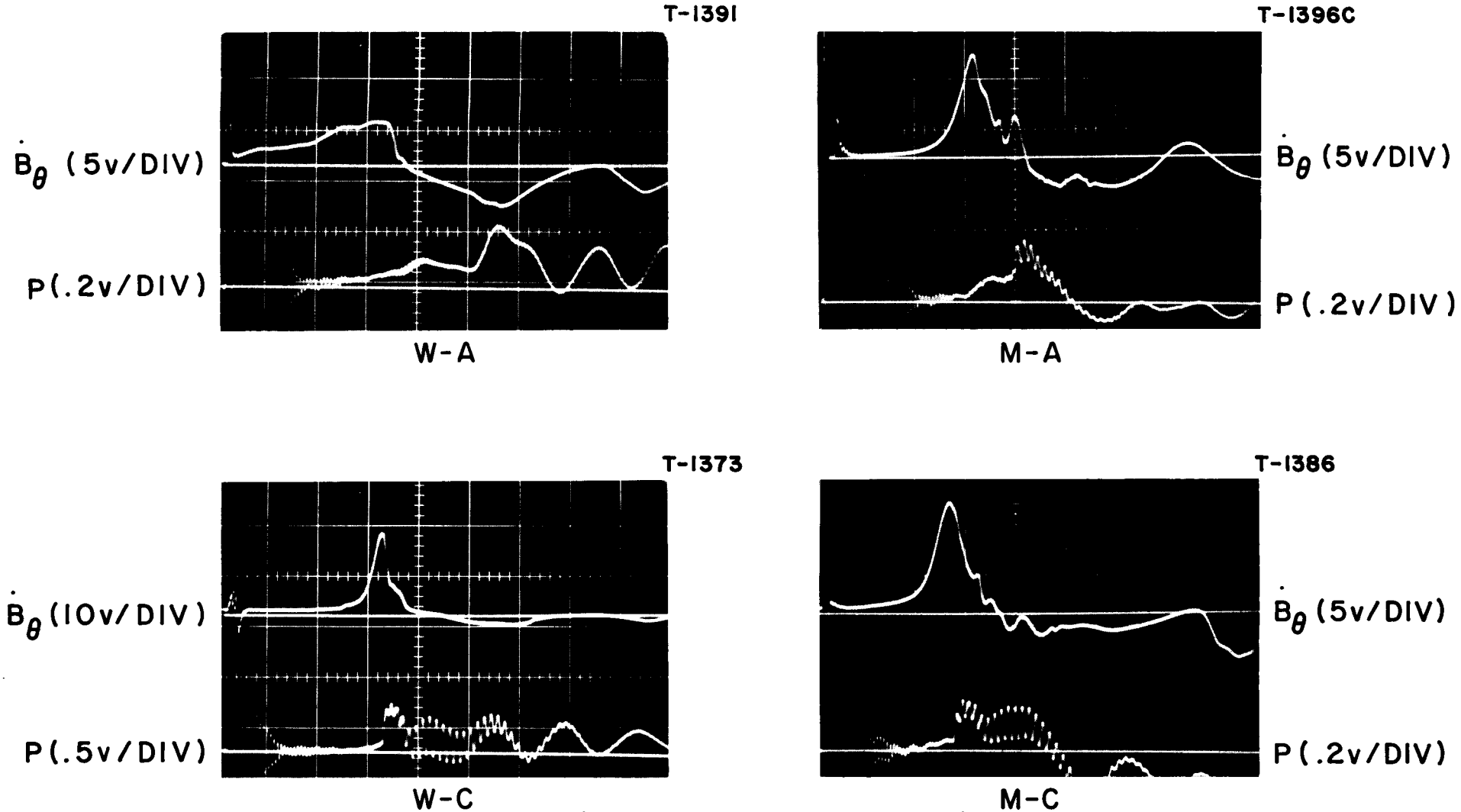

FIGURE 22

SIMULTANEOUS B_θ, PRESSURE MEASUREMENTS AT R=$2\frac{1}{4}$ INCHES FOR VARIOUS AXIAL POSITIONS

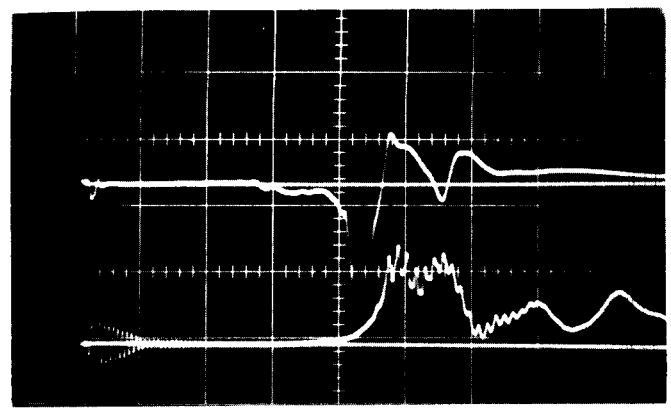

$\dot{B}_\theta$

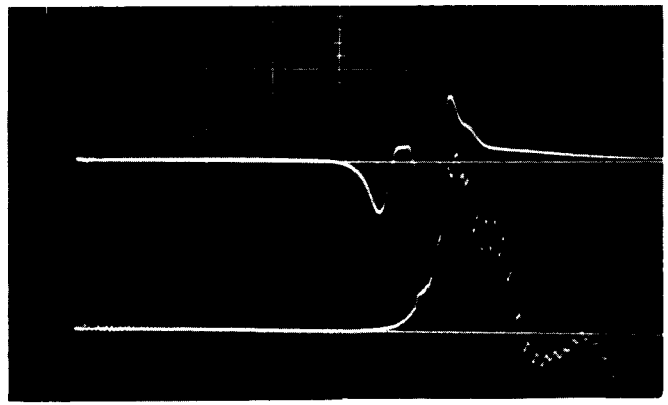

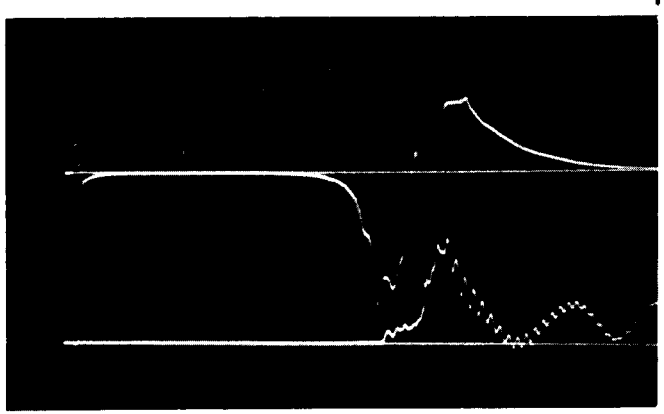

$\dot{B}_\theta$

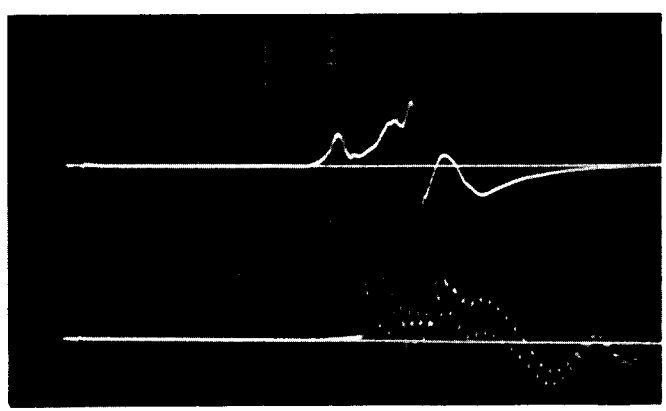

$\dot{B}_\theta$ SCALE - 10v/DIV
TIME SCALE - 1 μsec/DIV

FIGURE 23

PRESSURE MEASUREMENT AT PINCH RADIUS (R=0) FOR VARIOUS AXIAL POSITIONS

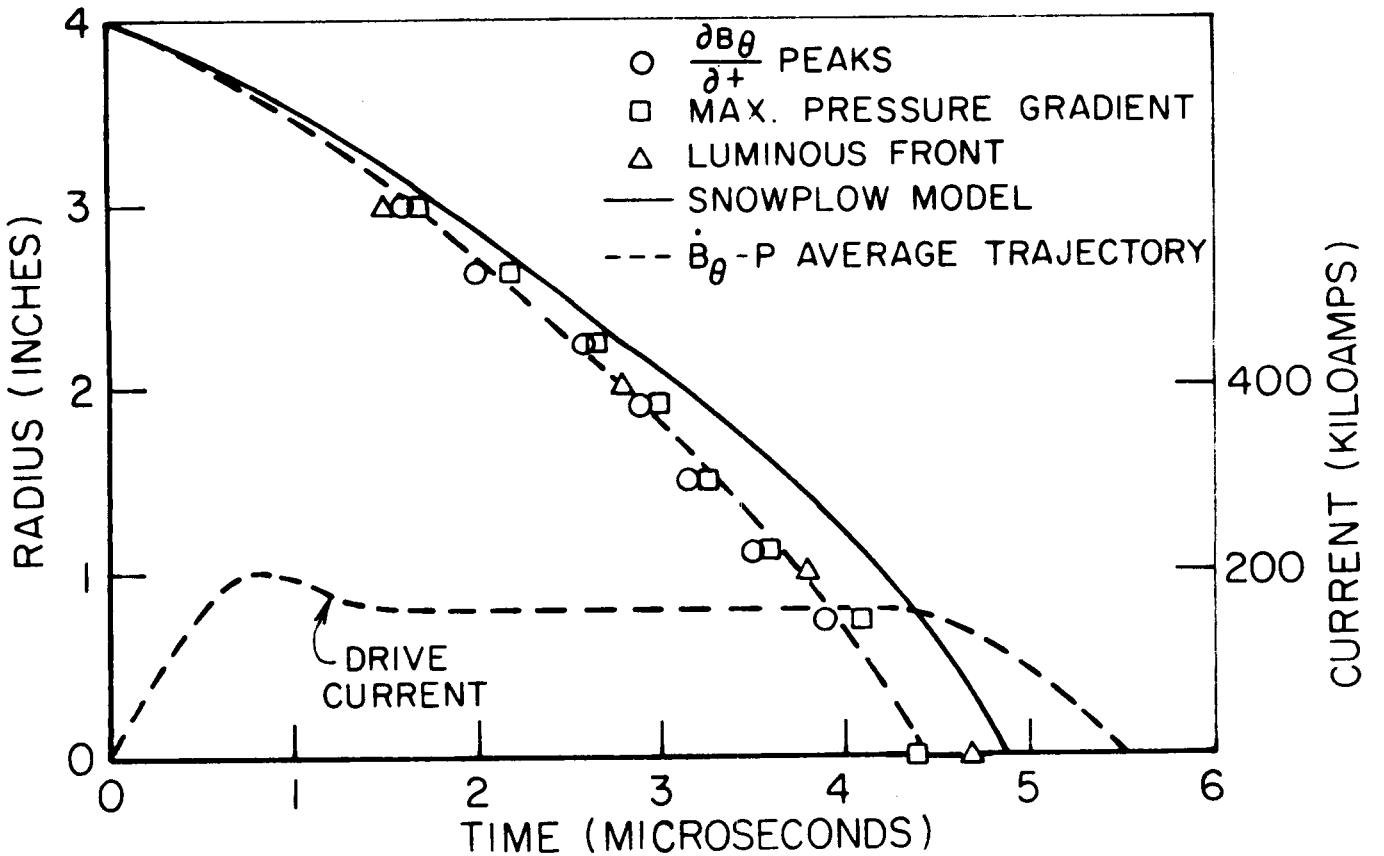

FIGURE 24

TRAJECTORIES OF $\dot{B}_\theta$ MAX, PRESSURE, LUMINOSITY & SNOWPLOW MODEL DRIVEN BY THE PULSE FORMING NETWORK

VI. High-Performance Capacitors and Low Impedance Pulse Network (Wilbur)

The program of design and construction of a series of low-inductance capacitors suitable for simple assembly into pulse line configurations has continued along the schedule outlined in the proposal [27], toward the objective of providing a power source which will transfer its energy to the plasma with optimum efficiency. To date, seven units have been received from the supplier, Corson Electric Manufacturing Corporation of East Hampton, Connecticut. Preliminary low voltage tests have shown the average unit has about 6.3 microfarads of capacitance and in the range of 15 to 20 nanohenries inductance. Inserting these values into the usual relation for the characteristic impedance of a distributed transmission line, $Z_o = \sqrt{L/C}$, one obtains a characteristic impedance for these units in the range of 50 to 60 milliohms.

In order to verify that the units would behave as a transmission line, a shorting ring with a resistance in the range of the calculated characteristic impedance of the capacitors was constructed and installed in the 8" pinch machine. Four capacitors were connected in series and discharged through the shorting ring. An oscillogram of the discharge current waveform in this test (Fig. 25a) demonstrates two important points: 1) The four units connected in series do have the flat-topped current response characteristic of a transmission line. 2) Since the current damps essentially to zero after the first pulse, the characteristic line impedance is approximately equal to the shorting ring resistance (56 milliohms).

When the shorting ring was removed and the capacitors were used to drive the 8" pinch discharge, the current waveform again exhibited a flat-topped pulse, characteristic of a transmission line (Figs. 25b,c). Note in both cases the current rings down in an overshoot pattern, as would be predicted because of the mismatch between the pinch and characteristic line impedances.

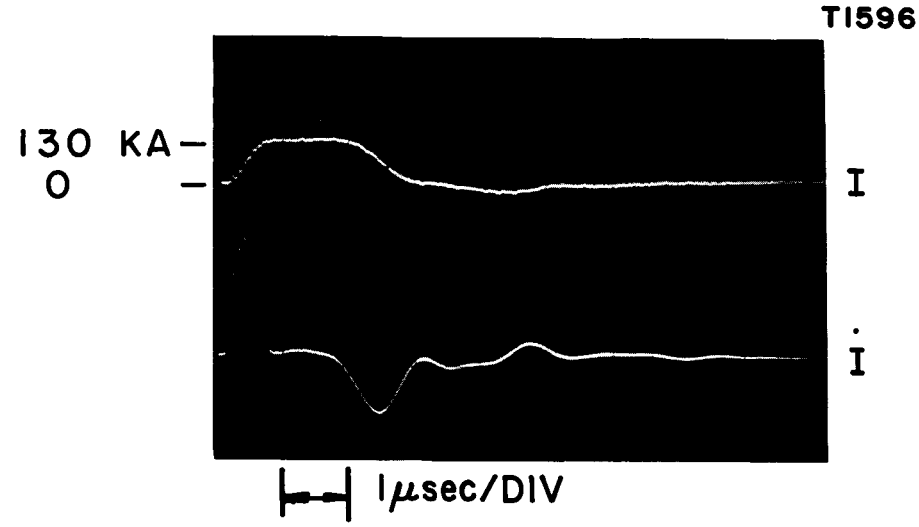

a) DISCHARGE CURRENT WAVEFORM OF 4 UNIT-LINE INTO 56 MILLIOHM SHORTING RING

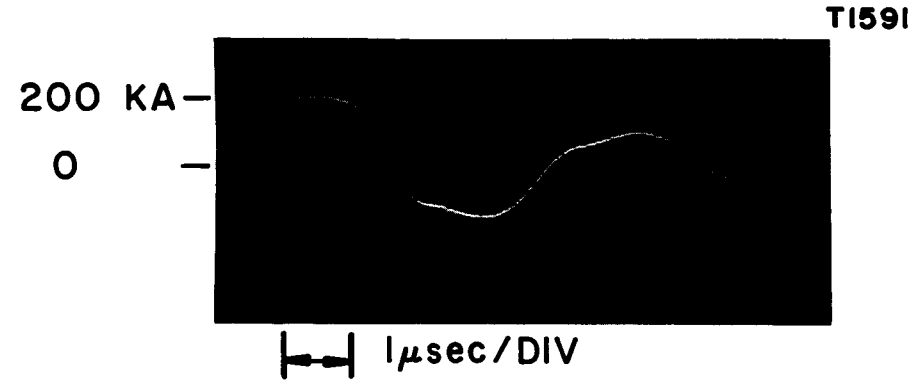

b) DISCHARGE CURRENT WAVEFORM OF 4 UNIT-LINE IN 100 μ ARGON

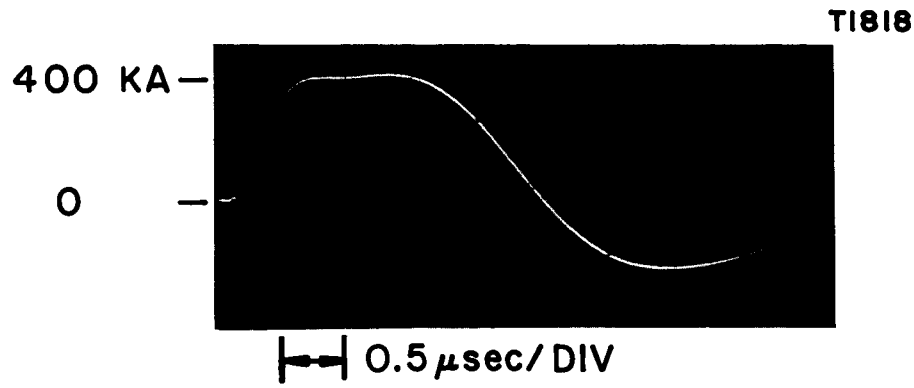

c) DISCHARGE CURRENT WAVEFORM OF 4 UNIT-LINE IN PARALLEL WITH 3 UNIT LINE IN 100 μ ARGON

APES-PPCB-67

FIGURE 25

A numerical analysis was undertaken in conjunction with this testing to determine an analytical model which would describe the discharge under the nonlinear conditions prevailing when the characteristic line impedance is near the pinch impedance. This analysis, in contrast to previous work, does not assume a current waveform; rather, the pinch process is described by the snowplow equation:

$$r \frac{d}{dt} \left[(r_1^2 - r^2) \frac{dr}{dt} \right] = - \frac{\mu_o I_T^2}{4\pi^2 \rho}$$

μ_o = permeability of free space

ρ = gas density

I_T = Total current through machine

r = current sheet radius

r_1 = initial current sheet radius

t = time

and the capacitor bank is represented by the equations describing a transmission line:

$$C \frac{\partial V}{\partial t} - \frac{\partial I}{\partial x} = 0$$

$$\frac{\partial V}{\partial x} - L \frac{\partial I}{\partial t} = 0$$

V = voltage on transmission line

I = current in transmission line

x = position on transmission line

t = time

L = inductance per unit length of line

C = capacitance per unit length of line

The unique current profile satisfying both sets of equations is then solved numerically on the IBM 7094 and 1620 computers. The analysis is assumed valid until pinch occurs or the voltage

applied across the machine reverses and secondary breakdown occurs. The current waveforms predicted by this analysis for the conditions of the experiments shown in Figs. 25b,c are displayed in Figs. 26 and 27. These show good qualitative agreement with the experimental results in that the current magnitude, rise time and pulse length fall within the accuracy of the measured quantities.

From this computer analysis program it has also been determined that the desired match of impedance between the line and the developing dynamical discharge can be achieved only by connecting four parallel lines of two or three units each to the 8" chamber. Tests of this arrangement now await delivery of the final group of capacitors from the supplier.

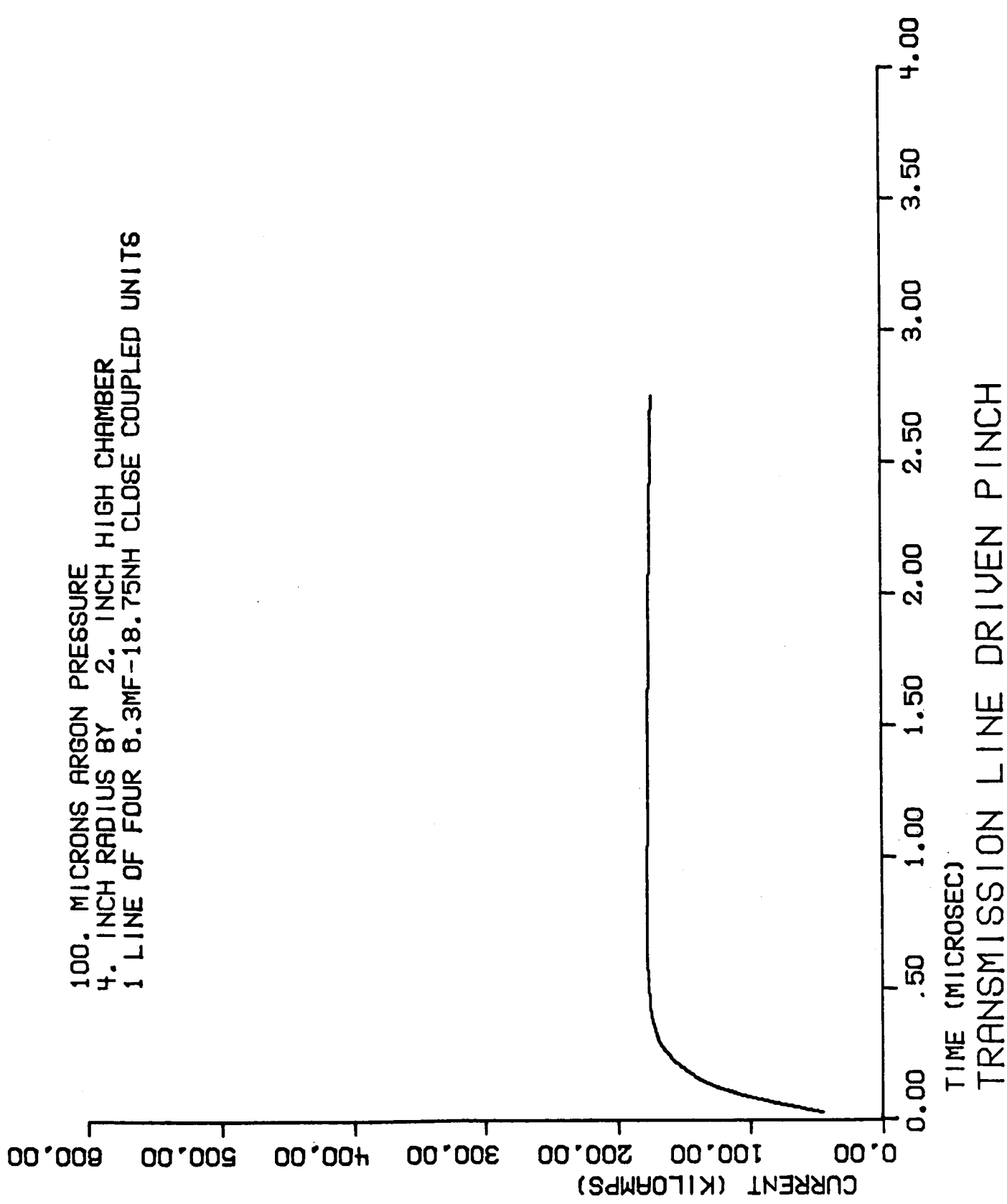

JP25-4237-67

FIGURE 26

JP25-4238-67

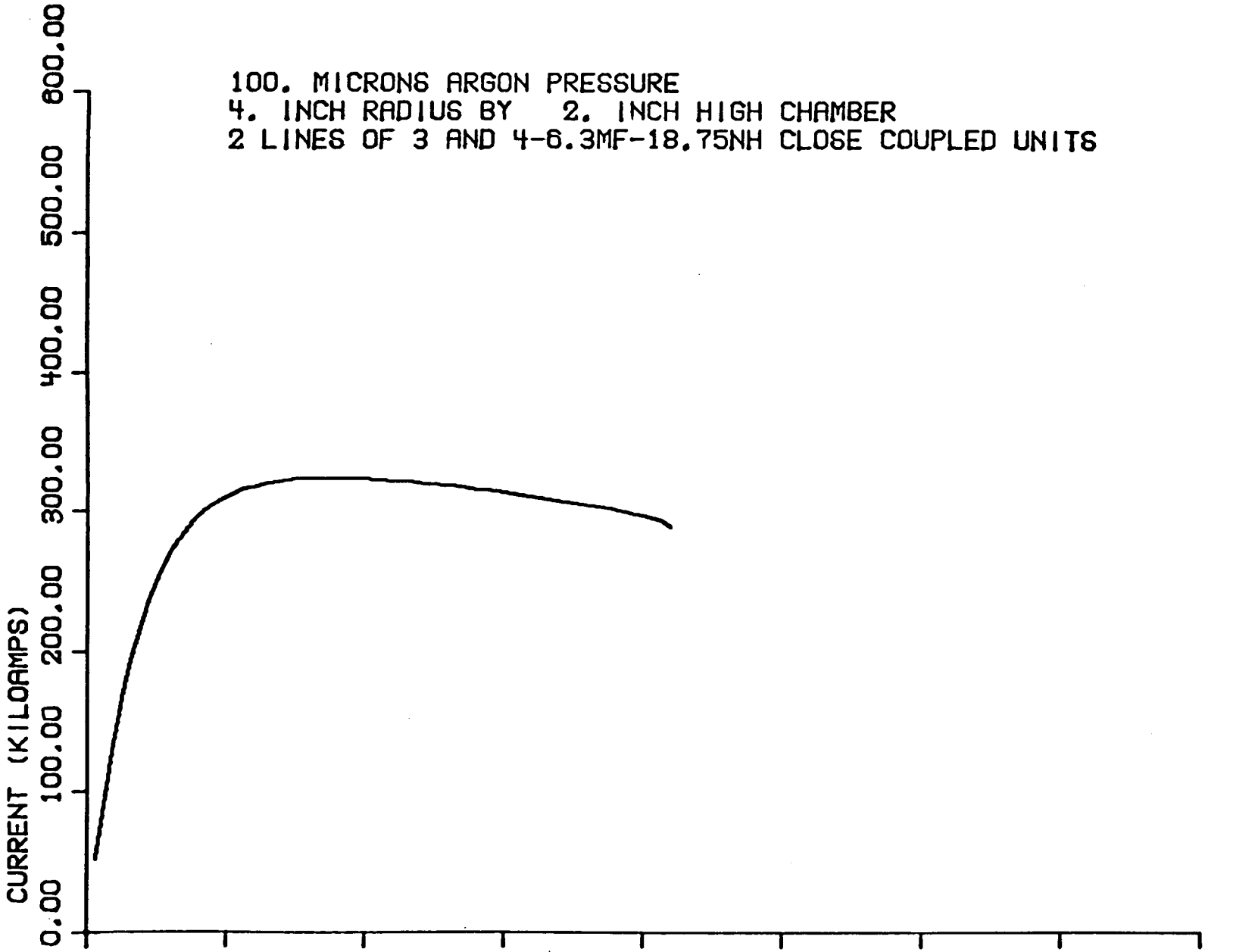

TRANSMISSION LINE DRIVEN PINCH

FIGURE 27

VII. Other Studies (Baumgarth, Bruckner, DiCapua, Oberth, Turchi)

In addition to the programs described separately above, the laboratory supports several other studies, both experimental and analytical, which are less advanced, and whose results are less clearly defined at this time. These include the development of a voltage dividing network that will unambiguously follow the excursions of arc voltage in the long-pulse studies of current-sheet stabilization and MPD simulation; a systematic examination of the effect of driving-current waveform on current sheet shape and amplitude; application of coaxial electric field probes to tailored-pulse discharges; further gasdynamic and magnetogasdynamic analysis of current sheet structure; and analytical formulation of "magnetic nozzle" processes appropriate to the experimental exhaust studies. As each of these efforts matures, it will be integrated into the more tightly-knit spectrum of active studies described in preceding sections, and its results will be appropriately reported.

Project References

1. "Proposed Studies of the Formation and Stability of an Electromagnetic Boundary in a Pinch." Proposal for NASA Research Grant NsG-306-63, 5 March 1962.

2. First Semi-Annual Progress Report for the period 1 July 1962 to 31 December 1962, Research Grant NsG-306-63, Aeronautical Engineering Report No. 634, Princeton University, Princeton, New Jersey.

3. "The Plasma Pinch as a Gas Accelerator," AIAA Electric Propulsion Conference, 11-13 March 1963, Preprint No. 63013.

4. Second Semi-Annual Progress Report for the period 1 January 1963 to 30 June 1963, Research Grant NsG-306-63, Aeronautical Engineering Report No. 634a, Princeton University, Princeton, New Jersey.

5. "Structure of a Large-Radius Pinch Discharge," AIAA Journal 1, 8, 1809-1814 (1963).

6. "Gas-Triggered Inverse Pinch Switch," Review of Scientific Instruments 34, 12, 1439-1440 (1963).

7. "A Gas-Triggered Inverse Pinch Switch," Technical Note, Aeronautical Engineering Report No. 660, Princeton University, Princeton, New Jersey, August 1963.

8. "Pulsed Electromagnetic Gas Acceleration," Paper No. II, 8, Fourth NASA Intercenter Conference on Plasma Physics in Washington, D. C., 2-4 December 1963.

9. "Current Distributions in Large-Radius Pinch Discharges," AIAA Aerospace Sciences Meeting, 20-22 January 1964, AIAA Preprint No. 64-25.

10. "Current Distributions in Large-Radius Pinch Discharges," AIAA Bulletin 1, 1, 12 (1964).

11. "Current Distributions in Large-Radius Pinch Discharges," AIAA Journal 2, 10, 1749-1753 (1964).

12. Third Semi-Annual Progress Report for the period 1 July 1963 to 31 December 1963, Research Grant NsG-306-63, Aeronautical Engineering Report No. 634b, Princeton University, Princeton, New Jersey.

13. "Pulsed Electromagnetic Gas Acceleration," Renewal Proposal for 15 months extension of NASA Research Grant NsG-306-63, Princeton University, Princeton, New Jersey, dated 15 January 1964.

Project References-continued

14. Fourth Semi-Annual Progress Report for the period 1 January 1964 to 30 June 1964, Research Grant NsG-306-63, Department of Aerospace and Mechanical Sciences Report No. 634c, Princeton University, Princeton, New Jersey.

15. "Gas-Triggered Pinch Discharge Switch," Princeton Technical Note No. 101, Department of Aerospace and Mechanical Sciences, Princeton University, Princeton, New Jersey, July 1964.

16. "Gas Triggered Pinch Discharge Switch," The Review of Scientific Instruments 36, 1, 101-102 (1965).

17. "Double Probe Studies in an 8" Pinch Discharge," M.S.E. Thesis of J. M. Corr, Department of Aerospace and Mechanical Sciences, Princeton University, Princeton, New Jersey, September 1964.

18. "Exhaust of a Pinched Plasma from an Axial Orifice," AIAA Bulletin 1, 10, 570 (1964).

19. "Exhaust of a Pinched Plasma from an Axial Orifice," AIAA Second Aerospace Sciences Meeting, New York, New York, 25-27 January 1965, Paper No. 65-92.

20. "Ejection of a Pinched Plasma from an Axial Orifice," AIAA Journal 3, 10, 1862-1866 (1965).

21. Fifth Semi-Annual Progress Report for the period 1 July 1964 to 31 December 1964, Research Grant NsG-306-63, Department of Aerospace and Mechanical Sciences Report No. 634d, Princeton University, Princeton, New Jersey.

22. "On the Dynamic Efficiency of Pulsed Plasma Accelerators," AIAA Journal 3, 6, 1209-1210 (1965).

23. "Linear Pinch Driven by a High-Current Pulse-Forming Network," AIAA Bulletin 2, 6, 309 (1965).

24. "Linear Pinch Driven by a High Current Pulse-Forming Network," 2nd AIAA Annual Meeting, San Francisco, California, 26-29 July 1965, Paper No. 65-336.

25. "The Design and Development of Rogowski Coil Probes for Measurement of Current Density Distribution in a Plasma Pinch," M.S.E. Thesis of Edward S. Wright, Department of Aerospace and Mechanical Sciences, Princeton University, Princeton, New Jersey, May 1965.

26. "The Design and Development of Rogowski Coil Probes for Measurement of Current Density Distribution in a Plasma Pinch," Department of Aerospace and Mechanical Sciences Report No. 740, Princeton University, Princeton, New Jersey, June 1965.

Project References-continued

27. "Pulsed Electromagnetic Gas Acceleration," Renewal Proposal for 12 months extension of NASA Research Grant NsG-306-63, Princeton University, Princeton, New Jersey, dated 7 June 1965.

28. "Miniature Rogowski Coil Probes for Direct Measurement of Current Density Distributions in Transient Plasmas," The Review of Scientific Instruments 36, 12, 1891-1892 (1965).

29. Sixth Semi-Annual Progress Report for the period 1 January 1965 to 30 July 1965, Research Grant NsG-306-63, Department of Aerospace and Mechanical Sciences Report No. 634e, Princeton University, Princeton, New Jersey.

30. "Cylindrical Shock Model of the Plasma Pinch," M.S.E. Thesis of Glen A. Rowell, Department of Aerospace and Mechanical Sciences, Princeton University, Princeton, New Jersey, February 1966.

31. "Cylindrical Shock Model of the Plasma Pinch," Department of Aerospace and Mechanical Sciences Report No. 742, Princeton University, Princeton, New Jersey, February 1966.

32. Seventh Semi-Annual Progress Report for the period 1 July 1965 to 31 December 1965, Research Grant NsG-306-63, Department of Aerospace and Mechanical Sciences Report No. 634f, Princeton University, Princeton, New Jersey.

33. "Electric and Magnetic Field Distributions in a Propagating Current Sheet," AIAA Bulletin 3, 1, 35 (1966).

34. "Electric and Magnetic Field Distributions in a Propagating Current Sheet," AIAA Fifth Electric Propulsion Conference, San Diego, California, 7-9 March 1966, Paper No. 66-200.

35. "Pulse-Forming Networks for Propulsion Research," paper presented at the Seventh Symposium on Engineering Aspects of Magnetohydrodynamics, Princeton University, Princeton, New Jersey, March 30-April 1, 1966 (p. 10-11 of Symposium proceedings).

36. "Dynamics of a Pinch Discharge Driven by a High Current Pulse-Forming Network," Ph.D. Thesis of Neville A. Black, Department of Aerospace and Mechanical Sciences, Princeton University, Princeton, New Jersey, May 1966.

37. "Dynamics of a Pinch Discharge Driven by a High Current Pulse-Forming Network," Aeronautical Engineering Report No. 778, Department of Aerospace and Mechanical Sciences, Princeton University, Princeton, New Jersey, May 1966.

Project References-continued

38. "Pulsed Plasma Propulsion," paper presented at the Fifth NASA Intercenter and Contractors Conference on Plasma Physics, Washington, D. C., 24-26 May 1966, p. 75-81, Part V of Proceedings.

39. "Pulsed Electromagnetic Gas Acceleration," Renewal Proposal for 24 months extension of NASA Research Grant NsG-306-63, Princeton University, Princeton, New Jersey, 25 May 1966.

40. "A Large Dielectric Vacuum Facility," AIAA Journal 4, 6, 1135 (1966).

41. "Structure of the Current Sheet in a Pinch Discharge," Ph.D. Thesis of Rodney L. Burton, Department of Aerospace and Mechanical Sciences, Princeton University, Princeton, New Jersey, August 1966.

42. "Structure of the Current Sheet in a Pinch Discharge," Department of Aerospace and Mechanical Sciences Report No. 783, Princeton University, Princeton, New Jersey, September 1966.

43. Eighth Semi-Annual Progress Report for the period 1 July 1966 to 31 December 1966, Research Grant NsG-306-63, Department of Aerospace and Mechanical Sciences Report No. 634g, Princeton University, Princeton, New Jersey.

44. "Electromagnetic Propulsion," Astronautics and Aeronautics 4, 69 (1966).

45. "Microwave Determination of the Electron Density Profile in a Propagating Current Sheet," Ph.D. Thesis of William R. Ellis, Jr., Department of Aerospace and Mechanical Sciences, Princeton University, Princeton, New Jersey, 1967.

46. "Current Status of Plasma Propulsion," AIAA Second Propulsion Joint Specialist Conference, Colorado Springs, Colorado, June 13-17, 1966, AIAA Paper No. 66-565.